2-2019

Insights Into Paleoenvironmental Conditions, Relative Sea-Level, and Carbonate Reservoir Quality Using Ichnology: Middle-Upper Miocene Slope Deposits, Great Bahama Bank

Ryan M. Mustacato
University of Nebraska-Lincoln, r.mustacato@gmail.com

INSIGHTS INTO PALEOENVIRONMENTAL CONDITIONS, RELATIVE SEA-LEVEL, AND CARBONATE RESERVOIR QUALITY USING ICHNOLOGY: MIDDLE-UPPER MIOCENE SLOPE DEPOSITS, GREAT BAHAMA BANK

by

Ryan M. Mustacato

A THESIS

Presented to the Faculty of

The Graduate College at the University of Nebraska

In Partial Fulfillment of Requirements

For the Degree of Master of Science

Major: Earth and Atmospheric Sciences

Under the Supervision of Professor Tracy D. Frank

Lincoln, Nebraska

February, 2019

INSIGHTS INTO PALEOENVIRONMENTAL CONDITIONS, RELATIVE SEA-LEVEL, AND CARBONATE RESERVOIR QUALITY USING ICHNOLOGY: MIDDLE-UPPER MIOCENE SLOPE DEPOSITS, GREAT BAHAMA BANK

Ryan M. Mustacato, M.S.

University of Nebraska, 2019

Advisor: Tracy D. Frank

Detailed ichnological and petrographic analyses were conducted on two biostratigraphically-constrained intervals (11.9-11.3 Ma and 10.7-9.4 Ma) from the Middle-Upper Miocene stratigraphy of the Great Bahama Bank's leeward margin to assess spatiotemporal trends in paleoenvironmental conditions and reservoir properties in carbonate slope deposits. Six ichnofacies, varied in expression, are documented: the *Skolithos* Ichnofacies (distal and impoverished expressions) the *Cruziana* Ichnofacies (proximal, archetypal, distal and impoverished expressions), the *Zoophycos* Ichnofacies, the *Nereites* Ichnofacies, the *Glossifungites* Ichnofacies, and the *Trypanites* Ichnofacies. An analysis of spatiotemporal ichnofacies trends reveals two distinct responses of the benthic community to significant environmental perturbations on the slope. An abrupt lateral expansion of impoverished *Cruziana* suites c. 11.6 Ma coincides with a period of highstand shedding and increased depositional stress on the slope. Additionally, an ichnofacies change c. 10.5 Ma, recorded by lateral dominance of the archetypal *Cruziana* ichnofacies on the slope, represents a prolonged period of quiescent conditions, characteristic of a sea-level lowstand. Petrographic analysis reveals that porosity is largely controlled by bioturbation in these deposits. Bioturbation characteristically results in porosity heterogeneity, as burrow fills, linings, spreiten, or halos differ significantly in

character to host sediment. Porosity heterogeneity is highest in non-impoverished *Cruziana* and *Glossifungites* fabrics and lowest in impoverished *Cruziana* fabrics, while *Zoophycos* and *Nereites* fabrics show intermediate porosity contrasts. Measurements indicate that distal *Cruziana* fabrics have the highest average porosities at 17.7 ± 5.9%, followed by *Zoophycos* fabrics at 14.8 ± 4.3%. Impoverished proximal and distal *Cruziana* fabrics possess comparable, but lower porosities at 13.3 ± 4.2% and 11.0 ± 4.2% respectively. *Nereites* and *Glossifungites* fabrics have intermediate porosities at 10.2 ± 3.6% and 11.3 ± 3.2% respectively. This study demonstrates the utility of trace fossil analysis in highlighting physiochemical change in carbonate slope environments and expands upon previous observations concerning impacts of bioturbation on porosity distribution in carbonates.

Table of Contents

LIST OF FIGURES PAGE

LIST OF TABLES

PAGE

1. INTRODUCTION

Bioturbation, the disruption of sedimentary deposits by living organisms, is a common post-depositional process, represented in the rock record by biogenic structures known as trace fossils. Trace fossil analysis (or Ichnology) is used to better understand depositional environments (Knaust & Bromley, 2012) and fluid flow through commercial reservoir rocks (Pemberton & Gingras, 2005). Trace fossils are significant interpretive devices because they are *in situ* representations of organism behaviors, and thus reflect animal responses to changes in environmental conditions such as water turbidity, sedimentation rate, substrate consistency, salinity, and oxygenation (Gingras et al., 2011). Trace fossil data organized into interpretive frameworks known as ichnofacies (Seilacher, 1967) and ichnofabrics (Bromley & Ekdale, 1986; Taylor & Goldring, 1993; Taylor et al., 2003) integrate with sedimentological data to yield high-resolution reconstructions of depositional environments. Although paleoenvironmental reconstruction is the primary utility of trace fossil analysis, an abundance of recent work indicates its equal value in understanding fluid flow and storage in reservoir rocks (reservoir quality). As it pertains to the current state of ichnology, it is evident that: (1) carbonate depositional environments receive less attention than siliciclastics (Buatois and Mángano, 2011), with a particular lack of study in slope environments (Hubbard et al., 2012), and (2) the impact of bioturbation on reservoir quality is variable, and more data (specifically from carbonate settings) are needed to advance current understanding.

Ichnological investigations of slope deposits are less common due to inherent difficulties. Trace-fossil assemblages show marked variability (Hubbard et al., 2012) and

often reflect the dynamic interplay between various sedimentation mechanisms and sub-environments. In the carbonate realm, ichnological investigations have traditionally emphasized either the deep-water (Bromley, 1967; Bromley & Ekdale, 1984a; Ekdale & Bromley, 1983, 1991; Frey & Bromley, 1985) or shallow-water (Curran, 1984, 1991; Jones & Pemberton, 1989; Knaust & Costamagna, 2012; Tudhope & Scoffin, 1984) realms, while less emphasis is given to the study of periplatform deposits (Ekdale & Bromley, 1984), contourites (Wetzel et al., 2008), and periplatform drifts (Reolid & Betzler, 2019) in slope environments.

Considering bioturbation and reservoir quality, recent studies document both positive and negative net effects, with a majority indicating net positive effects. The review paper of Pemberton & Gingras (2005) reports biogenically enhanced permeability in Pleistocene deposits at Willipa Bay, Washington (originally described in Gingras et al., 1999a), the Super-K interval of the Arab-D reservoir, Gwahar Field, Saudi Arabia, the Terang-Sirasun gas field, Offshore Bali, the Sag River Formation of the Prudhoe Bay oil field, Alaska, and numerous other reservoirs. Abundant additional examples of biogenically enhanced reservoir quality are detailed by various researchers (Baniak et al., 2013, 2015; Bednarz & McIlroy, 2012; Cunningham et al., 2009; Dawson, 1978; Gingras et al., 2004; Gordon et al., 2010; La Croix et al., 2013; Lemiski et al., 2011), yet other findings (Dawson, 1981; Knaust, 2009) document net negative effects of bioturbation on reservoir quality. While examples of enhancement outnumber those of reduction, it is increasingly evident that biogenic heterogeneity can have net positive and negative effects within the same formation (Buatois et al., 1999, 2002; La Croix et al., 2017; Tonkin et al., 2010; Spila et al., 2007). Furthermore, most studies of biogenic

heterogeneity are conducted in siliciclastic settings, while fewer involve carbonate deposits. As it pertains to carbonates, additional complexities are involved in that original early diagenesis exerts substantial controls on reservoir quality.

Thus, the objectives of this research are two-fold. The first is to examine and document the ichnology of an understudied depositional environment to provide insights into paleoenvironmental conditions associated with dynamic carbonate slopes. The second is to produce novel data concerning biogenic effects on sediment properties to elucidate how bioturbation influences carbonate reservoir heterogeneity and quality.

2. SETTING

The Great Bahama Bank (GBB) is a modern, archetypal carbonate platform environment situated southeast of the Florida coast and north of Cuba (Fig. 1a). The modern platform was formed by coalescence of three smaller platforms, which resulted from progradation of bank margins and infilling of subsurface depressions during the Cenozoic (Eberli & Ginsberg, 1987; 1989). In addition, prograding systems built the western margin of the bank more than 25 km westward into the Straits of Florida (Eberli & Ginsberg, 1987; 1989), concomitant with the GBB developing from a platform with low-angle slope into a steep-sided platform during the Neogene (Betzler et al., 1999, 2000a; Reijmer et al., 1992, 2002).

Ocean Drilling Program (ODP) Leg 166 drilled seven sites along the prograding western margin of the western GBB (Fig. 1b) to document the sedimentary record of Neogene sea-level changes (Eberli et al., 1997). From seismic, logging, and core data, much work was done to elucidate indications of sea-level changes on two different scales (Anselmetti et al., 2000; Bernet et al., 2000; Betzler et al., 1999, 2000b; Eberli, 2000;

Eberli et al., 2002; Frank & Bernet, 2000; Isern & Anselmetti, 2001; Kroon et al., 2000; Reuning et al., 2002; Spezzaferri et al., 2002; Williams et al., 2002). Higher-frequency, meter-scale alternations between lighter carbonate-rich intervals abundant in platform-derived material (interpreted as highstand deposits) and darker intervals abundant in siliciclastic and pelagic material (interpreted as lowstand/transgressive deposits), correlate with orbitally-induced (20-40 k.y.) sea-level and climate changes (Eberli, 2000). In addition, lower-frequency changes on a scale of 0.5-2.0 m.y. were defined by alternations between high sedimentations rates (up to 20 cm/k.y.), associated with highstand production and shedding from the platform, and low sedimentation rates (5 cm/k.y), associated with platform shutdown and pelagically-dominated sedimentation (Eberli, 2000). Moreover, these changes correlate with progradational pulses imaged in seismic data. In total, 17 depositional sequences, delimited by seismic sequence boundaries, were defined and separated into highstand and lowstand (including transgressive) systems tracts (Bernet et al., 2000; Eberli, 2000).

This study focuses on the Middle to lower-Upper Miocene (Late Seravallian – Early Tortonian) stratigraphy of Sites 1005, 1003, 1007 and 1006. Two biostratigraphically-constrained core intervals comprise the successions investigated herein. The lower interval from 11.9 - 11.3 Ma, is bounded by planktonic foraminiferal zone N13 at the base and nannofossil zone NN7 at the top, while the upper interval from 10.7 – 9.4 Ma, spans the entirety of nannofossil zone NN9 (Fig. 2). The entire studied interval (11.9 – 9.4 Ma) encompasses the highstand systems tract (HST) of depositional sequence *k*, the lowstand systems tract (LST) of depositional sequence *i*, and at Sites 1005, 1007, and 1006, the basal HST of sequence *i* (Eberli et al., 1997) (Fig. 3). Seismic

sequence boundary I marks the transition from the HST of depositional sequence *k* to the LST of depositional sequence *i* (Eberli et al., 1997).

2.1 Site 1005

Site 1005, the most proximal, is located on the middle-upper slope approximately 1.2 km from the platform edge in 350 m of water (Eberli et al., 1997). The succession studied herein covers a depth range from 497-672 mbsf, and includes lithologic units III and IV (Eberli et al., 1997). Average core recovery in this section is 35.6% (calculated from Eberli et al., 1997). Unit III comprises a majority of the LST of depositional sequence *i*, and is characterized by decimeter-scale alternations between gray to light gray, well-cemented biowackestones, and grey to olive grey, compacted biowackestones (Eberli et al., 1997). Lithologic Unit IV *encompasses* the HST of depositional sequence *k*, and consists of a monotonous series of foraminifer wackestones with the same cyclic variations described in Unit III (Eberli et al., 1997). Unit IV's upper boundary is marked by a series of gradational, heavily bioturbated, fining-upward beds with a dramatic decrease in the thickness of the poorly cemented and compacted intervals (Eberli et al., 1997). Sequence boundary I, which separates the two depositional sequences, was placed at 550 mbsf, with an estimated age of 10.2 Ma (Eberli et al., 1997). Based on biostratigraphic data, sedimentation rates were 13 cm/k.y in the middle Miocene and slowed to 11 cm/k.y in the lower-Upper Miocene (Eberli et al., 1997).

2.2 Site 1003

Site 1003, situated on the middle-slope, is roughly 4 km from the platform margin in 481 m of water (Eberli et al., 1997). This study's interval spans a depth range between 473-646 mbsf, and includes lithologic units III, IVa and IVb (Eberli et al., 1997).

Average core recovery in this section is 31% (calculated from Eberli et al., 1997). Unit III, comprising the upper LST of sequence *i*, is an interval with cyclic alternations of light well-cemented and darker less-cemented wackestones to mudstones (Eberli et al., 1997). Subunit IVa, which encompasses the upper HST of depositional sequence *k* and the lower LST of depositional sequence *i*, is characterized by laminated, normally graded packstone to grainstone beds (Eberli et al., 1997). Subunit IVb comprises the lower HST of depositional sequence *k* and consists of bioturbated to structureless packstones (Eberli et al., 1997). Sequence boundary I was positioned at 520 mbsf, with an estimated age of 10.6 Ma. Based on biostratigraphic data, sedimentation rates were 12 cm/k.y in the middle Miocene and slowed to 5 cm/k.y in the lower-Upper Miocene (Eberli et al., 1997).

2.3 Site 1007

Site 1007, located at the toe-of-slope is approximately 11 km from the platform margin in 647 m of water (Eberli et al., 1997). This study's succession spans a depth range between 436-543 mbsf, and includes lithologic units IVa and IVb (Eberli et al., 1997). Average core recovery in this section is 75.2% (calculated from Eberli et al., 1997). Subunit IVa comprises the LST and part of the HST of depositional sequence *i* and consists primarily of light gray to gray foraminifer wackestone, marked by alternating, decimeter- to meter-scale intervals of darker and lighter color (Eberli et al., 1997). As in other sites, lighter intervals are well-cemented and darker intervals show signs of compaction (Frank & Bernet, 2000). The base of subunit IVa is defined at the top of a hardground (Eberli et al., 1997). Subunit IVb, comprising the HST of depositional sequence *k*, consists primarily of light gray, gray, and olive gray wackestones with decimeter- to meter-scale intervals of densely and weakly cemented sediment (Eberli et

al., 1997). Sequence boundary I was placed at 490 mbsf, with an estimated age of 10.9 Ma (Eberli et al., 1997). Based on biostratigraphic data, sedimentation rates were 18 cm/k.y in the middle Miocene and slowed to 4 cm/k.y. in the lower-Upper Miocene (Eberli et al., 1997).

2.4 Site 1006

Site 1006, the most distal, is located approximately 30 km from the platform edge in 658 m of water (Eberli et al., 1997). The succession investigated herein spans a depth range between 543-630 mbsf, and includes lithologic units IV and V (Eberli et al., 1997). Average core recovery in this section is 91.3% (calculated from Eberli et al., 1997). Lithologic unit V comprises the upper LST and lower HST of sequence *k*, and is characterized by alternating intervals of light greenish gray to olive nannofossil chalk and light gray nannofossil chalk with planktonic foraminifers (Eberli et al., 1997). Lithologic unit IV comprises the entire LST and the lower HST of depositional sequence *i*, and is composed primarily of alternating intervals of light gray and light greenish gray nannofossil chalk with foraminifers (Eberli et al., 1997). The transition from Unit IV to V is punctuated by a series of firmgrounds (Eberli et al., 1997). Sequence boundary I was placed at 570 mbsf, with an estimated age of 10.7 Ma (Eberli et al., 1997). Based on biostratigraphic data, sedimentation rates were 5 cm/k.y in the middle Miocene and slowed to 3 cm/ k.y. in the lower-upper Miocene (Eberli et al., 1997).

3. METHODS

3.1 Core Description

Core descriptions conducted at the IODP Core Repository – MARUM, followed methodologies outlined in Knaust (2017). Colors and thicknesses of individual beds were documented and measured, and bioturbation intensities were quantified by visual estimation. The scale used was that of Taylor and Goldring (1993), while visual estimations were made using schematic diagrams from MacEachern et al. (2008). Initial identification of trace fossils was carried out by referencing core examples and descriptions from Knaust (2017). Additional observations such as burrow diameters, cross-cutting relationships, and ichnodiversities were documented where possible. In addition, high-resolution photographs were taken at regular intervals for further analysis.

3.2 Core Image Modification

Core images were modified after a method first described by Dorador & Rodríguez-Tovar (2014) to increase trace fossil visibility. Images were imported into Adobe Photoshop and cropped to remove non-core material. A levels adjustment was applied to alter image shadows, midtones, and highlights. For optimal effects, input values for shadows were increased 20-30 points from the default 0 value and highlights were decreased 20-30 points from the default 255 value. Midtone values were unaltered or lowered minimally, depending on individual images. A brightness/contrast adjustment was then applied to broaden overall ranges of tonal values and shadows in images. Favorable results were attained by increasing contrast values roughly 40 points and decreasing brightness values a similar amount. Greatly-enhanced burrow visibility was achieved, but severe color imbalances persisted. To ameliorate color imbalances, a vibrance adjustment was employed, which entailed decreasing saturation values by 20-25 points and increasing vibrance values by 10-15 points. A final levels adjustment was used

to further color-balance images, which involved minimal alteration to values, but was done to closely match altered image color to that of the originals.

3.3 Ichnological Analysis

An effort was made to adhere to the method of ichnological analysis outlined by McIlroy (2008), which integrates concepts from the ichnofabric approach and ichnofacies paradigm. Initial descriptions of bed-scale changes in bioturbation intensity, trace fossils, and ichnodiversity were updated or re-analyzed using enhanced, high-resolution core photographs. Ichnogenera were identified based on examples presented in the ichnological literature (Bromley & Ekdale, 1986; Buatois and Mángano, 2011; Chamberlain, 1978; Frey & Howard, 1985; Frey & Pemberton, 1985; Gingras et al., 2007; Knaust & Bromley, 2012; Knaust, 2017; MacEachern et al., 2007a, 2007b; MacEachern & Bann, 2008; Miller, 2007; Pemberton, 1992; Seilacher, 2007). Identified ichnogenera were combined with prior lithologic, sedimentary structure, geophysical, and geochemical data (Eberli et al., 1997) to define trace fossil suites or ichnofabrics. Trace fossil suites were then incorporated into an ichnofacies model, which in tandem with the established sequence stratigraphic framework, allowed for interpretation of depositional conditions and relative sea level.

3.4 Age Estimates

Age estimates discussed in proceeding sections were calculated based on the available biostratigraphy (Eberli et al., 1997), matched to depth and core number (see figures 13-16). Two assumptions are made, that: 1.) sedimentation rate (previously estimated in Eberli et al., 1997) was constant throughout the biostratigraphic zone, and 2.) the entire biostratigraphic zone is represented in the studied interval. Incomplete core

recovery is another potential source of error for these ages. However, these ages are merely estimates, and are utilized to interpret relative ichnofacies changes through time, both within individual sections and from section to section across the transect.

3.5 Petrographic Analysis

Fifty-two core plugs collected at the IODP Bremen Core Repository – Marum were vacuum impregnated with blue epoxy and thin sectioned to examine porosity. A four-step process (Fig. 4) was completed for each thin section to estimate porosity percentages and visualize distributions. First, full thin section scans were generated using a Prior Optiscan II system. Second, full-scan images were input into Adobe Photoshop and edited with the background eraser tool to remove non-sample porosity, ensuring that resultant images contained sample material only. Third, edited images were entered into JMicrovision image analysis software (www.jmicrovision.com), where a background tool was employed to isolate a color threshold representative of the blue epoxy. Once defined, JMicrovision output the percentage of the image falling within that threshold, generating porosity estimates. Lastly, images were re-inserted into Adobe Photoshop, where a layer mask tool was utilized to remove the background image and isolate porosity. This process allowed for both precise estimates of porosity and detailed visualization of porosity distributions within burrow fabrics.

4. RESULTS

4.1 Systematic Ichnology

In this study, 54 fabrics (Table 1), associated with six ichnofacies (varied in expression) are documented: the *Skolithos* Ichnofacies (distal and impoverished

expressions) the *Cruziana* Ichnofacies (proximal, archetypal, distal and impoverished expressions), the *Zoophycos* Ichnofacies, the *Nereites* Ichnofacies, the *Glossifungites* Ichnofacies, and the *Trypanites* Ichnofacies.

4.1.1 Impoverished *Skolithos*

Suites resembling an impoverished expression of the *Skolithos* ichnofacies (Fig. 5) comprise light gray to gray, or tan bioclastic packstones-grainstones with abundant visible sedimentary structures including: planar laminae, scoured contacts with normally graded beds and fining upward sequences. Other primary features include planktonic and benthic foraminifers, shell fragments, echinoderm spines, megafossils, lithoclasts, and red algae. Bioturbation is sporadic with intensities ranging from BI 1 to 5 and ichnodiversity is low. Recognized ichnogenera include: *fugichnia*, *navichnia*, *crypto-bioturbation*, rare *Skolithos* and *Arenicolites*. Inferred ethologies comprise escape, sediment swimming and locomotion under the sediment-water interface, equilibrichnia and rare filter-feeding. Opportunistic use of resources during short colonization windows in soupy-loose substrate is evidenced by the absence of cross-cutting, well-defined burrows, and low ichnodiversity.

4.1.2 Distal *Skolithos*

Suites attributed to the distal *Skolithos* ichnofacies (Fig. 6a) comprise light gray to gray, or tan bioclastic packstones-grainstones with subordinate sedimentary structures as planar laminae. Other primary features include planktonic and benthic foraminifers, and gastropods. Bioturbation intensity is moderate (BI 2-4), with an even distribution, and ichnodiversity is low-moderate. Identified ichnogenera include: *Cylindrichnus*, *Diplocraterion*, *Macaronichnus (?)*, *Rosselia*, and *Palaeophycus*. Inferred ethologies

comprise filter-feeding, interface feeding, shallow deposit feeding, equilibriirichnia, and predation from passive carnivores. Sediment colonization can generally be described as opportunistic, but the expression also incorporates elements of equilibrium colonization.

4.1.3 Proximal *Cruziana*

Suites attributed to the proximal *Cruziana* ichnofacies (Fig. 6b, c) are distinguished in light gray to gray bioclastic packstones and subordinate foraminifer wackestones with subordinate sedimentary structures such as planar laminae. Other primary features include planktonic and benthic foraminifers, shell fragments, gastropods, and echinoderm spines. Bioturbation intensity is moderate-high (3-4) with an even to occasionally pervasive distribution. Recognized ichnogenera include: *Diplocraterion*, *Cylindrichnus*, *Macaronichnus (?)*, *Ophiomorpha*, *Planolites*, *Palaeophycus*, *Rosselia*, *Teichichnus* and rare *Schaubcylindrichnus (?)*. Inferred ethologies include filter-feeding, interface feeding, shallow deposit feeding, equilibrichnia, living, and passive carnivore predation. Increased proportions of filter-feeding, equilibrichnia, and the lack of deep deposit feeding distinguish these suites from archetypal *Cruziana* fabrics. Sediment colonization is indicative of an equilibrium community adjusted to moderate colonization windows.

4.1.4 Impoverished *Cruziana*

Suites ascribed to the impoverished *Cruziana* ichnofacies (Fig. 7) comprise light gray, gray, light beige, or beige foraminifer wackestones and subordinate bioclastic packstones with common sharp contacts and planar laminae. Other primary features include abundant planktonic and subordinate benthic foraminifers. Bioturbation intensity is frequently high (BI 3-5) but ichnodiversity is exceedingly low. Fabrics are conspicuous

by the presence of color mottling overprinted by few discrete traces of facies-crossing forms. Recognized ichnogenera include: *Helminthopsis*, *Ophiomorpha*, *Phycosiphon*, *Planolites*, *Palaeophycus*, and *Thalassinoides*. Inferred ethologies are scarce and include: shallow deposit feeding, grazing, stabilizing, living, systematic feeding, and predation from passive carnivores. Suites can be separated further by overriding ethology. Some are dominated by *Planolites* and *Palaeophycus*, with subordinate *Ophiomorpha*. Others contain abundant *Planolites* and common *Palaeophycus* but in addition incorporate *Helminthopsis*, *Phycosiphon*, and *Thalassinoides*. The former, dominated by shallow deposit feeding and passive predation, is indicative of an impoverished proximal *Cruziana* expression, while the latter, with increased elements of systematic feeding and grazing, conforms to an impoverished distal *Cruziana* expression. All suites show some indication of opportunistic colonization of a substrate with a poor consistency.

4.1.5 Archetypal *Cruziana*

Suites ascribed to the archetypal *Cruziana* ichnofacies (Fig. 8) comprise gray to dark gray or beige to dark beige foraminifer wackestones to packstones with few-no visible sedimentary structures, often exhibiting gradational contacts between beds. Other primary features include planktonic and benthic foraminifers. Bioturbation is pervasive (BI 5-6) and ichnodiversity is high. Identified ichnogenera include *Asterosoma*, *Chondrites*, *Cosmorhaphe*, *Cylindrichnus*, *Helminthopsis*, *Ophiomorpha*, *Palaeophycus*, *Phoebichnus (?)*, *Phycosiphon*, *Planolites*, *Rosselia*, *Rhizocorallium*, *Schaubcylindrichnus (?)*, *Taenidium*, *Teichichnus*, *Thalassinoides*, and *Zoophycos*. Inferred ethologies are numerous and include: shallow & deep deposit feeding, grazing, systematic feeding, equilibrichnia, domichnia, filter-feeding and passive carnivore

structures. Distinguishing features of the ichnofacies include large burrow sizes (centimeter-scale diameters) and an abundance of large, vertical to sub-vertical feeding and dwelling structures. Sediment colonization is representative of a climax community in an increasingly cohesive substrate.

4.1.6 Distal *Cruziana*

Suites with a distal *Cruziana* ichnofacies association (Fig. 9) comprise gray to beige to dark beige foraminifer wackestones to packstones with gradational contacts. Other primary features are planktonic and benthic foraminifers and gastropods. Bioturbation is pervasive (BI 4-6) and ichnodiversity is moderate-high. Recognized ichnogenera include *Asterosoma*, *Chondrites*, *Cosmorhaphe*, *Cylindrichnus*, *Helminthopsis, Palaeophycus*, *Phycosiphon*, *Planolites*, *Scolicia*, *Thalassinoides*, and *Zoophycos*. Inferred ethologies are shallow & deep deposit feeding, interface feeding, systematic feeding, grazing, and rare filter-feeding and passive carnivore structures. Suites are distinguished from archetypal *Cruziana* by diminished trace fossil diameters, increased proportions of systematic feeding, and reduced presence of filter-feeding and passive carnivore structures. Sediment colonization is representative of an equilibrium community in an increasingly cohesive substrate.

4.1.7 *Zoophycos*

Suites of the *Zoophycos* ichnofacies (Fig.10) are distinguished in dark beige, dark gray, or dark olive gray foraminifer wackestones and nannofossil chalks with few sedimentary structures manifest as rare gradational contacts. Other primary components include planktonic and benthic foraminifers and disseminated pyrite. Bioturbation intensity is high (BI 5-6) with a pervasive distribution and ichnodiversity is low-

moderate. Recognized ichnogenera include: *Chondrites*, *Cosmorhaphe*, *Helminthopsis*, *Planolites*, *Phycosiphon*, *Scolicia*, *Thalassinoides*, and *Zoophycos*. Inferred ethologies are specialized and include shallow & deep deposit feeding, systematic feeding, and grazing. Distinctive features comprise increased abundances of systematic and specialized feeding, diminished trace fossil size, pervasive and intense mining of the sediment, and dark color of the deposits. Copious cross-cutting and overprinting points to equilibrium colonization of progressively stiffer substrate during long colonization windows.

4.1.8 *Nereites*

Suites of the *Nereites* Ichnofacies (Fig. 11) are common in light gray to light tan nannofossil chalks with planktonic & benthic foraminifers, shell fragments, pisoids, and some disseminated pyrite. They are characterized by: (1) grazing or systematic feeding as the dominant behavior, with common evidence of deposit and detritus feeding, (2) combinations of deep-tier mining structures and complex grazing structures, (3) moderate-high ichnodiversity, (4) moderate bioturbation intensity, and (5) mm-cm scale burrow diameters. Recognized ichnogenera include abundant *Chondrites, Cosmorhaphe*, *Helminthopsis*, common *Zoophycos,* subordinate *Scolicia* and *Planolites*. Increased abundances of complex, systematic feeding structures, particularly *Cosmorhaphe*, are a fundamental characteristic of these suites.

4.1.9 *Glossifungites*

The *Glossifungites* Ichnofacies (Fig. 12a, b), a substrate specific ichnofacies, is defined in this study by: (1) the presence of unlined, passively filled, open domiciles used for dwelling, predation, or suspension feeding, (2) subordinate deposit feeding structures,

(3) subdued ichnodiversity, (4) variable bioturbation intensity, and (5) variable burrow size. Recognized ichnogenera include: abundant *Thalassinoides*, common *Chondrites* and *Planolites*. Passively filled structures exhibiting a clear lithologic contrast between burrow fill and surrounding sediment is diagnostic in core and represents firmground colonization of the sediment. A slight departure from typical expressions exist however. Often *Thalassinoides* and *Planolites* tubes show evidence of slight compaction, suggesting a stiff-firm substrate during burrow emplacement rather than a completely firm substrate.

4.1.10 *Trypanites*

The *Trypanites* ichnofacies (Fig. 12c) is recognized in fully-cemented, light-gray to light beige foraminifer wackestones with associated sharp contacts. Ichnogenera are difficult to discern, and potentially include *Rogerella* and *Trypanites*. Structures can be inferred to represent borings or domiciles in a hard substrate.

4.2 Ichnofacies Trends by Site

4.2.1 Site 1005

At proximal Site 1005, (Fig. 13) the basal succession encompasses suites of the distal *Cruziana* and *Zoophycos* ichnofacies (668-662 m [~11.9-11.8 Ma]) overlain by impoverished proximal and distal *Cruziana* suites (658-644 m [~11.8-11.7 Ma]). Above, (640-636 m [~11.65-11.6 Ma]) distal *Cruziana* suites reoccur and are capped by a *Glossifungites* surface. The remaining basal succession (622-599 m [~11.5-11.3 Ma]) is dominated by impoverished proximal *Cruziana* suites (622-603 m [~11.5-11.4 Ma]) that transition into impoverished distal *Cruziana* suites (603-599 m [~11.4-11.3 Ma]). The upper succession includes proximal *Cruziana* suites at the base (575-571 m [~10.65-10.6]

Ma) that give way upward to an interval (571-567 m [~10.6-10.5 Ma]) of impoverished proximal *Cruziana* suites. Above, another short interval (565-562m [~10.45-10.4 Ma]) comprises suites of the archetypal *Cruziana* ichnofacies. The remaining succession (554-498 m [~10.4-9.4 Ma]) is dominated by suites representing an impoverished expression of the proximal *Cruziana* ichnofacies. Impoverished *Skolithos* suites are conspicuous and comprise a transient interval in this part of the section from 546-543 m (10.2-10.1 Ma).

Overall, the succession is dominated by fabrics representing an impoverished proximal *Cruziana* expression and contains the lowest diversity in terms of ichnofacies associations. Conspicuous in the succession are the presence of archetypal *Cruziana* suites from 565-562 m (~10.45-10.4) Ma and impoverished *Skolithos* suites from (~10.2-10.1 Ma). Although impoverished suites dominate the entire succession, they are more pronounced in NN9 than in NN7-N13.

4.2.2 Site 1003

At lower-middle slope Site 1003 (Fig. 14), the basal succession contains suites of the distal *Cruziana* and *Zoophycos* ichnofacies (642-637 m [~11.9-11.85 Ma]) overlain by impoverished proximal and distal *Cruziana* suites (637-629 m [~11.85 – 11.75 Ma]). Up section is an interval (629-618 m [~11.75-11.7 Ma]) that transitions between proximal *Cruziana*, distal *Cruziana* and *Zoophycos* suites. Above, a conspicuous interval (618-610 m [~11.7-11.65 Ma]) comprises suites attributed to the distal *Skolithos* ichnofacies, then capped by a *Glossifungites* surface. Above this surface is another short interval (608-599 m [~11.65-11.55 Ma]) with recurring suites of the *Zoophycos* and distal *Cruziana* ichnofacies. Suites attributed to various impoverished expressions of the *Skolithos* and *Cruziana* ichnofacies dominate the remaining basal succession (599-559 m [~11.55 –

11.3 Ma]). The upper succession includes suites with an impoverished *Skolithos* or proximal *Cruziana* expression at the base (526-512 m [~10.7-10.3 Ma]) overlain by a conspicuous interval (507-502 m [~10.2 – 10.05 Ma]) with suites of the archetypal *Cruziana* ichnofacies. The remaining interval (502-473 m [~10.05 – 9.4 Ma]) is dominated by suites with an impoverished *Cruziana* expression.

The succession is more diverse in terms of ichnofacies associations and includes greater proportions of non-impoverished suites. Though impoverished *Cruziana* expressions are again prominent they comprise only a slight majority, as impoverished *Skolithos* suites are more abundant at this site. Conspicuous in the succession are archetypal *Cruziana* suites from 507-502 m (10.2 – 10.05 Ma) and distal *Skolithos* suites from 618-610 m (11.7 – 11.65 Ma). As in Site 1005, impoverished suites are more abundant during NN9 than in NN7-N13.

4.2.3. Site 1007

At toe-of-slope Site 1007 (Fig. 15) the basal succession includes an interval with suites of the *Zoophycos* and distal *Cruziana* ichnofacies at the base (541-532 m [~11.9 – 11.75 Ma]) overlain by impoverished suites of the distal *Cruziana* ichnofacies (532-527 m [~11.75 – 11.65 Ma]). Above (527-513 m [~11.65 – 11.45 Ma]) are transitions between suites of the proximal *Cruziana*, distal *Cruziana* and *Zoophycos* ichnofacies. The upper lower interval (509-504 m [~11.4 -11.3 Ma]) is comprised of suites with an impoverished proximal *Cruziana* expression, then capped by multiple suites attributed to the *Glossifungites* and *Trypanites* ichnofacies. The upper succession is composed of an interval at the base (478-466 m [~10.7 – 10.2 Ma]) with abundant suites attributed to the impoverished *Cruziana* ichnofacies. Above this lies a conspicuous interval (462-456 m

[~10.15 – 9.95 Ma]) with suites of the archetypal *Cruziana* ichnofacies. The remaining upper succession (456-436 m [~9.95 – 9.4 Ma]) includes transitions between impoverished distal *Cruziana*, distal *Cruziana*, and *Zoophycos* suites, with the impoverished suites occurring from 448-442 m (9.75 – 9.55 Ma).

This succession contains reduced abundances of impoverished suites compared to more proximal Sites 1003 & 1005 continuing a trend of decreasing impoverishment distally. In addition, suites attributed to the distal *Cruziana* and *Zoophycos* ichnofacies are proportionally more prevalent at Site 1007 than the more proximal sites. Continuing other trends, as in Sites 1005 and 1003, the succession in NN9 contains: (1) a conspicuous interval with archetypal *Cruziana* suites, and (2) higher proportions of impoverished suites compared to NN7-N13.

4.2.4 Site 1006

The succession at distal Site 1006 (Fig. 16) comprises regular alternations between suites of the *Zoophycos* and *Nereites* ichnofacies. Conspicuous in the succession are two *Glossifungites* surfaces c. 11.6 and 11.4 Ma. The *Zoophycos* ichnofacies is marginally more abundant in NN7-N13 than in NN9.

4.3 Porosity Attributes

4.3.1 Distal *Skolithos* & Proximal *Cruziana* fabrics

Distal *Skolithos* & proximal *Cruziana* fabrics are rare, with one distal *Skolithos* from Site 1003 and one proximal *Cruziana* from Site 1007. The distal *Skolithos* fabric (Fig. 17a) contains a vertical tube of an inferred *Diplocraterion* trace with slightly higher porosity than the surrounding host sediment. The tube predominantly contains moldic porosity of bioclastic material while the surrounding matrix is predominantly interparticle

microporosity within the matrix. The total porosity for this fabric is 12.3%. The proximal *Cruziana* fabric (Fig. 17b) did not capture any particular trace characteristic of the ichnofacies expression, however clear porosity heterogeneity can be seen. Total porosity of the fabric is 6.9%.

4.3.2 Impoverished *Cruziana* fabrics

Impoverished *Cruziana* microfabrics (Fig. 18) often encompass wackestones-packstones with ample neritic or bioclastic components, diminished pelagic material, and low lithologic heterogeneity. Therefore, contrasts between burrow fills, linings, and host rock are frequently inconspicuous, resulting in mottled textures. Generalized feeding and dwelling behaviors dictate microfabrics, as low-diversity assemblages are prevalent, while complex feeding, dwelling, and grazing structures are rare. Ten samples were attributed to suites resembling an impoverished proximal *Cruziana* expression, while seven were from suites with an impoverished distal expression. The former, consists of eight samples from Site 1005 and two from Site 1003 with porosities ranging from 2.8 – 24.6% and an average of 13.3 ± 4.2 %, while the latter contains four samples from Site 1005, one from Site 1003, and two from Site 1007 with porosities ranging between 4.1 – 22.1% and an average of 11.0 ± 4.2 %. In either expression, moldic porosity is abundant, intraparticle porosity is common, and microporosity within the matrix is subordinate. A difference between the two is in proximal fabrics, micropores constitute molds of fine-grained bioclastic carbonate instead of interparticle matrix microporosity common to distal fabrics.

4.3.3 Archetypal *Cruziana* fabrics

Only one microfabric, from Site 1007 is attributed to the archetypal *Cruziana* ichnofacies. This particular fabric (Fig. 19a) contains a high abundance of complex, cross-cutting, feeding and dwelling structures with cm-scale diameters. Imaged is the porosity distribution within a conspicuous meniscate trace fossil (Fig. 19b) identified here as *Taenidium*, with abundant microporosity and subordinate intraparticle porosity constituting the active fill. The fill (Fig. 19c) is more porous than the enclosing host sediment, displaying moderate porosity heterogeneity. Overall porosity of this fabric is 11.5%.

4.3.4 Distal *Cruziana* fabrics

Typical distal *Cruziana* microfabrics (Fig. 20) comprise pervasively reworked sediment by deposit feeders and grazers overprinted by larger domicile structures. Burrow diameters are mm-cm scale, and contrasts between burrow fill and host sediment are often conspicuous. Nine fabrics, one from Site 1005, five from Site 1003, and three from Site 1007 are attributed to this expression. Total porosity measurements range from 3.7 – 24.5% with an average of 17.7 ± 5.9 %, the highest of all ichnofacies expressions. Porosity types include moldic, intraparticle, and microporosity.

4.3.5 *Zoophycos* fabrics

Thoroughly-bioturbated chalks, wackestones, and rare packstones with abundant planktonic foraminifera typify *Zoophycos* microfabrics (Fig. 21). Prominent behaviors captured in thin section include systematic sediment mining and grazing. Porosity contrasts between burrow fill and surrounding host sediment can be conspicuous or discrete. Twelve samples, four from Site 1003, one from Site 1007, and seven from Site 1006 are attributed to the ichnofacies. Total porosity measurements are wide ranging,

from 5.7 – 29.7% with an average value of 14.8 ± 4.3%. Three porosity types: intraparticle, moldic, and microporosity are equally abundant. Moldic porosity is prevalent in samples from Site 1003, while intraparticle and microporosity dominate in samples from Sites 1007 & 1006.

4.3.6 *Nereites* fabrics

Nereites microfabrics (Fig. 22) encompass moderately-bioturbated nannofossil chalks with complex grazing structures. Contrasts between burrow fill and host sediment are occasionally conspicuous, but mostly discrete. Eight samples, all from distal Site 1006 fall within the ichnofacies. Total porosity measurements range from 5.4 – 15%, with an average of 10.2 ± 3.6%. Burrows contain intraparticle porosity predominantly, while microporosity in the surrounding host sediment is common. Moldic porosity is scarce or non-existent.

4.3.7 *Glossifungites* & *Trypanites* fabrics

Glossifungites microfabrics (Fig. 23a) encompass mainly domicile and some deposit feeding structures in foraminifer wackestones and nannofossil chalks. Characteristic to microfabrics are compositional and grain-size disparities between burrow fill and surrounding material, where burrow fill is regularly allochem-rich compared to host sediment. Only two samples, one from Site 1007, the other from Site 1006, with porosities of 14.5% and 8.1% respectively, average to 11.3 ± 3.3% for the ichnofacies. Intraparticle porosity is common and matrix microporosity is subordinate. Important ichnotaxa in thin section include *Thalassinoides* and *Planolites*. Only one *Trypanites* microfabric (Fig. 23b) is captured in thin section, with a porosity of 2.0%.

5. INTERPRETATION & DISCUSSION

5.1 Conceptual Framework

Marine softground ichnofacies (Seilacher, 1967) have a passive relationship to bathymetry (Ekdale, 1988; Frey, Pemberton & Saunders, 1990) in that trace fossil distributions are controlled by conditions (i.e. substrate consistency, food resources, energy conditions, salinity, and oxygenation) that tend to change with, but can be separate from, water depth. This study provides further support for the notion that depositional conditions (which can be independent of bathymetry and context-dependent) control ichnofossil assemblages. As will be presented here, substrate consistency, sedimentation rate, and sedimentation rate variability are evident as major controls on ichnofacies distributions in these deposits. Moreover, the expressions documented herein relate to specific depositional regimes unique to the GBB slope, which are known to be strongly controlled by relative sea level fluctuations. Therefore, to gain insight into how depositional conditions, and thus sea level, may have evolved in this setting during the middle-late Miocene, it is useful to: (1) provide a short background on depositional conditions and environments traditionally associated with each ichnofacies, (2) discuss how the ichnofacies presented here differ from known examples, and what each may represent in the context of GBB depositional conditions, and (3) attempt to link spatiotemporal ichnofacies trends to potential variations in depositional regime caused by fluctuating relative sea level.

5.2 Traditional Ichnofacies Conditions and Stressed Departures

The archetypal *Skolithos* Ichnofacies indicates relatively high levels of depositional energy, and is typically established in moderately well-sorted, loose or shifting particulate (sand-prone) substrates (MacEachern et al., 2007a). It is prevalent in shallow-marine environments where abrupt changes in depositional rate, erosion, and physical reworking of the sediment are common (MacEachern et al., 2007a). If such conditions persist in other environments (e.g. submarine canyons and deep-marine channels), the ichnofacies may be established in deeper water settings (Crimes et al., 1981; Frey & Howard, 1990; Heard & Pickering, 2008). Its distal expression is considered to be intergradational with the proximal *Cruziana* ichnofacies, both of which are often recognized in relatively clean, silty and muddy sand substrates (MacEachern et al., 2007a). Both generally correspond to environments with gradational transitions from mainly suspended sediment settling to shifting substrate conditions under higher energy, usually in shallow subtidal settings (MacEachern et al., 2007a). The archetypal *Cruziana* ichnofacies is most characteristic of poorly sorted and unconsolidated cohesive substrates in shallow-marine settings with normal salinities, abundant oxygen in depositional waters, abundant food resources, and moderate to low depositional energies (MacEachern et al., 2007a). Bathymetrically, it is typical in environments below fair-weather and above storm-weather wave base where depositional energies are moderate, however, it is also established in lower energy deposits in deeper waters (MacEachern et al., 2007a). Examples of *Cruziana* expressions are also known from slope environments (e.g. Buck & Bottjer, 1985; Ineson, 1987; Savrda et al., 2001; Wetzel et al., 2008) where sufficient oxygen and food are available in deeper water settings (Hubbard et al., 2012). Such environments may include tectonically active slopes with narrow shelves, areas of

significant seasonal coastal downwelling of cold waters, slopes dominated by strong contour currents, regions with high surface-water productivity, and areas proximal to conduits of focused sedimentation (Hubbard et al., 2012). Its distal expression is considered transitional between the archetypal *Cruziana* and *Zoophycos* ichnofacies and is associated with soft, cohesive substrates under persistently quiescent, fully-marine conditions (MacEachern et al., 2007a). The *Zoophycos* ichnofacies has the broadest bathymetric range and is generally considered as an intermediary between the *Cruziana* and *Nereites* ichnofacies. In popular bathymetric schemes, it covers a broad area across the shelf-slope break, where depositional rates are characteristically slow, uniform, and continuous, representative of persistent quiescence (MacEachern et al., 2007a). Re-evaluations of the *Zoophycos* ichnofacies (Seilacher, 1978; Frey and Seilacher, 1980) indicate a diagnostic condition is lowered oxygen levels associated with abundant organic material. The *Nereites* ichnofacies is characterized by settings with slow, continuous suspended sediment deposition, locally punctuated by sediment gravity flows in lower-bathyal to abyssal environments (MacEachern et al., 2007a). Settings are generally well-oxygenated and food resources are commonly sparse. In slope settings, it has been documented (Callow et al., 2013; Cummings and Hodgson, 2011; Heard and Pickering, 2008; Hubbard and Shultz, 2008; Kane et al., 2007) in close proximity to basin-floor depozones (Hubbard et al., 2012). The last two ichnofacies, the *Glossifungites* and the *Trypanites* ichnofacies, are distinct in that they are substrate-specific. The *Glossifungites* ichnofacies is characteristic of firm but unlithified substrates that frequently demarcate discontinuity surfaces of either sequence stratigraphic importance or autocyclic derivation, while the *Trypanites* ichnofacies is characteristic of fully lithified marine

substrates (i.e., hardgrounds), which may reflect depositional omission as well as erosional exhumation (MacEachern et al., 2007a).

Typical ichnofacies associations are indeed critical for palaeoenvironmental reconstruction, but deviations from the norm are perhaps more informative, as departures from normal are strong indicators of palaeoenvironmental change or stress. Non-normal marine salinity (brackish or hypersaline), lowered oxygen in depositional waters, rapid or inconsistent sedimentation rate, poor substrate stability, and lowered food supply are all potential causes of change or stress (Gingras et al., 2011). Organism responses to each are distinct, and specific alterations to trace fossil assemblages reflect such responses. Trace fossil assemblages associated with brackish water (Gingras et al., 1999b; Pemberton et al., 1982, Pemberton & Wightman, 1992) are characterized by: (1) a low diversity of forms, (2) a preponderance of morphologically simple structures, (3) high abundances of single ichnospecies, (4) diminutive trace fossils, and (5) some ichnospecies present in high densities. Lower dissolved oxygen levels induce a marked reduction in burrow size and diversity of ichnogenera (Bromley & Ekdale, 1984b; Ekdale & Mason, 1988; Savrda & Bottjer, 1986; 1991). On the contrary, if trace fossil size is large, it is a strong indication that dissolved oxygen content is high enough to support large animals on the seafloor (Gingras et al., 2007). Organism responses to sedimentation stress are of particular importance in this study. Generally, sedimentation stress manifests in two different ways. The first is consistently high sedimentation rates. Suites subject to consistently high sedimentation rates are characterized by reduced bioturbation intensity and uniformity, and lack structures that record specialized and elaborate feeding strategies (MacEachern et al., 2007b). The second is episodic sedimentation, for example

in the form of turbidites or tempestites. Much work has been done to elucidate organism responses to such sedimentation mechanisms and define recurring trends (Crimes et al., 1981; Wetzel, 1991; Wetzel & Uchman, 2001; Miller, 1993; Seilacher, 1982; Uchman, 2001; 2004). Frequently, there is a juxtaposition of pre-event or ambient suites with post-event suites, the former typically resembling proximal, archetypal, or distal *Cruziana* expressions, the latter incorporating more elements of the *Skolithos* ichnofacies. This has been deemed the "mixed *Skolithos*-*Cruziana* Ichnofacies" but the two are better considered as composite suites (Pemberton & Frey, 1984). In shallower sand-prone settings, ambient suites may correspond to distal or archetypal *Skolithos* expressions (MacEachern & Hobbs, 2004), while in quieter settings, event bed suites may alternate with *Zoophycos* or even *Nereites* ichnofacies elements.

5.3 Sediment Dynamics on the Leeward Slope of the Great Bahama Bank

Relative sea level unequivocally dictated sedimentation on the GBB slope. It is well-established that during the Miocene, highstand shedding (Droxler & Schlager, 1985; Schlager et al., 1994) operated on the GBB (Eberli & Ginsburg, 1989; Isern & Anselmetti, 2001; Reuning et al., 2002; Wilber et al., 1990). The standard model postulates that during highstands, the neritic carbonate factory produced and exported substantial amounts of aragonite-rich sediment down the slope as gravity-driven flows (turbidites), and during lowstands, the shallow-water factory essentially shut down, starving the slope of sediment except for fallout from the pelagic realm. Repeated shutdown and re-activation of the carbonate factory produced the characteristic dark and light lithologies discussed previously, which reflect differences in bulk concentrations of carbonate, insolubles (quartz and clays), and organic matter (Frank & Bernet, 2000).

However, it is probable that a slight departure from the standard model functioned on the GBB during the Miocene. Ample evidence (Bernet et al., 2000; Betzler et al., 1999, 2000a; Eberli, 2000) indicates that sediment export to the slope was not confined to highstands but also occurred during lowstands; and the focus of sedimentation shifted between lowstands and highstands. Moreover, the geometry and composition of highstand and lowstand turbidites differ. Lowstand turbidites are laterally restricted and are composed of mixed shallow-water and pelagic particles, whereas highstand turbidites are laterally extensive with abundant shallow-water particles (Betzler et al., 2000a). Sea-level controlled re-sedimentation from the platform top was the main depositional mechanism affecting middle, lower, and toe-of-slope locations (Sites 1005, 1003, & 1007), and produced the characteristic strata of periplatform oozes intercalated with turbidites (Anselmetti et al., 2000). By contrast, commencing c. 12.4 Ma (middle NN7) in basinal areas (Site 1006), sedimentation was largely-controlled by ocean currents at the confluence of the Santaren Channel and Straits of Florida, producing an 800-m thick drift deposit known as the "Santaren Drift" (Anselmetti et al., 2000). The two sedimentation mechanisms (downslope shedding & contour current drifts) operated simultaneously on the slope and inter-finger at the toe-of-slope Site 1007 (Anselmetti et al., 2000). In the intervals studied here, however, drifts deposited sediment solely at distal Site 1006 and had yet to begin influencing toe-of-slope Site 1007. Sea level is thought not only to have influenced re-sedimentation from the platform top, but also the erosive and depositional potential of the contour current, in that short-term sea level falls intensify currents in seaways due to restriction of the channel area (Richardson & Knauss, 1971).

While sea level fluctuations were undeniably a major depositional control, changing slope morphology also imparted a considerable influence (Betzler et al., 1999; 2000a). Slope morphology of the GBB transitioned gradually from a distally steepened carbonate ramp in the Miocene to a flat-topped carbonate platform in the Pliocene (Betzler et al., 1999, 2000a; Reijmer et al., 1992, 2002), causing a concomitant shift in gravity flow depocenters from an outer ramp position (Site 1003) to a basin floor setting (Site 1007) (Betzler et al., 1999). This transformation is thought to have been triggered by an intensification of bottom currents during the Tortonian (Betzler et al., 1999; 2014). During the middle-late Miocene, the interval studied herein, this transformation was in progress and the GBB was an inchoate flat-topped platform. On a flat-topped platform, a sea-level fall of 5-10 m would be sufficient to significantly reduce production of neritic components (Eberli, 2000), whereas on a distally-steepened ramp a similar fall would have a much smaller impact on rates of shallow water production. Furthermore, current research has shown that Quaternary sedimentation on the GBB slope produced morphologies analogous to siliciclastic settings such as mass transport complexes resulting from slope failure (Jo et al., 2015), channel-levee-lobe systems (Mulder et al., 2012), plunge pools and cyclic steps (Betzler et al., 2014; Schnyder et al., 2018; Wunsch et al., 2017). Thus, ichnofacies distributions on the GBB should also reflect such potential sedimentation changes imparted by an evolving slope morphology.

5.4 Ichnofacies & Paleoenvironmental Conditions on the Great Bahama Bank

5.4.1 Impoverished Expressions

Impoverished *Skolithos* suites are interpreted to represent post-event colonization of turbidite deposits. Successions with ample occurrences characterize periods with

increased frequency and intensity of re-sedimentation from the platform top, typical of highstand conditions. Spatially, their profusion at Site 1003 provides further evidence that the lower-slope was a main depocenter (Betzler et al., 1999) during the middle-late Miocene. Impoverished *Cruziana* suites, in contrast, are more spatially complex, with interpretation more dependent on location along the slope. One inferred scenario for impoverished *Cruziana* suites is they characterize a recovery or ambient suite in turbidite or bypass prone settings where sedimentation stabilized, but the benthic community had not fully recovered or adapted to a recent rapid change. Longer stretches of quiescence between re-sedimentation events could lead to the development of either impoverished proximal and impoverished distal *Cruziana* expressions, the latter representing longer times between events. Another potential scenario is that such suites correspond to times of pelagically-dominated sedimentation admixed with smaller pulses of re-sedimentation from the platform top. In terms of relative sea level, it is possible these suites characterize either late-transgressive or early-highstand deposits before major turbidite export begins, or latest highstand or early-lowstand when major turbidite deposition wanes. In addition, less prolonged occurrences of impoverished suites could also represent times of lowstand turbidite export, which in theory should be less pronounced and frequent due to a diminished neritic factory.

Spatially, the abundance of impoverished *Cruziana* and lack of impoverished *Skolithos* suites at Site 1005 indicates it was not a turbidite depocenter, but nonetheless was stressful for the benthic community. Poor substrate consistency and episodic sedimentation are the likely major depositional stressors. In this setting, soupy-soft substrates were regularly disrupted by bypassing gravity-driven flows during both

lowstands and highstands, biasing behaviors towards general deposit feeding and passive predation during rarer intermittent times of quiescence. Low-diversity, low-complexity, shallow-tier trace fossil assemblages indicate that organisms colonized the sediment quickly and efficiently between shedding events but failed to establish complex communities. This interpretation of ichnofacies at Site 1005 is consistent with previous work identifying it as a site of sediment bypass (Betzler et al., 2000a). In general, if successions (as in the upper half of NN7-N13 at Site 1003) demonstrate continuous alternations between impoverished *Skolithos* and *Cruziana* suites, it can be interpreted to indicate prolonged periods of shedding and environmental instability at that location. As eluded to previously, numerous studies have also shown this juxtaposition of *Skolithos*/*Cruziana* assemblages in turbidite and tempestite prone settings with rapid changes in depositional rate and substrate consistency (MacEachern & Hobbs 2004; Pemberton & Frey, 1984; Vossler & Pemberton, 1989).

Potential barriers to interpreting impoverished suites are lithologic heterogeneity and soupground taphonomic biases (Bromley, 1996). Lithologic heterogeneity and grain size distribution influence burrow recognition in carbonates (Archer, 1984), such that low lithologic contrast makes burrow identification extremely difficult. Soupground conditions carry a taphonomic bias (Bromley & Ekdale, 1984a; Wetzel, 1991) against preservation of structures in that they are more easily destroyed after emplacement. In this regard, overestimation of impoverished suites at Site 1005 due to low lithologic contrast or taphonomic bias is a possibility, whereby smaller grazing and mining structures may have been either obscured or destroyed. However, even in beds with both high lithologic contrast and well-defined burrows at Site 1005, suites were still devoid of

complex forms and dominated by facies crossers such as *Planolites* and *Palaeophycus*. These observations bolster the hypothesis that impoverished suites were indeed a result of stressed depositional conditions rather than the sole product of low lithologic contrast or taphonomic bias (although these factors are suspected to have imparted some influence). Further supporting evidence for actual depositional stress is the prevalence of abundant sharp contacts between beds at Site 1005 (more than any other site) indicating episodic rather than gradual changes in erosive and depositional processes.

5.4.2 Non-Impoverished Expressions

Distal *Skolithos* and proximal *Cruziana* suites on the GBB are unique in that they provide evidence for increased sedimentation rate without signs of mass wasting. In this regard, either exceedingly high rates of pelagic sedimentation or increased rates of non-catastrophic re-sedimentation from the platform top are indicated. A depositional mechanism producing such conditions is challenging to ascertain, but recent evidence for the existence of channelized “delta drift” deposits (Lüdmann et al., 2018) on carbonate slopes fits this description. Such deposits have been identified from the Maldives and a similar “periplatform drift” is documented from the GBB (Betzler et al., 2014), however “delta drifts” have yet to be described in Miocene deposits from the GBB. Moreover, Reolid & Betzler (2019) documented the ichnology of the Maldives delta drift deposit and it was dominated by *Zoophycos* ichnofacies elements. Thus, at this juncture, the impact of this mechanism in these deposits is purely speculative and needs further investigation. However, other recent work (Mulder et al., 2012) revealed the existence of several small- and large-scale morphologies analogous to those found in siliciclastic settings, with inferred processes including mass transport complexes, gravity currents

initiated by density cascading, and overspilling channeled turbidity currents. As discussed previously, traditional shallow-marine ichnofacies expressions have been described in such settings (see Hubbard et al., 2012 for review). Archetypal *Cruziana* fabrics are interpreted to represent times with low-moderate sedimentation rates, abundant food supply, and considerable amounts of dissolved oxygen in depositional waters (MacEachern et al., 2007a). In the context of the GBB these conditions are most likely during times of extended quiescence and environmental stability during lowstand, perhaps with increased pelagic or non-catastrophic re-sedimentation from higher up on the slope. Distal *Cruziana* and *Zoophycos* suites are interpreted to reflect times of quiescence with slow, steady sedimentation, increased pelagic and organic matter input, improved substrate consistency, and potentially lowered oxygen levels (MacEachern et al., 2007a). The alternations between *Nereites* and *Zoophycos* ichnofacies expressions at distal Site 1006 are interpreted here to be largely independent from sea level controlled sediment export from the platform top. Instead it is more plausible they represent fluctuations in ocean current intensity, erosive power, and depositional rate, such that increased current velocity brought more oxygenated waters to the site but precluded deposition of abundant food resources (Wetzel et al. 2008), leading to expressions of the *Nereites* ichnofacies. By contrast, slower currents caused increased deposition of organic material and reduced oxygen in the sediment and depositional waters (Wetzel et al. 2008), resulting in *Zoophycos* ichnofacies expressions. It is clear that the ichnology reflects a different sedimentation mechanism at Site 1006 relative to other sites.

5.5 Significance of Ichnofacies Trends

Increased carbonate production and sediment export to the slope during highstands create conditions that favor impoverished ichnofossil assemblages characteristic of stressed *Cruziana* expressions, or mixed associations of the *Cruziana* and *Skolithos* ichnofacies. Thus, in this setting, these ichnofacies can help in the recognition of highstand deposits. In contrast, lowstand conditions generate more diverse ichnofossil assemblages characteristic of the archetypal, distal *Cruziana* ichnofacies, and the *Zoophycos* ichnofacies, Therefore, in this study they serve to elucidate lowstand deposits. Slight departures from each defined ichnofacies may represent either transgressive, early highstand, or late highstand deposits. Thus, tracking alternations from stressed suites to archetypal or intergradational ones through space and time can provide insights into sea level changes (Fig. 24).

From c. 11.9 to 11.8 Ma (lower-middle N13), distal *Cruziana* and *Zoophycos* suites appear on the middle slope (Site 1005), lower slope (Site 1003), and toe-of-slope (Site 1007), suggesting quiescence along the entire transect, characteristic of lowstand conditions (Fig. 24). C. 11.8 Ma (upper N13), stressed conditions (designated by impoverished ichnofacies expressions) arise on the middle and lower slope but fail to affect the toe-of-slope, indicating laterally-restricted shedding in this interval. A major change in ichnofacies distribution occurs c. 11.65 Ma (middle-upper NN7) and is marked by the development of *Glossifungites* surfaces at the middle slope (Site 1005) and lower slope (Site 1003). Above these surfaces, signs of stress, evident as impoverished ichnofacies expressions, begin to permeate throughout entire successions until the end of NN7 (11.3 Ma). The middle slope remains stressed for the rest of NN7, but the lower and toe-of-slope contain more nuanced ichnofacies changes. Impoverished *Skolithos* suites

begin to appear on the lower slope c. 11.55 Ma (middle-upper NN7), potentially marking the initiation of a fully functioning and exporting shallow water platform during highstand. For a brief time, c. 11.45 Ma (upper NN7) the lower and toe-of-slope are free of depositional stress, indicated by transient occurrences of non-impoverished ichnofacies expressions. This suggests a potential higher-order lowstand imposed on the lower-order highstand trend. After 11.45 Ma to the end of NN7, the entire transect contains impoverished ichnofacies expressions, indicating stressed conditions during highstand shedding. Considering the entire interval, lowstand conditions prevailed c. 11.9 – 11.65 Ma (middle-upper NN7), whereas highstand conditions characterized c. 11.65 – 11.3 Ma (upper NN7).

In NN9, from c. 10.7 – 10.5 Ma (lower NN9) an abundance of impoverished suites points to stressed conditions dominating along the transect, with the exception of middle slope Site 1005. This pattern is difficult to explain. The most plausible explanation is that in this part of the interval, Site 1005 was no longer a site of direct sediment bypass and may have been marginally impacted by bypassing currents (i.e. overspilling of channelized turbidity currents). Nonetheless, this was a time dominated by stress on the slope, still characteristic of highstand conditions. A major change in the ichnofacies distribution occurs c. 10.5 Ma (lower NN9), in which the archetypal *Cruziana* ichnofacies begins to appear along the transect. It occurs first at the middle slope c. 10.5 – 10.45 Ma (lower NN9), then appears shortly after on the lower and toe-of-slope c. 10.2 – 10.1 Ma (lower-middle NN9). Overall, this time could reflect a prolonged lowstand in which quiescent sedimentation and optimal conditions prevailed for a considerable time. Subsequently, stressed conditions returned to the middle and lower

slope and continued until the end of the NN9 (9.4 Ma) indicating another period of shedding characteristic of a highstand in sea level.

Overall, two key ichnofacies changes at c. 11.6 (middle-upper NN7) and 10.5 Ma (lower NN9) record animal responses to major environmental perturbations on the slope. The shift from predominantly non-impoverished to impoverished suites along the slope with firmgrounds developing on the middle and lower slope ~11.6 Mya is interpreted to mark the end of lowstand conditions and initiation of a prolonged period of highstand shedding. The second, marked by a shift from impoverished to non-impoverished suites along the slope c. 10.5 Ma (lower NN9) is interpreted to signal the initiation of lowstand conditions which lasted a considerable time. A return of impoverished suites along the slope indicates that highstand shedding resumed c. 10 Ma (middle NN9). The first lowstand interval falls within dates previously defined for the Mi 5 glaciation (Haq et al., 1987 [12.5 Ma]; Westerhold et al. 2005 [11.7 Ma]) and the second corresponds to dates defined for the Mi 6 glaciation (Haq et al., 1987 [10.5 Ma]; Westerhold et al., 2005 [10.4 Ma]). The second glaciation at 10.5 Ma is interpreted by Haq et al. (1987) to be concomitant with a major global, eustatic sea level drop, resulting in sea level falling 80 m below present levels. A fall of this magnitude should shut down the neritic carbonate factory for an extended period, and thus could explain the lengthy persistence of quiescent conditions along the GBB slope. Evolving slope morphology towards a steeply sided, rimmed platform could have also played a role because more substantial attenuations of the neritic factory would be expected to occur during lowstands. Finally, previously defined (Eberli et al., 1997) seismic Sequence Boundary I (placed 10.2 Ma at

Site 1005, 10.6 Ma at Site 1003, 10.9 Ma at Site 1007, and 10.7 Ma at Site 1006) coincides with this major change in the ichnofacies distribution.

5.6 Bioturbation & Porosity

On the slope of the Great Bahama Bank, biogenic reworking noticeably alters grain distributions within sediments, characteristically resulting in porosity heterogeneity; where burrow fills, linings, spreiten, or halos contrast markedly with enclosing host sediment. Perhaps more so than average porosity (Fig. 25), it is this porosity heterogeneity that will have the larger impact on fluid flow in the different ichnofacies expressions.

Pemberton & Gingras (2005) identified five different scenarios for textural heterogenieties: (1) surface constrained textual heterogeneities, (2) non-constrained textual heterogeneities, (3) weakly defined textural heterogeneities, (4) diagenetic textual heterogeneities, and (5) cryptic bioturbation. Surface-constrained textural heterogeneities consist of discrete, sediment-filled trace fossils that penetrate a low permeability surface representing a depositional discontinuity, whereas non-constrained textural heterogeneities consist of discrete, sediment-filled burrows encased by a low-permeability substrate, unrelated to a discontinuity surface. Weakly defined textural heterogeneities result from ichnofossils infilled with subtly different sediment from that of the surrounding host rock. Diagenetic textural heterogeneities typically result from the establishment of preferred diagenetic pathways in burrow fills. Cryptic bioturbation is very subtle, characterized by non-discrete biogenic structures that completely alter the sediment, mostly resulting from the activity of meiofauna or small infauna.

Biogenic textural heterogeneities often establish dual-porosity (permeability contrast between matrix and burrows is less than two orders of magnitude) and dual-permeability (permeability contrast between matrix and burrows is greater than three orders of magnitude) networks (Pemberton & Gingras, 2005), which can profoundly dictate fluid flow. Surface and non-constrained textural heterogeneities generally result in substantial permeability contrasts between burrow and matrix with fluid flow largely restricted to burrow conduits (Pemberton & Gingras, 2005), whereas weakly-defined textural heterogeneities can generate biogenically sorted flow conduits with less significant permeability contrasts. Dual-porosity and permeability networks are usually limited in vertical extent but can potentially be vast in aerial extent (Pemberton & Gingras, 2005). It is within this framework that specific ichnofacies expressions on the GBB slope are discussed. Critical to note is that even though textural and porosity heterogeneity can be characterized in this study, whether dual porosity or permeability networks have been established cannot be resolved in the absence of permeability data. Therefore, fluid flow within different fabrics can only be inferred based on the porosity distribution.

Non-impoverished *Cruziana* fabrics (proximal, archetypal and distal expressions) are strongly associated with non-constrained textural heterogeneities (Fig. 26), often exhibiting the highest porosity contrasts between burrow fill and host sediment. Specifically, distal *Cruziana* fabrics incorporate abundant non-constrained textural heterogeneities with high average porosities. Therefore, fluid flow should be more concentrated within burrow fills, and may result in the establishment of dual-permeability networks in such fabrics. Conversely, impoverished *Cruziana* suites are strongly

associated with weakly-defined textural heterogeneities (Fig. 27), often integrating moderate average porosities with lower heterogeneity. Thus, it can be expected that fluid flow in such fabrics would be less confined to burrow conduits and may lead to the establishment of dual porosity networks, or no biogenic flow network at all. *Zoophycos* fabrics incorporate high average porosities with a predominance of non-constrained textural heterogeneities and subordinate, weakly defined textural heterogeneities, while *Nereites* fabrics include analogous proportions of textural elements but contain lower average porosity values. Dual-porosity networks may be preferentially established in *Zoophycos* and *Nereites* fabrics, and fluid flow would not be as anisotropic as in non-impoverished *Cruziana* fabrics. *Glossifungites* microfabrics are diagnostic of surface-constrained textural heterogeneities and boast lower average porosity values. Unfortunately, too few quality samples were collected to adequately infer fluid flow characteristics in such fabrics.

6. CONCLUSIONS

Detailed ichnological core and petrographic analyses of Middle-Upper Miocene slope deposits from the Great Bahama Bank demonstrate the utility of trace fossil analysis to elucidate sea-level-induced, spatiotemporal changes in paleoenvironmental conditions and porosity heterogeneity in carbonate reservoir rocks. Numerous conclusions result from this research.

1.) Ichnological analysis corroborates evidence that sedimentation on the slope was dynamic, showing marked contrasts in depositional conditions and environments,

reflected by numerous ichnofacies expressions (impoverished, non-impoverished, and transitional) traditionally uncharacteristic of deeper water settings.

2.) Major benthic stressors on the GBB slope during the Middle-Late Miocene are determined to be variable sedimentation rates and poor substrate consistency, caused by turbidite re-sedimentation from the platform top.

3.) Of the sites influenced by platform re-sedimentation, proximal Site 1005 is indicated as the most stressed environment due to high rates of disruption from bypassing turbidity currents. Lower-slope Site 1003, although less stressed than Site 1005, is determined as a main turbidite depocenter during the study interval. Site 1007 is comparably less stressed than Site 1003, thus continuing a trend of decreasing signs of stress distally.

4.) Spatiotemporal alternations between non-impoverished vs. impoverished suites can be utilized to distinguish lowstand vs. highstand conditions on the leeward slope Great Bahama Bank.

5.) Analysis of spatiotemporal trends in ichnofacies highlights two key responses of the benthic community to fluctuating environmental conditions. Beginning c. 11.6 Ma (middle-upper NN7), successions transition from being dominated by non-impoverished expressions to impoverished ones, interpreted to indicate the end of lowstand conditions and the initiation of a prolonged period of highstand shedding on the platform. The second, c. 10.5 Ma (lower NN9), is indicated by the expansion of the archetypal *Cruziana* ichnofacies on the slope, and is interpreted as a period of lowstand conditions lasting until highstand conditions resumed c. 10 Ma (middle NN9).

6.) The most complex and diverse benthic communities (climax communities), which produced suites attributed to the archetypal *Cruziana* ichnofacies, shows a diachronous

expansion along the slope. These climax communities were present at 10.5-10.4 Ma on the middle slope (Site 1005, 565-562 m), 10.2-10.1 Ma on the lower slope (Site 1003, 507-502 m), and 10.1-10 Ma at the toe-of-slope (Site 1007, 462-456 m). It is proposed here that a pronounced shutdown of the carbonate factory, caused by a combination of a significant sea level lowering (Haq et al., 1987) and a changing slope morphology (Betzler et al., 1999, 2000a), allowed for quiescent conditions to persist for an extended period, thus maintaining optimal conditions for benthic organisms.

7.) Ichnological analysis corroborates evidence for two different sedimentation mechanisms operating on the slope as ichnofacies trends at Site 1006 (drift deposits) are separate and largely-unrelated to those seen at sites where sea-level-controlled re-sedimentation from the platform top is the dominant mechanism.

8.) Non-constrained and weakly-defined textural heterogeneities dominate middle-upper Miocene GBB slope deposits. Non-impoverished *Cruziana* fabrics show greater proportions of non-constrained textural heterogeneities, high average porosities, and high porosity heterogeneity, and thus are more likely to result in the establishment of dual-permeability flow networks. Impoverished *Cruziana* suites (especially from middle and lower slope Sites 1005 & 1003) commonly comprise weakly-defined textural heterogeneities, moderate porosities, and low porosity heterogeneity, and therefore are more prone to establish dual porosity flow networks or no biogenic flow network.

Two future research directions are evident as a result of this analysis. First, further ichnologic investigations of carbonate slope environments influenced by highstand shedding are needed to test the efficacy and validity of impoverished vs. non-impoverished suites as indicators of sea level fluctuations. Secondly, it is recommended

that spot-permeability, or bulk permeability and dispersion characteristics are measured, to investigate if porosity contrasts correspond to permeability contrasts. Those data can then be utilized to characterize deposits as either dual-porosity or dual-permeability systems.

7. REFERENCES

Anselmetti, F.S., Eberli, G.P. and Ding, Z. (2000) From the Great Bahama Bank into the Straits of Florida: A margin architecture controlled by sea-level fluctuations and ocean currents. *Geol. Soc. Am. Bull.,* **112**, 829-844.

Archer, A.W. (1984) Preservational Control of Trace-Fossil Assemblages: Middle Mississippian Carbonates of South-Central Indiana. *J. Paleontol.,* **58**, 285-297.

Baniak, G.M., Gingras, M.K. and Pemberton, S.G. (2013) Reservoir characterization of burrow-associated dolomites in the Upper Devonian Wabamun Group, Pine Creek gas field, central Alberta, Canada. *Mar. Petrol. Geol.,* **48**, 275-292.

Baniak, G.M., Gingras, M.K., Burns, B.A. and Pemberton, S.G. (2015) Petrophysical Characterization of Bioturbated Sandstone Reservoir Facies In the Upper Jurassic Ula Formation, Norwegian North Sea, Europe. *J. Sed. Res.,* **85**, 62-81.

Bednarz, M. and McIlroy, D. (2012) Effect of phycosiphoniform burrows on shale hydrocarbon reservoir quality. *AAPG Bull.,* **96**, 1957-1980.

Bernet, K.H., Eberli, G.P. and Gilli, A. (2000) Turbidite frequency and composition in the distal part of the Bahamas Transect. In: *Proc. ODP, Sci. Results,*166 (Eds P.K. Swart, Eberli, G.P. Eberli, Malone, M.J. Malone, and J.F Sarg), College Station, TX (Ocean Drilling Program), 45-60.

Betzler, C., Reijmer, J.J.G., Bernet, K., Eberli, G.P. and Anselmetti, F.S. (1999) Sedimentary patterns and geometries of the Bahamian outer carbonate ramp (Miocene–Lower Pliocene, Great Bahama Bank). *Sedimentology,* **46**, 1127-1143.

Betzler, C., Pfeiffer, M. and Saxena, S. (2000a) Carbonate shedding and sedimentary cyclicities of a distally steepened carbonate ramp (Miocene, Great Bahama Bank). *Int. J. Earth Sci.,* **89**, 140-153.

Betzler, C., Kroon, D. and Reijmer, J.J.G. (2000b) Synchroneity of major Late Neogene sea level fluctuations and paleoceanographically controlled changes as recorded by two carbonate platforms. *Paleoceanography,* **15**, 722-730.

Betzler, C., Lindhorst, S., Eberli, G.P., Lüdmann, T., Möbius, J., Ludwig, J., Schutter, I., Wunsch, M., Reijmer, J.J.G. and Hübscher, C. (2014) Periplatform drift: The combined result of contour current and off-bank transport along carbonate platforms. *Geology,* **42**, 871-874.

Bromley, R.G. (1967) Some observations on burrows of thalassinidean Crustacea in chalk hardgrounds. *Q. J. Geol. Soc. London,* **123**, 157-177.

Bromley, R.G. (1996) Trace Fossils: Biology, Taphonomy, Applications (Ed. R.G. Bromley) 2nd edn, Taylor & Francis, New York, 361 pp.

Bromley, R.G. and Ekdale, A.A. (1984a) Trace Fossil Preservation in Flint in the European Chalk. *J. Paleontol.,* **58**, 298-311.

Bromley, R.G. and Ekdale, A.A. (1984b) Chondrites: A Trace Fossil Indicator of Anoxia in Sediments. *Science,* **224**, 872-874.

Bromley, R.G. and Ekdale, A.A. (1986) Composite ichnofabrics and tiering of burrows. *Geological Magazine,* **123**, 59-65.

Buatois, L.A. and Mángano, M.G. (2011) Ichnology: Organism-Substrate Interactions in Space and Time. Cambridge University Press, Cambridge, 358 pp.

Buatois, L.A., Carr, T. and Mangano, G. (1999) Sedimentology and ichnology of paleozoic estuarine and shoreface reservoirs, Morrow Sandstone, Lower Pennsylvanian of Southwest Kansas, USA. Kansas Geological Survey, Lawrence, KS, 35 pp.

Buatois, L.A., Mángano, M.G., Alissa, A. and Carr, T.R. (2002) Sequence stratigraphic and sedimentologic significance of biogenic structures from a late Paleozoic marginal- to open-marine reservoir, Morrow Sandstone, subsurface of southwest Kansas, USA. *Sed. Geol.,* **152**, 99-132.

Buck, S.P. and Bottjer, D.J. (1985) Continental slope deposits from a Late Cretaceous, tectonically active margin, Southern California. *J. Sed. Res.,* **55**, 843.

Callow, R.H.T., McIlroy, D., Kneller, B. and Dykstra, M. (2013) Integrated ichnological and sedimentological analysis of a Late Cretaceous submarine channel-levee system: The Rosario Formation, Baja California, Mexico. *Mar. Petrol. Geol.,* **41**, 277-294.

Chamberlain, K.C. (1978) Recognition of trace fossils in cores. In: *Trace Fossil Concepts* (Ed. P.B. Basan), *SEPM Short Course*, 5, 33-183.

Crimes, T.P., Homewood, P. and Goldring, R. (1981) Trace fossil assemblages of deep-sea fan deposits, Gurnigel and Schlieren flysch (Cretaceous-Eocene), Switzerland. *Eclogae Geol. Helv.,* **74**, 953-995.

Cummings, J.P. and Hodgson, D.M. (2011) Assessing controls on the distribution of ichnotaxa in submarine fan environments, the Basque Basin, Northern Spain. *Sed. Geol.,* **239**, 162-187.

Cunningham, K.J., Sukop, M.C., Huang, H., Alvarez, P.F., Curran, H.A., Renken, R.A. and Dixon, J.F. (2009) Prominence of ichnologically influenced macroporosity in the karst Biscayne aquifer: Stratiform 'super-K' zones. *Geol. Soc. Am. Bull.,* **121**, 164.

Curran, H.A. (1984) Ichnology of Pleistocene Carbonates on San Salvador, Bahamas. *J. Paleontol.,* **58**, 312-321.

Curran, H.A. and White, B. (1991) Trace Fossils of Shallow Subtidal to Dunal Ichnofacies in Bahamian Quaternary Carbonates. *PALAIOS,* **6**, 498-510.

Dawson, W.C. (1978) Improvement of Sandstone Porosity During Bioturbation: ABSTRACT. *AAPG Bull.,* **62**, 508-509.

Dawson, W.C. (1981) Secondary burrow porosity in quartzose biocalcarenites Upper Cretaceous. Texas: U.S.A. *VIII Congreso Geológico Argentino*, *Actas II*, 637–649.

Dorador, J. and Rodríguez-Tovar, F. (2014) Digital image treatment applied to ichnological analysis of marine core sediments. *Facies,* **60**, 39-44.

Droxler, A.W. and Schlager, W. (1985) Glacial versus interglacial sedimentation rates and turbidite frequency in the Bahamas. *Geology,* **13**, 799-802.

Eberli, G.P. (2000) The record of Neogene sea-level changes in the prograding carbonates along the Bahamas Transect—Leg 166 synthesis. In: *Proc. ODP, Sci. Results,***166** (Eds P.K. Swart, Eberli, G.P. Eberli, Malone, M.J. Malone, and J.F Sarg), College Station, TX (Ocean Drilling Program), 167–177.

Eberli, G.P. and Ginsburg, R.N. (1987) Segmentation and coalescence of Cenozoic carbonate platforms, northwestern Gereat Bahama Bank. *Geology,* **15**, 75-79.

Eberli, G.P. and Ginsburg, R.N. (1989) Cenozoic Progradation of Northwestern Great Bahama Bank, a Record of Lateral Platform Growth and Sea-level Fluctuations. In: *Controls on Carbonate Platform and Basin Development* (Eds P. Crevello, J. Wilson, F. Sarg and F. Read)*, SEPM Spec. Publ.,* 44, 339-351.

Eberli, G.P., Swart, P.K., Malone, M.J., et al. (1997) *Proc. ODP, Init. Repts.,* **166**: College Station, TX (Ocean Drilling Program), 850 pp.

Eberli, G.P., Anselmetti, F.S., Kroon, D., Sato, T. and Wright, J.D. (2002) The chronostratigraphic significance of seismic reflections along the Bahamas Transect. *Mar. Geol.,* **185**, 1-17.

Ekdale, A.A. (1988) Pitfalls of Paleobathymetric Interpretations Based on Trace Fossil Assemblages. *PALAIOS,* **3**, 464-472.

Ekdale, A.A. and Bromley, R.G. (1983) Trace fossils and ichnofabric in the Kjølby Gaard Marl, uppermost Cretaceous, Denmark. *Bull. Geol. Soc. Denmark,* **31**, 107-119.

Ekdale, A.A. and Bromley, R.G. (1984) Comparative Ichnology of Shelf-Sea and Deep-Sea Chalk. *J. Paleontol.,* **58**, 322-332.

Ekdale, A.A. and Bromley, R.G. (1991) Analysis of Composite Ichnofabrics: An Example in Uppermost Cretaceous Chalk of Denmark. *PALAIOS,* **6**, 232-249.

Ekdale, A.A. and Mason, T.R. (1988) Characteristic trace-fossil associations in oxygen-poor sedimentary environments. *Geology,* **16**, 720-723.

Frank, T.D. and Bernet, K. (2000) Isotopic signature of burial diagenesis and primary lithological contrasts in periplatform carbonates (Miocene, Great Bahama Bank). *Sedimentology*, **47**, 1119-1134.

Frey, R.W. and Bromley, R.G. (1985) Ichnology of American chalks: the Selma Group (Upper Cretaceous), western Alabama. *Can. J. Earth Sci.,* **22**, 801-828.

Frey, R.W. and Howard, J.D. (1985) Trace fossils from the Panther Member, Star Point Formation (Upper Cretaceous), Coal Creek Canyon, Utah. *J. Paleontol.,* **59**, 370-404.

Frey, R.W. and Howard, J.D. (1990) Trace Fossils and Depositional Sequences in a Clastic Shelf Setting, Upper Cretaceous of Utah. *J. Paleontol.,* **64**, 803-820.

Frey, R.W. and Pemberton, S.G. (1985) Biogenic structures in outcrops and cores; I, Approaches to ichnology. *Bull. Can. Petrol. Geol.,* **33**, 72-115.

Frey, R.W. and Seilacher, A. (1980) Uniformity in marine invertebrate ichnology. *Lethaia,* **13**, 183-207.

Frey, R.W., Pemberton, S.G. and Saunders, T.D.A. (1990) Ichnofacies and Bathymetry: A Passive Relationship. *J. Paleontol.,* **64**, 155-158.

Gingras, M.K., Pemberton, S.G., Mendoza, C.A. and Henk, F. (1999a) Assessing the anisotropic permeability of Glossifungites surfaces. *Petrol. Geosci.,* **5**, 349-357.

Gingras, M.K., Pemberton, S.G., Saunders, T. and Clifton, H.E. (1999b) The ichnology of modern and Pleistocene brackish-water deposits at Willapa Bay, Washington; variability in estuarine settings. *PALAIOS,* **14**, 352-374.

Gingras, M. K., Mendoza, C. A., & Pemberton, S. G. (2004) Fossilized worm burrows influence the resource quality of porous media. *AAPG Bull.*, **88**, 875-883.

Gingras, M.K., Bann, K.L., MacEachern, J.A., Waldron, J. and Pemberton, S.G. (2007) A Conceptual Framework for the Application of Trace Fossils. In: *Applied Ichnology* (Eds. J.A. MacEachern, K.L. Bann, M.K. Gingras and S.G. Pemberton), *SEPM Short Course Notes*, 52, 1-26.

Gingras, M.K., MacEachern, J.A. and Dashtgard, S.E. (2011) Process ichnology and the elucidation of physico-chemical stress. *Sed. Geol.,* **237**, 115-134.

Gordon, J.B., Pemberton, S.G., Gingras, M.K. and Konhauser, K.O. (2010) Biogenically enhanced permeability: A petrographic analysis of Macaronichnus segregatus in the Lower Cretaceous Bluesky Formation, Alberta, Canada. *AAPG Bull.,* **94**, 1779-1795.

Grammer, G.M., Harris, P.M. and Eberli, G.P. (2004) Integration of outcrop and modern analogs in reservoir modeling: overview with examples from the Bahamas. In: *Integration of Outcrop and Modern Analogs in Reservoir Modeling* (Eds G.M. Grammer, P.M. Harris and G.P. Eberli), *AAPG Mem.*, 80, 1-22.

Haq, B.U., Hardenbol, J. and Vail, P.R. (1987) Chronology of Fluctuating Sea Levels Since the Triassic. *Science,* **235**, 1156-1167.

Heard, T.G. and Pickering, K.T. (2008) Trace fossils as diagnostic indicators of deep-marine environments, Middle Eocene Ainsa-Jaca basin, Spanish Pyrenees. *Sedimentology*, **55**, 809-844.

Hubbard, S.M. and Shultz Michael, R. (2008) Deep Burrows in Submarine Fan-Channel Deposits of the Cerro Toro Formation (Cretaceous), Chilean Patagonia: Implications For Firmground Development and Colonization in the Deep Sea. *PALIOS*, **23**, 223-232.

Hubbard, S.M., MacEachern, J.A. and Bann, K.L. (2012) Slopes. In: *Trace fossils as indicators of sedimentary environments* (Eds. D. Knaust and R.G. Bromley), *Dev. Sedimentol.*, 64, 607-642.

Ineson, J.R. (1987) Trace fossils from a submarine fan-slope apron complex in the Cretaceous of James Ross Island, Antarctica. *Bull. Brit. Antarct. Surv.,* **74**, 1-16.

Isern, A.R. and Anselmetti, F. (2001) The influence of carbonate platform morphology and sea level on fifth-order petrophysical cyclicity in slope and basin sediments adjacent to the Great Bahama Bank. *Mar. Geol.,* **177**, 381-394.

Jo, A., Eberli, G.P. and Grasmueck, M. (2015) Margin collapse and slope failure along southwestern Great Bahama Bank. *Sed. Geol.,* **317**, 43-52.

Jones, B. and Pemberton, S.G. (1989) Sedimentology and ichnology of a Pleistocene unconformity-bounded, shallowing-upward carbonate sequence; the Ironshore Formation, Salt Creek, Grand Cayman. *PALAIOS,* **4**, 343-355.

Kane, I.A., Kneller, B.C., Dykstra, M., Kassem, A. and McCaffrey, W.D. (2007) Anatomy of a submarine channel–levee: An example from Upper Cretaceous slope sediments, Rosario Formation, Baja California, Mexico. *Mar. Petrol. Geol.,* **24**, 540-563.

Knaust, D. (2009) Ichnology as a tool in carbonate reservoir characterization: a study from the Permian-Triassic Khuff Formation in the Middle East. *GeoArabia,* **14**, 17-38.

Knaust, D. (2017) Atlas of Trace Fossils in Well Core : Appearance, Taxonomy and Interpretation. Springer International Publishing, 209 pp.

Knaust, D. and Bromley, R.G. (2012) Trace Fossils as Indicators of Sedimentary Environments*, Dev. Sedimentol., 64*. Elsevier, Amsterdam, 960 pp.

Knaust, D. and Costamagna, L.G. (2012) Ichnology and sedimentology of the Triassic carbonates of North-west Sardinia, Italy. *Sedimentology,* **59**, 1190-1207.

Kroon, D., Williams, T., Pirmez, C., Spezzaferri, S., Sato, T., and Wright, J.D. (2000) Coupled early Pliocene–middle Miocene bio-cyclostratigraphy of Site 1006 reveals orbitally induced cyclicity patterns of Great Bahama Bank carbonate production. In: *Proc. ODP, Sci. Results,***166** (Eds P.K. Swart, Eberli, G.P. Eberli, Malone, M.J. Malone, and J.F Sarg), College Station, TX (Ocean Drilling Program), 155–166.

La Croix, A.D., Gingras, M.K., Pemberton, S.G., Mendoza, C.A., MacEachern, J.A. and Lemiski, R.T. (2013) Biogenically enhanced reservoir properties in the Medicine Hat gas field, Alberta, Canada. *Mar. Petrol. Geol.,* **43**, 464-477.

La Croix, A. D., MacEachern, J. A., Ayranci, K., Hsieh, A., & Dashtgard, S. E. (2017) An ichnological-assemblage approach to reservoir heterogeneity assessment in bioturbated strata: Insights from the Lower Cretaceous Viking Formation, Alberta, Canada. *Mar. Petrol. Geol.*, **86**, 636-654.

Lemiski, R.T., Hovikoski, D.J., Pemberton, D.S.G. and Gingras, D.M. (2011) Sedimentological ichnological and reservoir characteristics of the low-permeability, gas-charged Alderson Member (Hatton gas field, southwest Saskatchewan): Implications for resource development. *Bull. Can. Petrol. Geol.,* **59**, 27-53.

Lüdmann, T., Betzler, C., Eberli, G.P., Reolid, J., Reijmer, J.J.G., Sloss, C.R., Bialik, O.M., Alvarez-Zarikian, C.A., Alonso-García, M., Blättler, C.L., Guo, J.A., Haffen, S., Horozal, S., Inoue, M., Jovane, L., Kroon, D., Lanci, L., Laya, J.C., Mee, A.L.H., Nakakuni, M., Nath, B.N., Niino, K., Petruny, L.M., Pratiwi, S.D., Slagle, A.L., Su, X., Swart, P.K., Wright, J.D., Yao, Z. and Young, J.R. (2018) Carbonate delta drift: A new sediment drift type. *Mar. Geol.,* **401**, 98-111.

MacEachern, J.A. and Bann, K.L. (2008) The Role of Ichnology in Refining Shallow Marine Facies Models. In: *Recent Advances in Models of Siliciclastic Shallow-Marine Stratigraphy* (Eds. G.J. Hampson, R.J. Steel, P.M. Burgess and R.W. Dalrymple), *SEPM Spec. Publ.*, 90, 73-116.

MacEachern, J.A. and Hobbs, T.W. (2004) The ichnological expression of marine and marginal marine conglomerates and conglomeratic intervals, Cretaceous Western Interior Seaway, Alberta and northeastern British Columbia. *Bull. Can. Petrol. Geol.,* **52**, 77-104.

MacEachern, J.A., Bann, K.L., Pemberton, S.G. and Gingras, M.K. (2007a) The Ichnofacies Paradigm: High-Resolution Paleoenvironmental Interpretation of the Rock Record. In: *Applied Ichnology* (Eds. J.A. MacEachern, K.L. Bann, M.K. Gingras and S.G. Pemberton), *SEPM Short Course Notes*, 52, 27-64.

MacEachern, J.A., Pemberton, S.G., Bann, K.L. and Gingras, M.K. (2007b) Departures from the Archetypal Ichnofacies: Effective Recognition of Physico-Chemical Stresses in the Rock Record. In: *Applied Ichnology* (Eds. J.A. MacEachern, K.L. Bann, M.K. Gingras and S.G. Pemberton), *SEPM Short Course Notes*, 52, 65-93.

McIlroy, D. (2008) Ichnological analysis: The common ground between ichnofacies workers and ichnofabric analysts. *Palaeogeogr. Palaeoclimatol. Palaeoecol.,* **270**, 332-338.

Miller, W.III. (1993) Trace fossil zonation in Cretaceous turbidite facies, northern California. *Ichnos,* **3**, 11-28.

Miller, W.III. (2007) Trace Fossils: Concepts, Problems, Prospects. Elsevier Science, Amsterdam, 632 pp.

Mulder, T., Ducassou, E., Eberli, G.P., Hanquiez, V., Gonthier, E., Kindler, P., Principaud, M., Fournier, F., Leonide, P.S., Billeaud, I., Marsset, B., Reijmer, J.J.G., Bondu, C., Joussiaume, R. and Pakiades, M. (2012) New insights into the morphology and sedimentary processes along the western slope of Great Bahama Bank. *Geology,* **40**, 603-606.

Pemberton, S. G. (1992) Applications of Ichnology to Petroleum Exploration: A Core Workshop (Ed. S.G. Pemberton), *SEPM Core Workshop*, 17, 430 pp.

Pemberton, S.G. and Frey, R.W. (1984) Ichnology of Storm-Influenced Shallow Marine Sequence: Cardium Formation (Upper Cretaceous) at Seebe, Alberta. In: *The Mesozoic of Middle North America* (Eds D.F. Stott and Glass, D.J. Glass), *Can. Soc. Petrol. Geol. Mem.,* **9**, 281-300.

Pemberton, S.G. and Gingras, M.K. (2005) Classification and characterizations of biogenically enhanced permeability. *AAPG Bull.,* **89**, 1493-1517.

Pemberton, S.G. and Wightman, D.M. (1992) Ichnological Characteristics of Brackish Water Deposits. In: *Applications of Ichnology to Petroleum Exploration: A Core Workshop* (Ed. S.G. Pemberton), *SEPM Core Workshop*, 17, 141-168.

Pemberton, S.G., Flach, P.D. and Mossop, G.D. (1982) Trace Fossils from the Athabasca Oil Sands, Alberta, Canada. *Science,* **217**, 825-827.

Reijmer, J.J.G., Schlager, W., Bosscher, H., Beets, C.J. and McNeill, D.F. (1992) Pliocene/Pleistocene platform facies transition recorded in calciturbidites (Exuma Sound, Bahamas). *Sed. Geol.,* **78**, 171-179.

Reijmer, J., Betzler, C., Kroon, D., Tiedemann, R. and Eberli, G. (2002) Bahamian carbonate platform development in response to sea-level changes and the closure of the Isthmus of Panama. *Int. J. Earth Sci.,* **91**, 482-489.

Reolid, J. and Betzler, C. (2019) The ichnology of carbonate drifts. *Sedimentology*

Reuning, L., Reijmer, J.J.G. and Betzler, C. (2002) Sedimentation cycles and their diagenesis on the slope of a Miocene carbonate ramp (Bahamas, ODP Leg 166). *Mar. Geol.,* **185**, 121-142.

Richardson, P.L. and Knauss, J.A. (1971) Gulf stream and Western boundary undercurrent observations at Cape Hatteras. *Deep-Sea Research and Oceanographic Abstracts,* **18**, 1089-1109.

Savrda, C.E. and Bottjer, D.J. (1986) Trace-fossil model for reconstruction of paleo-oxygenation in bottom waters. *Geology,***14**, 3.

Savrda, C.E. and Bottjer, D.J. (1991) Oxygen-related biofacies in marine strata: an overview and update. *Geol. Soc. London Spec. Publ.,* **58**, 201-219.

Savrda, C.E., Krawinkel, H., McCarthy, F.M.G., McHugh, C.M.G., Olson, H.C. and Mountain, G. (2001) Ichnofabrics of a Pleistocene slope succession, New Jersey margin:

relations to climate and sea-level dynamics. *Palaeogeogr. Palaeoclimatol. Palaeoecol.,* **171**, 41-61.

Schlager, W., Reijmer, J.J.G. and Droxler, A. (1994) Highstand shedding of carbonate platforms. *J. Sed. Res.,* **64**, 270.

Schnyder, J.S.D., Eberli, G.P., Betzler, C., Wunsch, M., Lindhorst, S., Schiebel, L., Mulder, T. and Ducassou, E. (2018) Morphometric analysis of plunge pools and sediment wave fields along western Great Bahama Bank. *Mar. Geol.,* **397**, 15-28.

Seilacher, A. (1967) Bathymetry of trace fossils. *Mar. Geol.,* **5**, 413-428.

Seilacher, A. (1978) Use of Trace Fossil Assemblages for Recognizing Depositional Environments. In: *Trace Fossil Concepts* (Ed. P.B. Basan), *SEPM Short Course*, 5, 175-201.

Seilacher, A. (1982) Distinctive Features of Sandy Tempestites. In: *Cyclic and Event Stratification* (Eds G. Einsele and A. Seilacher), pp. 333-349. Springer-Verlag Berlin Heidelberg, Berlin.

Seilacher, A. (2007) Trace Fossil Analysis. Springer-Verlag Berlin Heidelberg, Berlin, 226 pp.

Spezzaferri, S., McKenzie, J.A. and Isern, A. (2002) Linking the oxygen isotope record of late Neogene eustasy to sequence stratigraphic patterns along the Bahamas margin: results from a paleoceanographic study of ODP Leg 166, Site 1006 sediments. *Mar. Geol.,* **185**, 95-120.

Spila, M.V., Pemberton, S.G., Rostron, B. and Gingras, M.K. (2007) Biogenic Textural Heterogeneity, Fluid Flow and Hydrocarbon Production: Bioturbated Facies Ben Nevis Formation, Hibernia Field, Offshore Newfoundland. In: *Applied Ichnology* (Eds. J.A. MacEachern, K.L. Bann, M.K. Gingras and S.G. Pemberton), *SEPM Short Course Notes*, 52, 354-371.

Taylor, A. M., & Goldring, R. (1993) Description and analysis of bioturbation and ichnofabric. *J. Geol. Soc. London*, **150**, 141-148.

Taylor, A.M., Goldring, R. and Gowland, S. (2003) Analysis and application of ichnofabrics. *Earth-Sci. Rev.,* **60**, 227-259.

Tonkin, N.S., McIlroy, D., Meyer, R. and Moore-Turpin, A. (2010) Bioturbation influence on reservoir quality: A case study from the Cretaceous Ben Nevis Formation, Jeanne d'Arc Basin, offshore Newfoundland, Canada. *AAPG Bull.,* **94**, 1059-1078.

Tudhope, A.W. and Scoffin, T.P. (1984) The effects of Callianassa bioturbation on the preservation of carbonate grains in Davies Reef Lagoon, Great Barrier Reef, Australia. *J. Sed. Res.,* **54**, 1091.

Uchman, A. (2001) Eocene flysch trace fossils from the Hecho Group of the Pyrenees, northern Spain. *Beringeria*, **28**, 3-41.

Uchman, A. (2004) Phanerozoic history of deep-sea trace fossils. *Geol. Soc. London Spec. Publ.,* **228**, 125-139.

Vossler, S.M. and George Pemberton, S. (1989) Ichnology and paleoecology of offshore siliciclastic deposits in the cardium formation (Turonian, Alberta, Canada). *Palaeogeogr. Palaeoclimatol. Palaeoecol.,* **74**, 217-239.

Westerhold, T., Bickert, T. and Röhl, U. (2005) Middle to late Miocene oxygen isotope stratigraphy of ODP site 1085 (SE Atlantic): new constrains on Miocene climate variability and sea-level fluctuations. *Palaeogeogr. Palaeoclimatol. Palaeoecol.,* **217**, 205-222.

Wetzel, A. (1991) Ecologic interpretation of deep-sea trace fossil communities. *Palaeogeogr. Palaeoclimatol. Palaeoecol.,* **85**, 47-69.

Wetzel, A. and Uchman, A. (2001) Sequential colonization of muddy turbidites in the Eocene Beloveža Formation, Carpathians, Poland. *Palaeogeogr. Palaeoclimatol. Palaeoecol.,* **168**, 171-186.

Wetzel, A., Werner, F. and Stow, D.A.V. (2008) Bioturbation and Biogenic Sedimentary Structures in Contourites. In: *Contourites* (Eds M. Rebesco, and A. Camerlenghi), *Dev. Sedimentol.*, 60, 183-202.

Wilber, R.J., Milliman, J.D. and Halley, R.B. (1990) Accumulation of bank-top sediment on the western slope of Great Bahama Bank: Rapid progradation of a carbonate megabank. *Geology,* **18**, 970.

Williams, T., Kroon, D. and Spezzaferri, S. (2002) Middle and Upper Miocene cyclostratigraphy of downhole logs and short- to long-term astronomical cycles in carbonate production of the Great Bahama Bank. *Mar. Geol.,* **185**, 75-93.

Wunsch, M., Betzler, C., Lindhorst, S., Lüdmann, T. and Eberli, G.P. (2017) Sedimentary dynamics along carbonate slopes (Bahamas archipelago). *Sedimentology*, **64**, 631-657.

8. FIGURE CAPTIONS

Fig. 1 – Map of Great Bahama Bank (A) and Site Map (B) depicting drillhole locations along ODP Leg 166 transect. After Grammer et al. (2004)

Fig. 2 – Line drawing from Western seismic line of the leeward margin of Great Bahama Bank, modified to show coring intervals NN9 (green) and NN7-N13 (orange) investigated in this study. After Anselmetti et al. (2000).

Fig. 3 – Depositional sequences and systems tracts defined by Eberli et al., 2000 and Bernet et al., 2000 modified to show coring intervals NN9 (green) and NN7-N13 (orange) and their relationship to previously defined sequences. After Eberli et al. (2000).

Fig. 4 – Image treatment and porosity estimation. **A.)** Full thin section scan of sample from Site 1003, Hole C, Core 20R, Section 3, Depth 136-140cm, using Prior OptiScan II. Scale bar = 5mm. **B.)** Thin section scan after editing in Adobe Photoshop. **C.)** Image after analysis in JMicrovision software. **D.)** Non-porosity sample material is removed in Adobe Photoshop to increase visibility of burrow porosity and overall porosity distribution.

Fig. 5 – Core examples of impoverished *Skolithos* fabrics. For each example, left-hand image is original core photo, right-hand image is enhanced photo. **A.)** Erosive, laminated turbidite package with singular *Planolites* above periplatform wackestone. 69-78cm. Site 1003, Core 4R, Section 3. **B.)** Escape trace left by an organism avoiding burial during turbidite deposition Site 1003, Core 13R, Section 1. **C.)** Additional example from Site 1003, Core 7R, Section 1. Trace fossil abbreviations are as follows: *fugichnia* (fu), *Planolites* (P).

Fig. 6 – Core examples of distal *Skolithos* and proximal *Cruziana* suites. For each example, left-hand image is original core photo, right-hand image is enhanced photo. **A.)** Rare distal *Skolithos* suite from Site 1003, Core 17R, Section 3, showing small limb of *Diplocraterion habichi* overprinting mottled background. **B-C.)** Proximal *Cruziana* suites from Site 1007, Core 23R, Section 1 and Site 1007, Core 24R, Section 2 showing rare occurrences of ?*Macaronichnus* (after MacEachern & Bann, 2008, p. 80; . Trace fossil abbreviations are as follows: *Diplocraterion habichi* (Dh), ?*Macaronichnus* (Ma?), *Ophiomorpha* (O), and ?*Schaubcylindrichnus* (S?).

Fig. 7 – Core examples of impoverished *Cruziana* suites. For each example, left-hand image is original core photo, right-hand image is enhanced photo. **A.)** Color mottling overprinted by few discrete traces of facies crossers such as *Palaeophycus*. Site 1003, Core 13R, Section 2. **B.)** Example of sediment homogenization. Vestiges of primary sedimentary fabric and erosive contact remain. Note rare occurrence of *Skolithos*. Site1003, Core 15R, Sec1, 58-69cm. Site 1003, Core 15R, Section 1. **C.)** Mottled fabric

overprinted by *Ophiomorpha* tube. Site 1005, Core 14R, Section 2. **D.)** Low-diversity assemblage of facies-crossing forms (i.e. *Planolites*, and potential *Thalassinoides*) during intermittent quiescence. Site 1005, Core 16R, Section 1, 19-27cm. Trace fossil abbreviations are as follows: *Ophiomorpha* (O), *Palaeophycus* (Pa), *Planolites* (P), *Skolithos* (Sk).

Fig. 8 – Core examples of archetypal *Cruziana* suites. For each example, left-hand image is original core photo, right-hand image is enhanced photo. All cores display pervasive bioturbation (BI5-6) with diverse assemblages of cm-scale deposit feeding and domicile structures. **A.)** Gray bioclastic packstone with abundant cross-cutting of complex, diverse forms (i.e. *Rosselia* and large *Ophiomorpha*). Site 1003, Core 6R, Section 3, 73-87cm. **B.)** Pervasive bioturbation in dark-beige, foraminifer wackestone with abundant meniscate trace fossils. Site 1007, Core 17R, Section 2, 53-67cm. **C.)** Pervasive bioturbation by ichnogenus *Palaeophycus*. Site 1003, Core 6R, Section 3. **D.)** Additional example of pervasive bioturbation and complex cross-cutting from proximal Site 1005, Core20R, Section 2. Trace fossil abbreviations are as follows: *Chondrites* (C), *Cosmorhaphe* (Cr), ?*Macaronichnus* (Ma?) (After Pemberton, 1992, p. 129), *Ophiomorpha* (O), *Palaeophycus* (Pa), *Planolites* (P), *Rosselia* (Rs), ?*Scolicia* (Sc?), *Taenidium* (Ta), *Thalassinoides* (Th), and *Zoophycos* (Zo).

Fig. 9 – Core examples of distal *Cruziana* suites. For each example, left-hand image is original core photo, right-hand image is enhanced photo. **A.)** Site 1007, Core 15R, Section 2. **B.)** Site 1003, Core18R, Section 3. **C.)** Site 1003, Core 3R, Section 1 **D.)** Site 1007, Core 23R Section 6. Trace fossil abbreviations are as follows: *Asterosoma* (As), *Chondrites*, (C), *Cosmorhaphe* (Cr), *Helminthopsis* (H), *Palaeophycus* (Pa), *Phycosiphon* (Ph), *Planolites* (P), *Thalassinoides* (Th), *Zoophycos* (Zo).

Fig. 10 – Core examples of *Zoophycos* suites. For each example, left-hand image is original core photo, right-hand image is enhanced photo. **A.)** Thoroughly-mined, dark-grey, bioclastic, mud-rich packstone with overprinting *Zoophycos*. Site 1003, Core 14R, Section 1, 65-75cm. **B.)** Comparable assemblage with decreased trace size in grey nannofossil chalk. Site 1006, Core 62X, Section 2, 75-89cm. **C.)** Thoroughly-bioturbated, dark beige foraminifer wackestone with slightly impoverished expression, dominated by facies-crossers *Chondrites* and *Planolites*. Site 1005, Core 31R, Section 3, 101-114cm. **D.)** Fully-bioturbated, dark-tan foraminifer wackestone with slightly higher diversity than other suites. Site 1007, Core 22R, Section 3. Trace fossil abbreviations are as follows: *Chondrites* (C), *Cosmorhaphe* (Cr), *Helminthopsis* (H), *Planolites* (P), and *Zoophycos* (Zo)

Fig. 11 – Core examples of *Nereites* suites. For each example, left-hand image is original core photo, right-hand image is enhanced photo. **A.)** High diversity assemblage of grazing and feeding structures in gray nannofossil chalk. Site 1006, Core 67X, Section 4, 96-110cm. **B.)** Comparable assemblage with prevalent *Cosmorhaphe* and small-scale *Zoophycos*. Site 1006, Core 61X, Section 5, 129-143cm. **C.)** *Cosmorhaphe* dominated assemblage with moderate bioturbation intensity. Site 1006, Core 61X, Section 6, 25-38cm. **D.)** *Chondrites* dominated assemblage with decreased grazing traces. Site 1006,

Core 67X, Section 5, 28-42cm. Trace fossil abbreviations are as follows: *Chondrites* (C), *Cosmorhaphe* (Cr), *Planolites* (P), *Scolicia* (Sc), and *Zoophycos* (Zo).

Fig. 12 – Core examples of substrate-specific ichnofacies. For each example, left-hand image is original core photo, right-hand image is enhanced photo. **A.)** *Glossifungites* surface from Site 1003, Core 17R, Section 2, showing slightly compacted, passively filled burrows. **B.)** *Glossifungites* surface similarly displaying slight burrow compaction. Site 1006, Core 68X, Section 4. **C.)** *Trypanites* surface developed in hardground. Site 1007, Core 22R, Section 1. Trace fossil abbreviations are as follows: *Chondrites* (C), *Planolites* (P), *Rogerella* (R), *Thalassinoides* (Th) and ?*Trypanites* (T?).

Fig. 13 – Graphic log of succession from Site 1005. Core status refers to core recovery (black = recovered core). Zone NN8 was not studied herein and is therefore omitted. Average core recovery of this interval is 35.6% (calculated from Eberli et al., 1997).

Fig. 14 – Graphic log of succession from Site 1003. Core status refers to core recovery (black = recovered core).). Zone NN8 was not studied herein and is therefore omitted. Average core recovery of this interval is 31% (calculated from Eberli et al., 1997).

Fig. 15 – Graphic log of succession from Site 1007. Core status refers to core recovery (black = recovered core).). Zone NN8 was not studied herein and is therefore omitted. Average core recovery of this interval is 75.2% (calculated from Eberli et al., 1997).

Fig. 16 – Graphic log of succession from Site 1006. Core status refers to core recovery (black = recovered core).). Zone NN8 was not studied herein and is therefore omitted. Average core recovery of this interval is 91.3% (calculated from Eberli et al., 1997).

Fig 17 – **A.)** Distal *Skolithos* fabric. Thin section scan (top) and analyzed image (bottom) capture rare vertical tube of either *Diplocraterion* or *Skolithos*. Note slightly augmented porosity within burrow fill compared to surrounding host rock. Site 1003, Core 17R, Sec3, 64-67cm. Scale bar = 5mm. Total porosity = 12.2%. **B.)** Proximal *Cruziana* fabric. Thin section scan (left) and analyzed image (right). Burrows are fairly indiscriminate, but porosity heterogeneity is clear. Site 1007, Core 23R, Sec2, 62-66cm. Scale bar = 5mm. Total porosity = 6.9%.

Fig. 18 – Impoverished *Cruziana* fabrics in thin section. **A.)** Modified core photo of light-grey bioclastic wackestone with biodeformational structures, lack of discrete trace fossils, and diminished trace preservation. Characteristic of an impoverished proximal *Cruziana* suite. Site1003, Core7R, Sec1, 84-97cm **B.)** Thin section scan (left) and modified version (right) elucidate sediment sorting undetected in core. Important to note are circular arrangements of coarser-grained material surrounding finer-grained particles. The right-hand image highlights areas with coarser material where porosity is concentrated. Burrows are unidentifiable, but the occurrence of sediment sorting points to deposit feeding as a potential behavior. Scale bar = 5mm. Total porosity = 8.2% **C.)** Photomicrograph of larger white box in B, encapsulates area of concentrated fine-sand sized allochems. Porosity is both intraparticle and moldic **D.)** Photomicrograph of small

white box in B, capturing porosity distribution within fine-grained sediment (potential burrow fill?). Porosity is greatly reduced and intraparticle porosity is absent. Little moldic porosity remains **E.)** Core photo of light-grey biowackestone-packstone with a low diversity-assemblage and improved trace fossil preservation, representing an impoverished distal *Cruziana* suite. Based on burrow diameter, *Thalassinoides* is inferred as the ichnogenus of the bottom-left-hand burrow. Site1003, Core15R, Sec1, 137-147cm **F.)** Thin section scan (left) and modified image (right). Note large contrasts in porosity distribution and pore size within burrow fill and outside matrix. Scale bar = 5mm. Total porosity = 22.1% **G.)** Photomicrograph of large box in F, demonstrates *Thalassinoides* burrow fill porosity vs. surrounding matrix porosity. Porosity type is moldic in both burrow fill and surrounding matrix, but pores are larger and more abundant within burrow fill **H.)** Photomicrograph of small box in F, exhibits a diminutive *Phycosiphon* mud-tube and halo. Halo porosity is moldic and is significantly higher than mud-tube porosity

Fig. 19 – Archetypal *Cruziana* fabric in thin section. **A.)** Modified core photo of intensely-bioturbated, dark-beige foraminifer wackestone with abundant meniscate traces. Site1007, Core17R, Sec2, 49-63cm **B.)** Thin section scan (left) and analyzed image (right) highlight porosity distribution within meniscate trace fossil and surrounding matrix. Note higher porosity of active burrow fill (upper left-hand corner of image) compared to surrounding matrix. Total porosity is 11.5%. Scale bar = 5mm **C.)** Photomicrograph of white square in F, exhibiting intraparticle and matrix microporosity within burrow fill. Intraparticle porosity is in the dissolved tests of globerinid foraminifera **D.)** Photomicrograph of white square in G, demonstrating ample micrite microporosity

Fig. 20 – Distal *Cruziana* fabric in thin section. **A.)** Modified core photo depicting horizontal *Palaeophycus* tunnel in dark-grey, bioclastic packstone-wackestone. From Site1003, Core16R, Sec2, 95-101cm. Note light-grey, passive fill is re-burrowed **B.)** Thin section scan (left) and analyzed image (right) exhibits porosity distributions within burrow fill and surrounding matrix. Note higher porosity burrow fill compared to matrix and near complete porosity destruction within burrow lining. Total porosity = 19.8%. Scale bar = 5mm **C.)** Photomicrograph of left-hand square in B, detailing burrow fill porosity. Porosity is moldic, with pervasive dissolution of bioclastic material **D.)** Photomicrograph of right-hand square in B, displaying porosity occlusion within mud-dominant burrow lining.

Fig. 21 – *Zoophycos* fabric in thin section. **A.)** Modified core photo of thoroughly mined, dark-grey, bioclastic packstone-wackestone with good trace fossil preservation. From Site1003, Core20R, Sec1, 56-69cm **B.)** Thin section scan (left) and modified image (right) of intensely-bioturbated fabric characteristic of the *Zoophycos* ichnofacies. Traces may be inferred but are not discernable; however, biogenic alteration of the sediment is evident. Note cluster of mud-filled spheres at top-right and center-left-middle with enclosing halo of porous sediment. Produces a heterogeneous porosity distribution. Total porosity = 21.2%. Scale bar = 5mm **C.)** Photomicrograph of white box in B, demonstrates porosity differences between mud-filled spheres and surrounding sediment.

Similar to *Phycosiphon*, however cluster of spheres is distinct **D.)** Higher-magnification photomicrograph of mud-filled ellipses and surrounding halo. Porosity within halo is primarily moldic, with subordinate microporosity

Fig. 22 – *Nereites* fabric in thin section. **A.)** Modified core photo of *Nereites* ichnofabric in beige nannofossil chalk, note contrasting burrow fills. Site 1006, Core61, Sec2, 81-95cm **B.)** Thin section scan (left) and edited image (right) capturing porosity difference between light burrow fill and dark matrix. Note horizontal (spreite?) burrow in upper third of image. Also, note vertical fracture porosity. Total porosity = 11.1%. Scale bar = 5mm **C.)** Photomicrograph of box in F, encapsulates potential spreite of horizontal burrow, filled with planktonic foraminifera. **D.)** Photomicrograph of box in G, exhibiting intraparticle and microporosity within potential spreite

Fig. 23 – Substrate-specific ichnofabrics in thin section. **A.)** *Glossifungites* microfabric. Passively-filled small *Thalassinoides* or large *Planolites* in nannofossil chalk. Site1006, Core67X, Sec2, 66-70cm. Note abundant allochems (planktonic foraminifers) in burrow fill (top-left & across center) with intraparticle porosity. Total porosity = 8.1%. Scale bar = 5mm **B.)** *Trypanites*? microfabric. Erosive contact between bioclastic packstone and foraminifer wackestone from Site1007, Core22R, Sec1, 21-24cm. Note pervasive cementation resulting in low average porosity (2.1%) and little porosity heterogeneity despite contrasting burrow fill and surrounding host rock. It is possible that cementation occurred post burrow emplacement and this fabric evolved from a soft-firm-to hardground.

Fig. 24 – Synthesis of ichnofacies trends on the Great Bahama Bank

Fig. 25 – Porosity by ichnofacies expression.

Fig. 26 – Non-constrained textural heterogeneities in thin section with increasing porosity heterogeneity. All fabrics are attributed to the distal *Cruziana* ichnofacies. **A.)** Thoroughly mined, highly porous background fabric overprinted by mud-filled *Planolites* occluding porosity. Site 1003, Core 20R, Sec4, 44-48cm. Scale bar = 5mm. Total porosity = 24.4%. **B & C.)** Fabrics from Site 1007, Core 23R, Sec4 (a) & Sec6 (b) with substantial intraparticle porosity concentrated within either large *Planolites* or small *Thalassinoides* burrows. Total porosities are 20.6% and 23.9% respectively. Scale bars = 5mm.

Fig. 27 – Weakly-defined textural heterogeneities in thin section, strongly associated with impoverished *Cruziana* suites. Microphotographs are in order of increasing porosity heterogeneity. **A.)** Site1005C, Core14R, Sec1, 121-125cm. Total porosity = 10.5%. **B.)** Site1005C, Core 26R. Total porosity = 15.7%. **C.)** Site 1005C, Core 15R, Sec3, 47-51 cm. Total porosity = 20.2%.

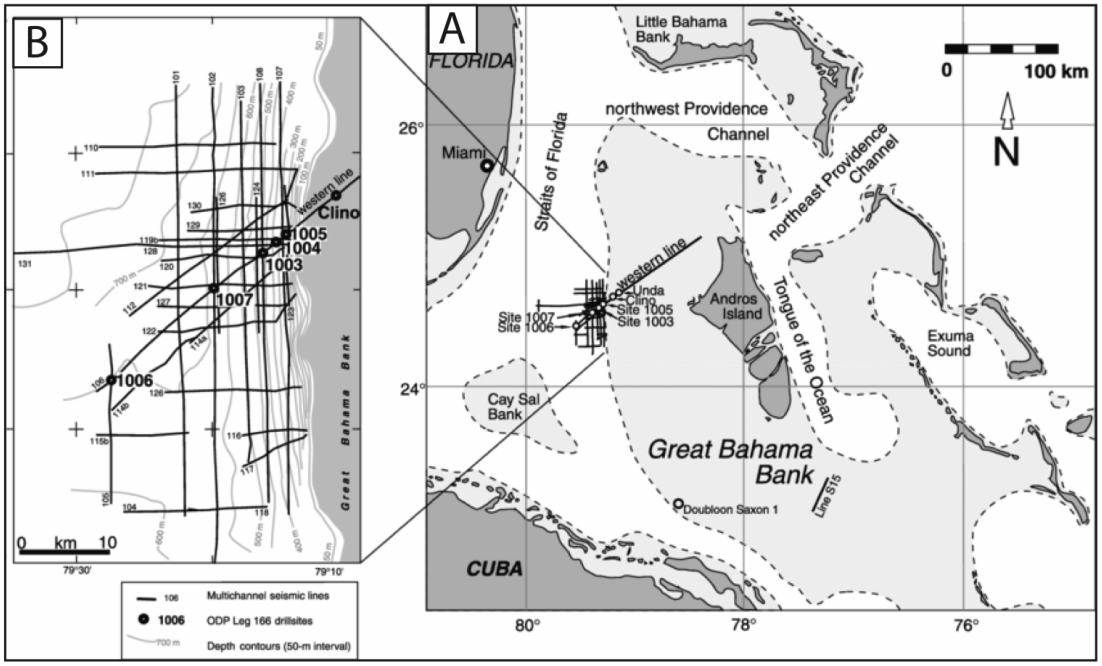
A
B
FLORIDA
Little Bahama Bank
northwest Providence Channel
Miami
Straits of Florida
northeast Providence Channel
0
100 km
N
26°
24°
Western line
Clino
1005
1004
1003
1007
1006
Site 1007
Site 1006
Linda
Cling
Site 1005
Site 1003
Andros Island
Tongue of the Ocean
Exuma Sound
Cay Sal Bank
Great Bahama Bank
Doubloon Saxon 1
Line 515
CUBA
80°
78°
76°
Great Bahama Bank
0 km 10
79°30'
79°10'
Multichannel seismic lines
ODP Leg 166 drillsites
Depth contours (50-m interval)

Figure 1

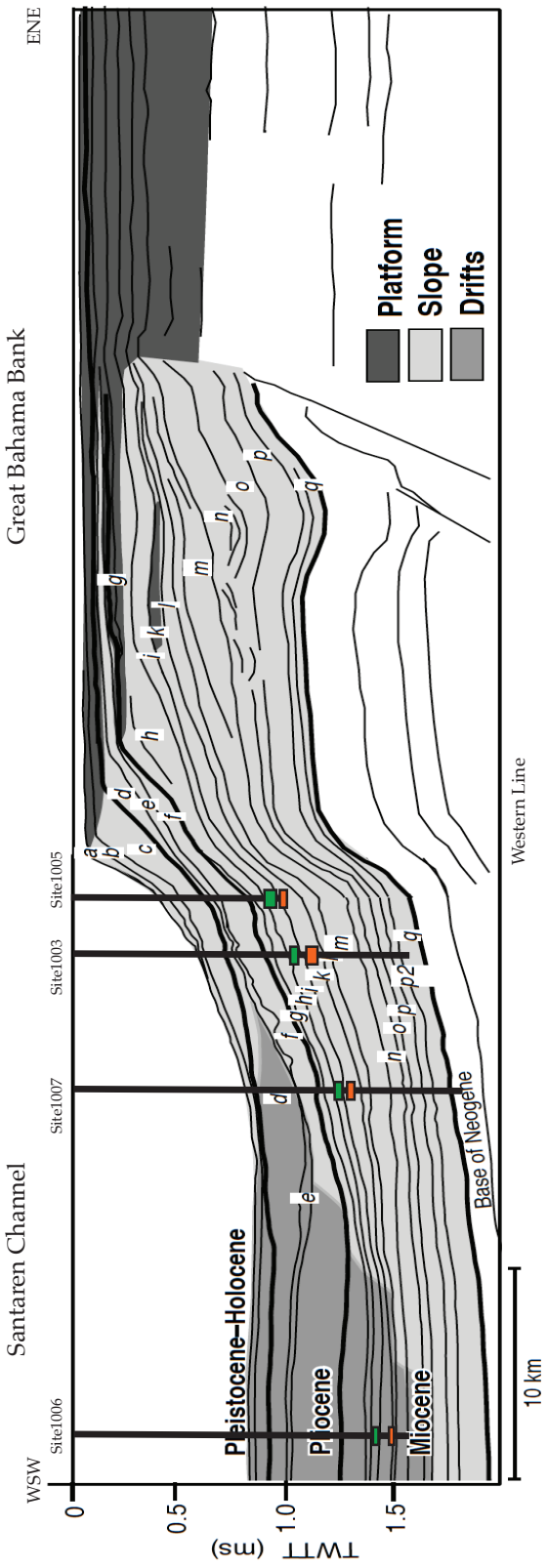
WSW
ENE
Great Bahama Bank
Santaren Channel
Western Line
Site1006
Site1007
Site1003
Site1005
Platform
Slope
Drifts
Pleistocene–Holocene
Pliocene
Miocene
Base of Neogene
10 km
TWTT (ms)
0
0.5
1.0
1.5

Figure 2

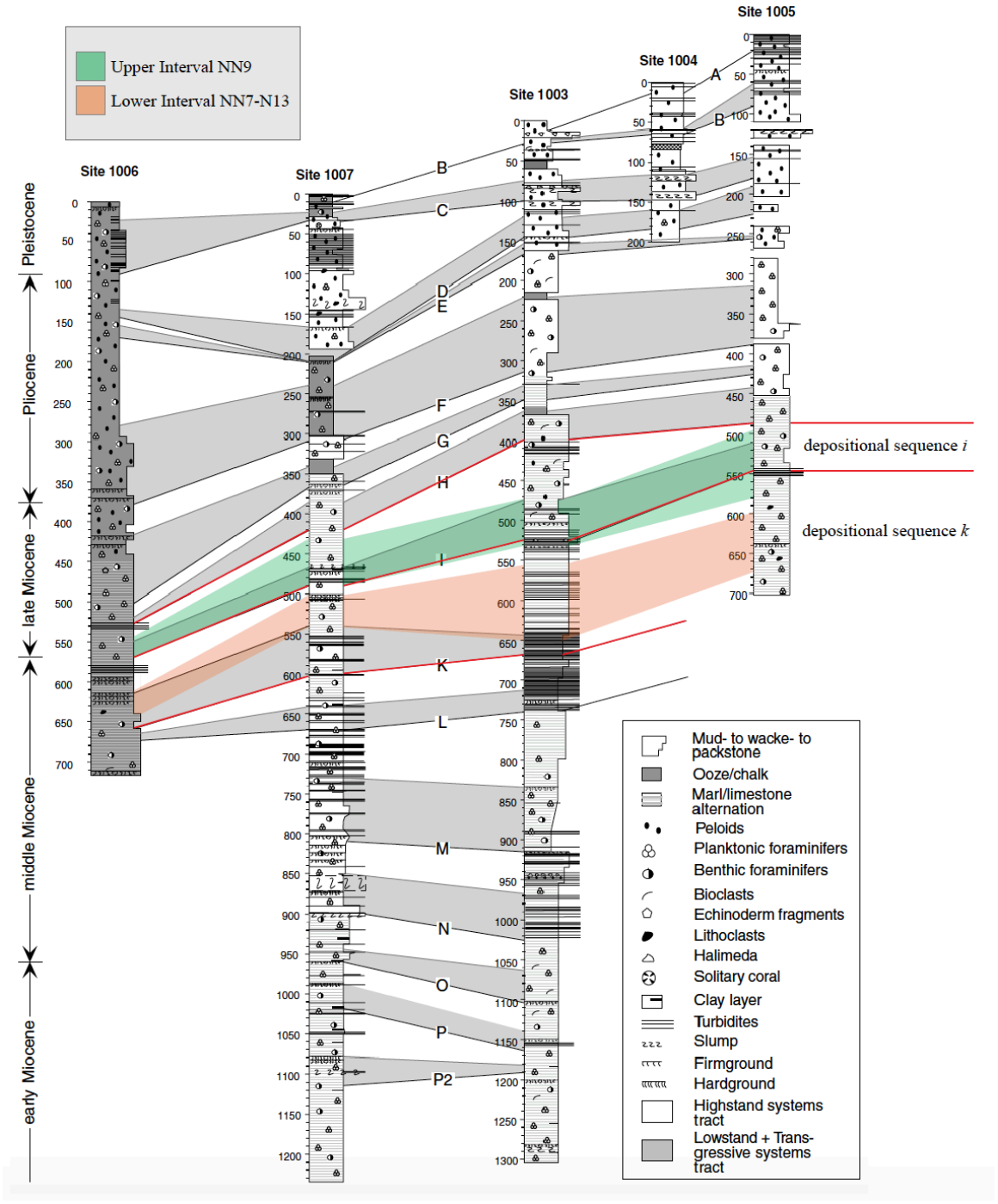
Upper Interval NN9
Lower Interval NN7-N13
Site 1006
Site 1007
Site 1003
Site 1004
Site 1005
A
B
B
C
D
E
F
G
H
I
K
L
M
N
O
P
P2
depositional sequence i
depositional sequence k
Pleistocene
Pliocene
late Miocene
middle Miocene
early Miocene
Mud- to wacke- to packstone
Ooze/chalk
Marl/limestone alternation
Peloids
Planktonic foraminifers
Benthic foraminifers
Bioclasts
Echinoderm fragments
Lithoclasts
Halimeda
Solitary coral
Clay layer
Turbidites
Slump
Firmground
Hardground
Highstand systems tract
Lowstand + Trans-gressive systems tract

Figure 3

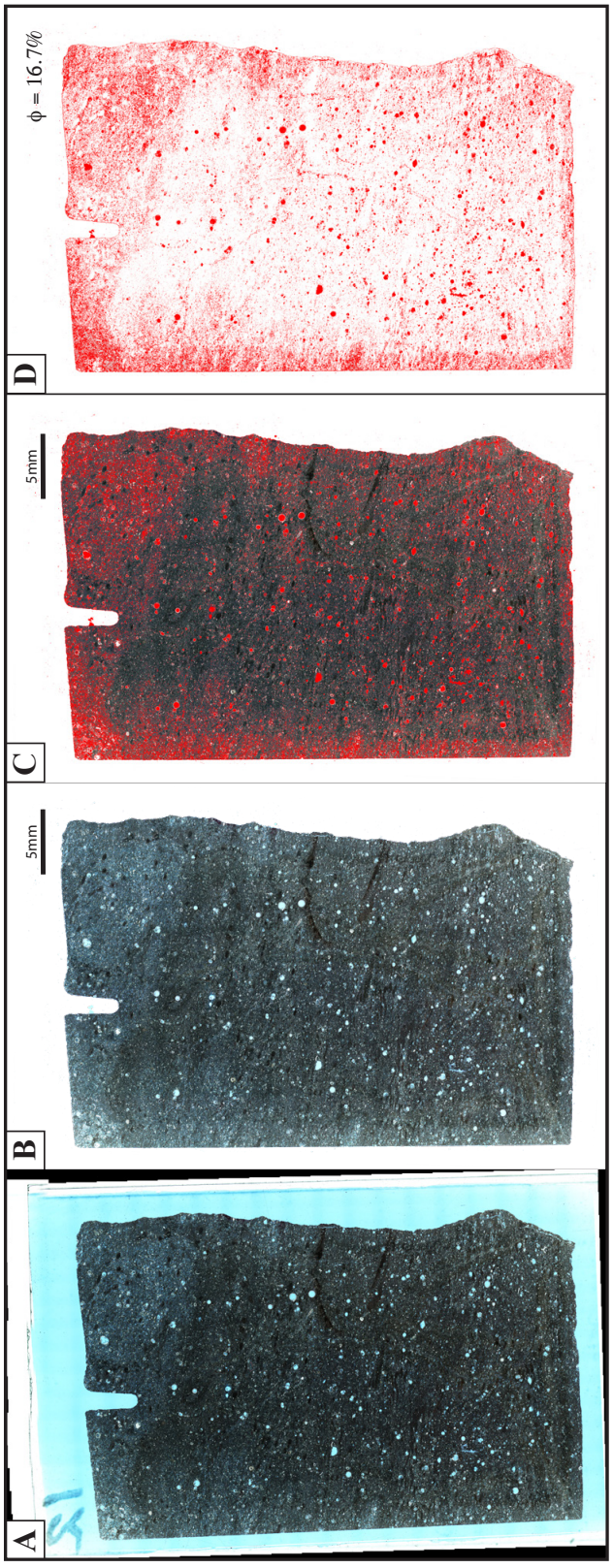

Figure 4

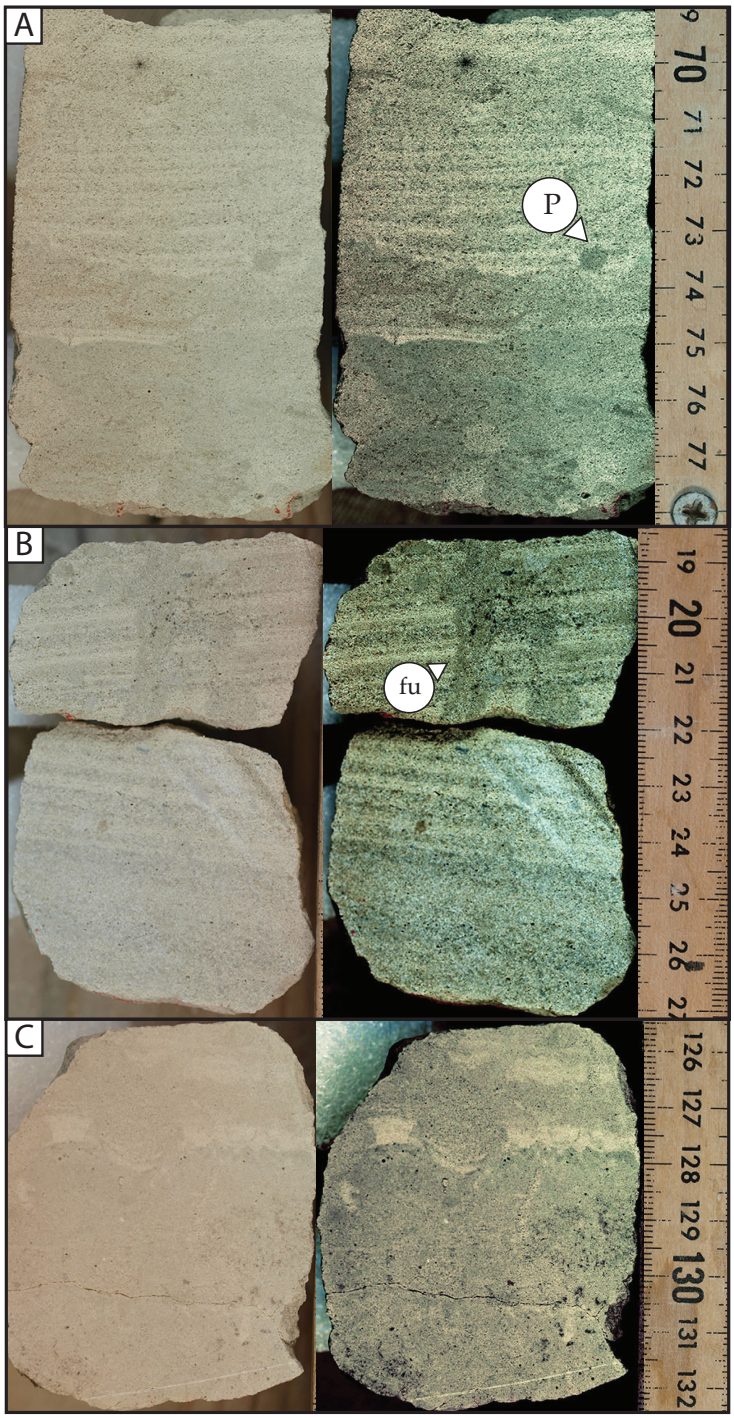

Figure 5

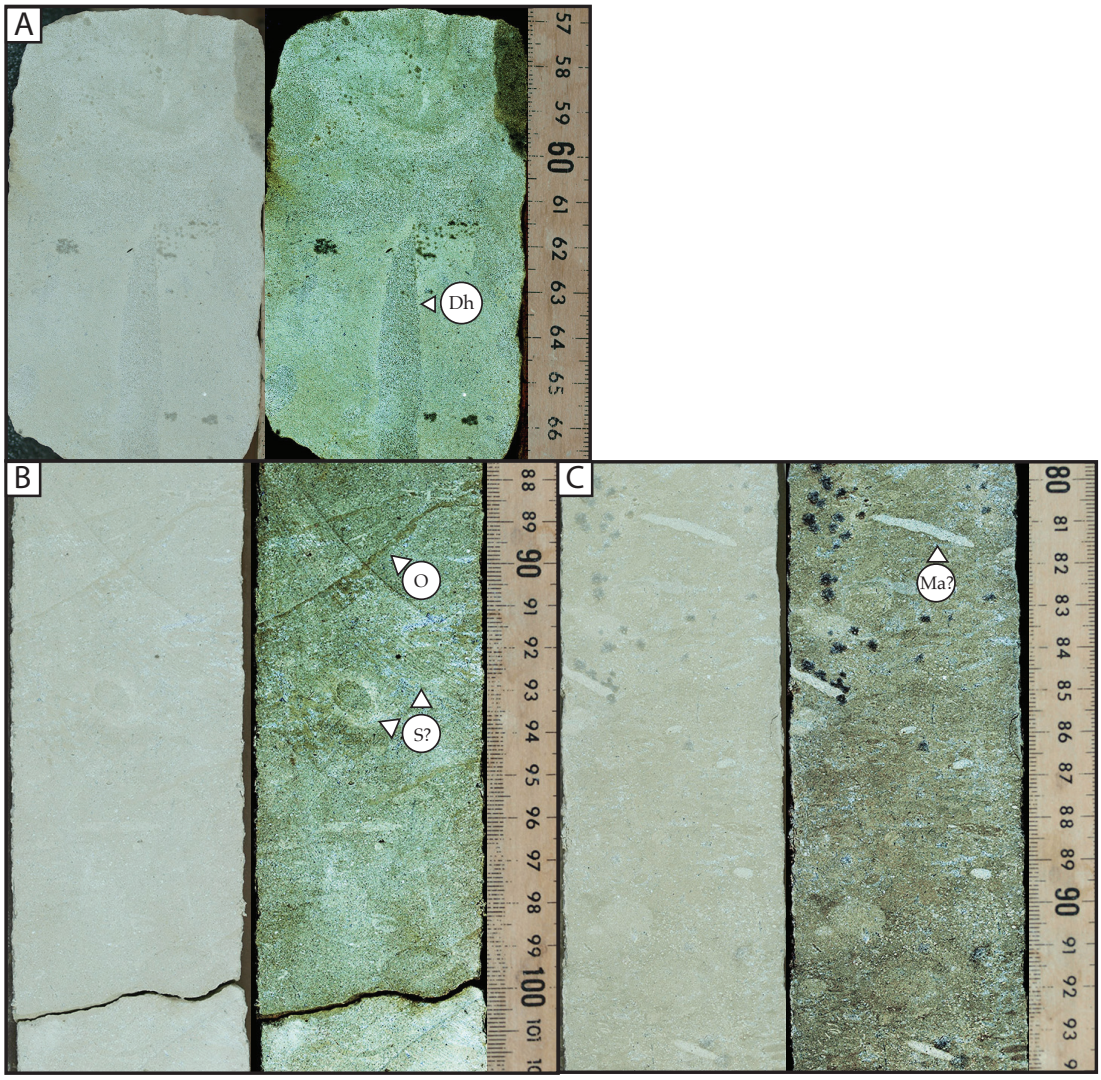

Figure 6

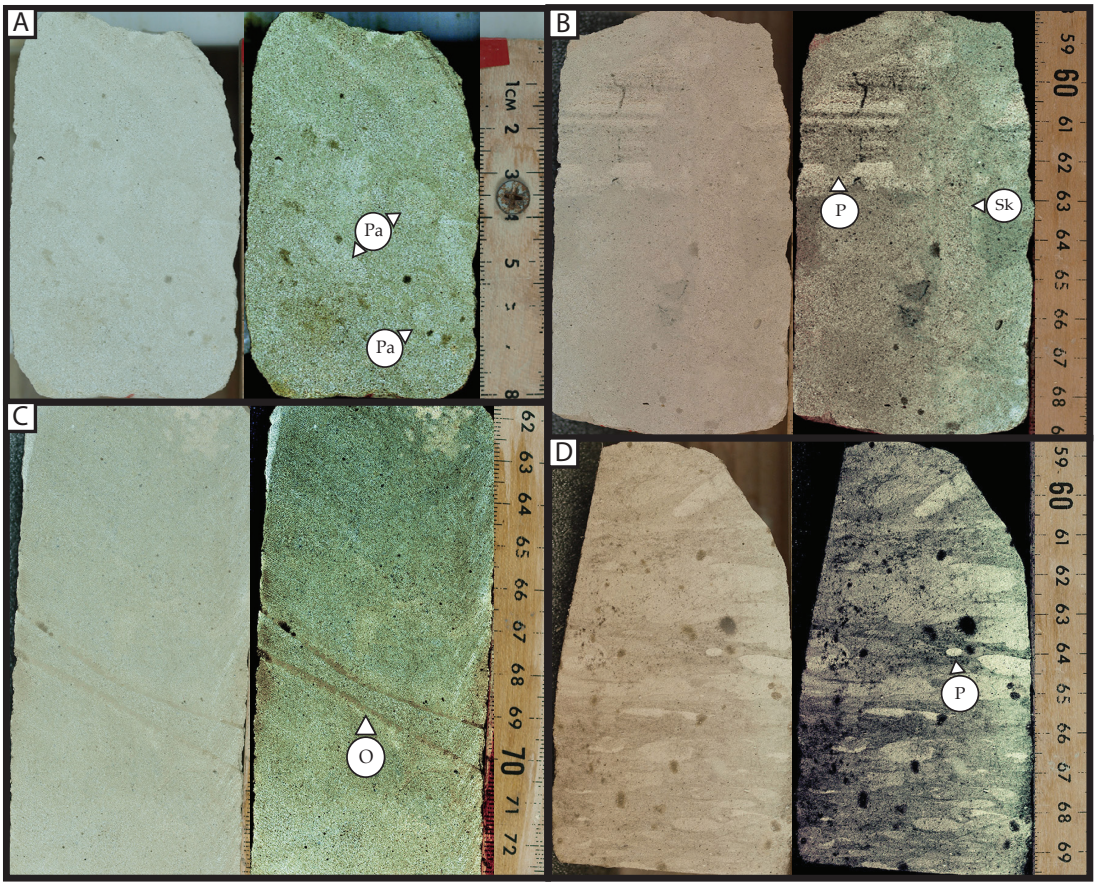

Figure 7

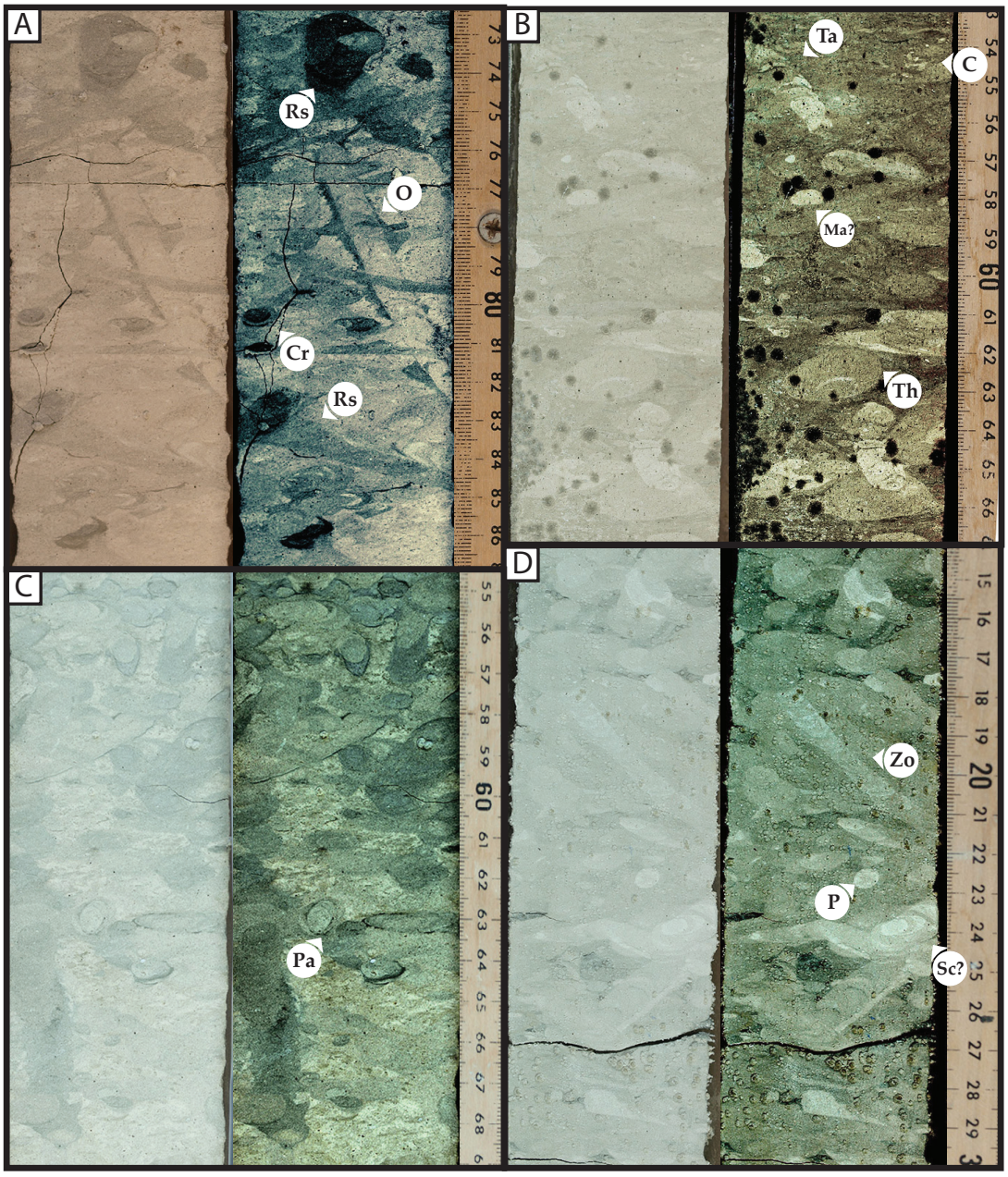

Figure 8

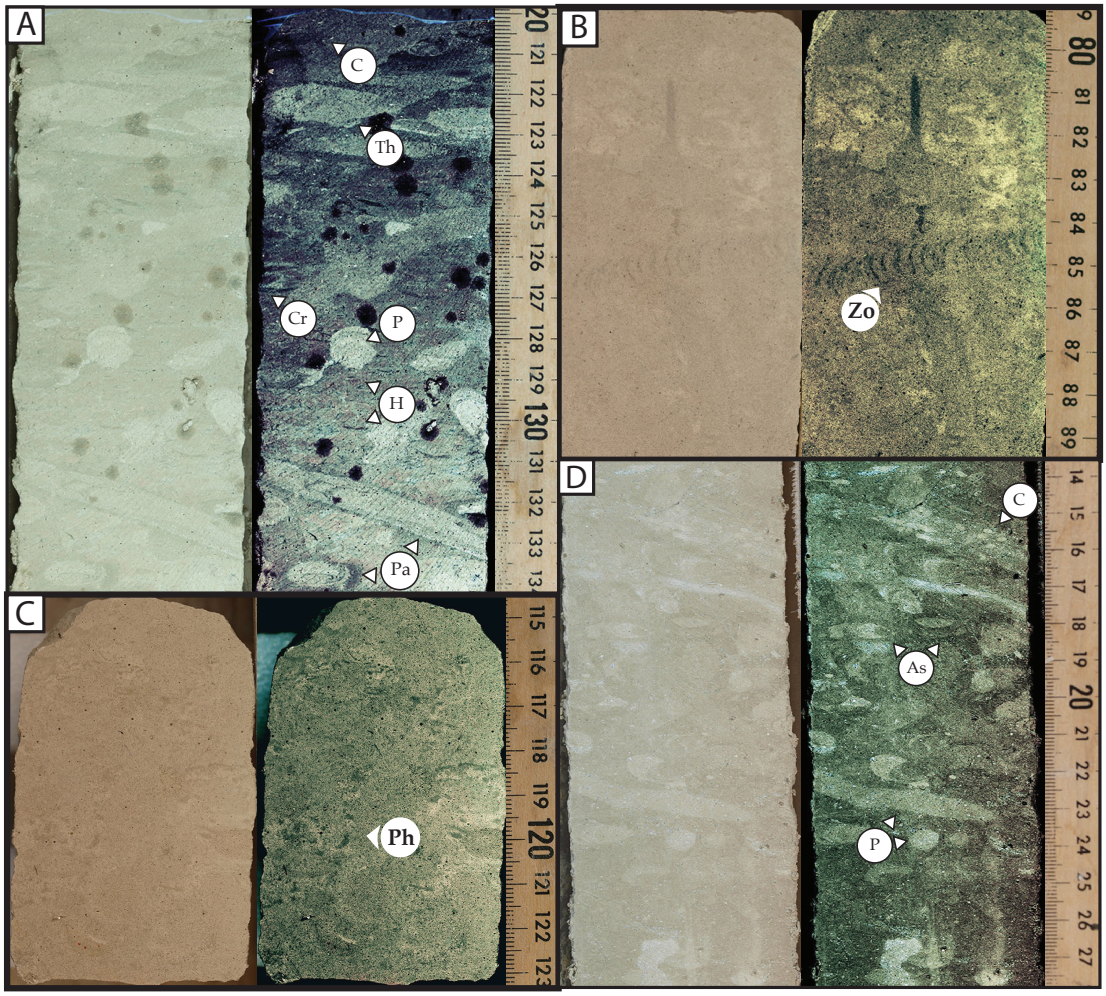

Figure 9

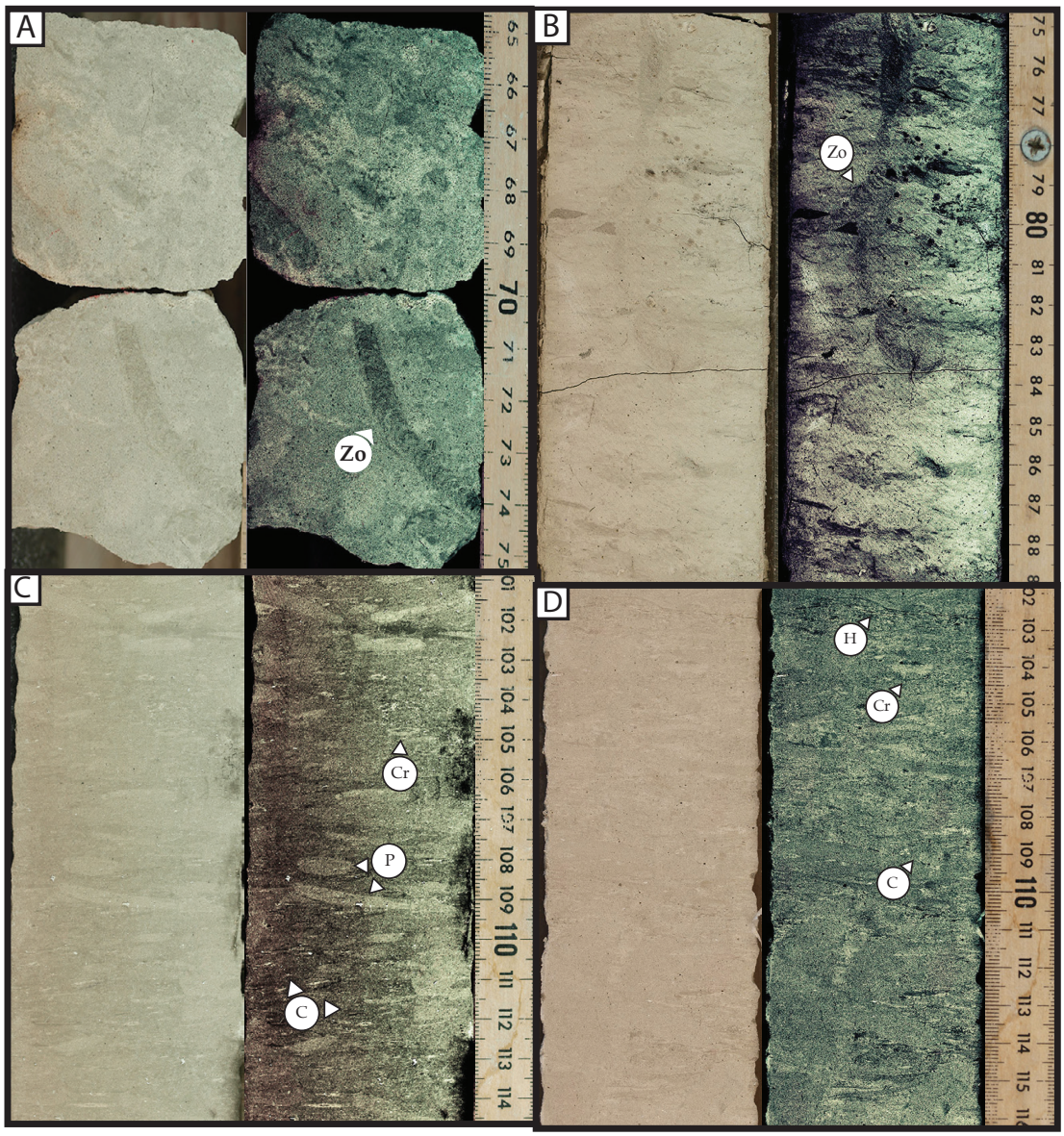

Figure 10

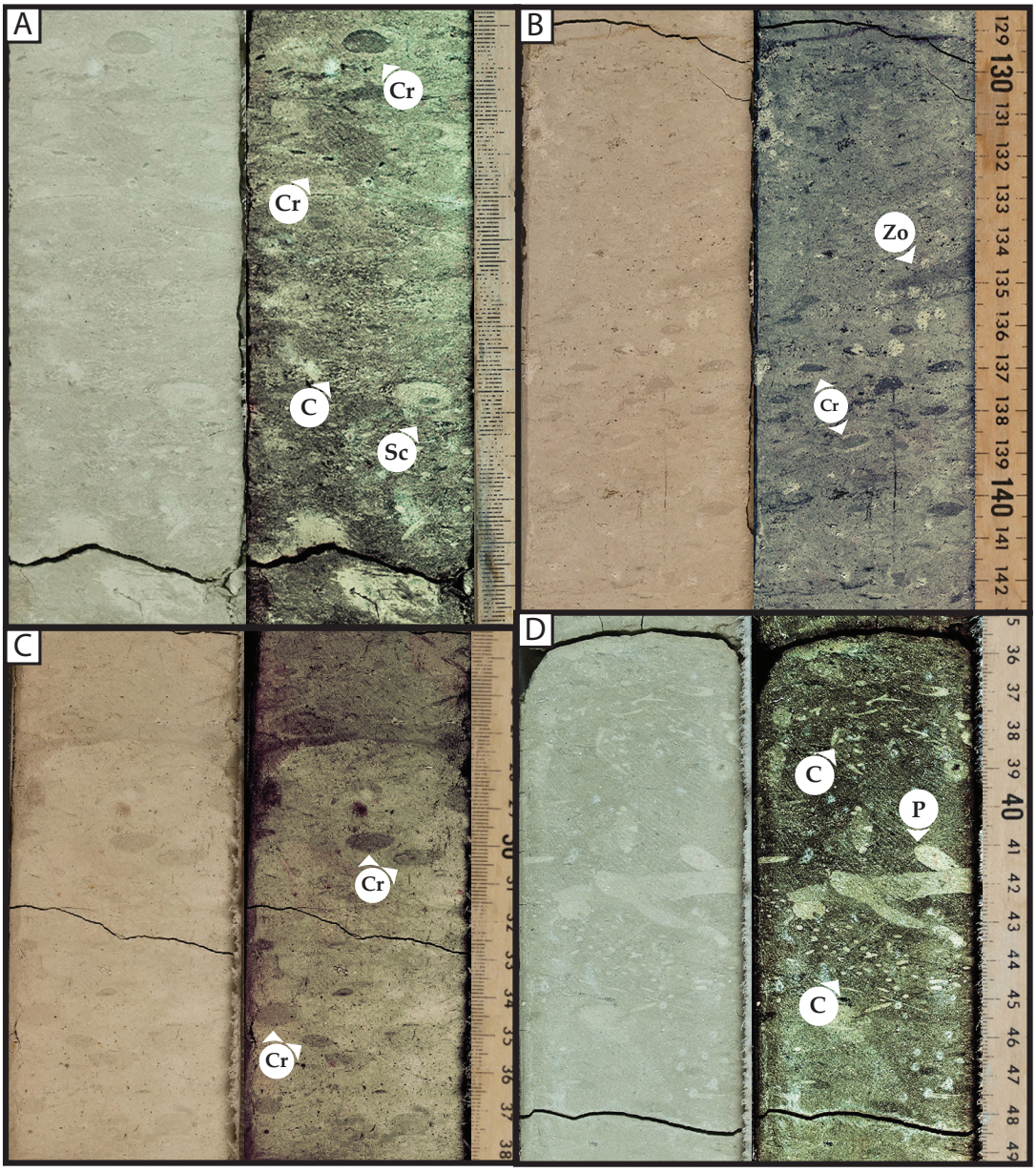

Figure 11

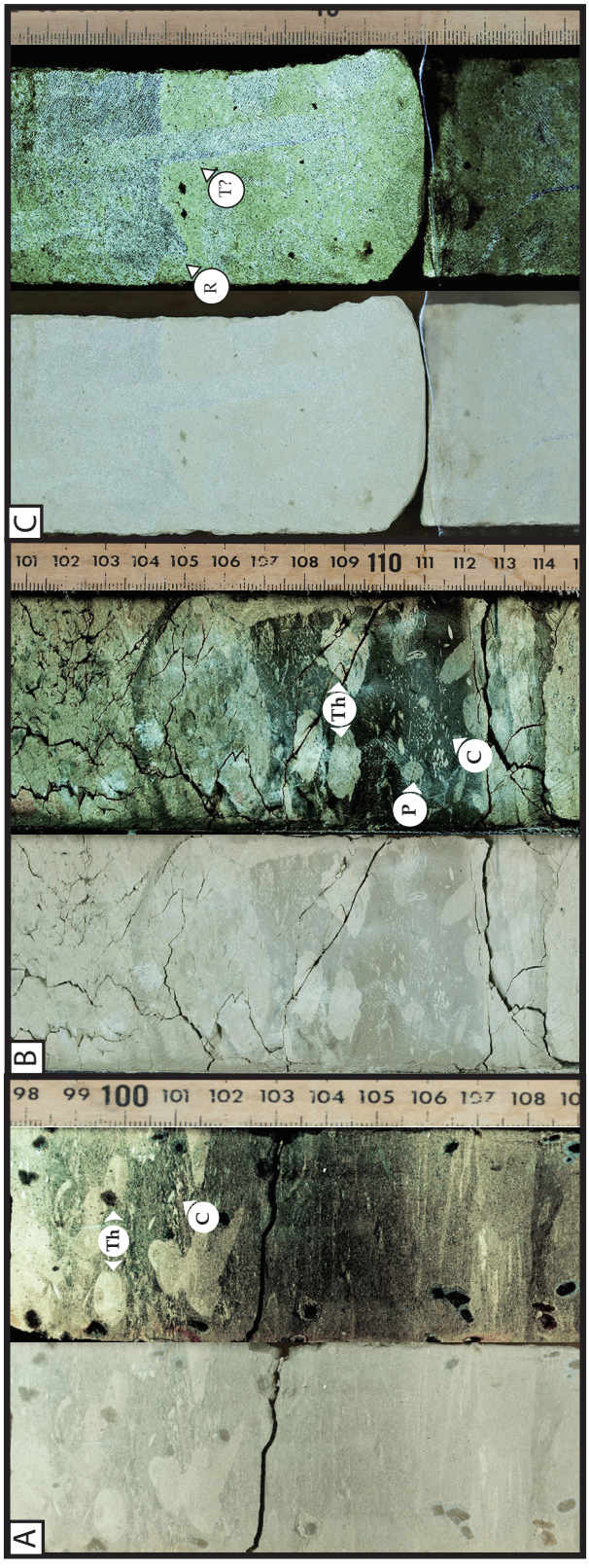
T?
R
C
101 102 103 104 105 106 107 108 109 110 111 112 113 114
Th
C
P
B
98 99 100 101 102 103 104 105 106 107 108
Th
C
A

Figure 12

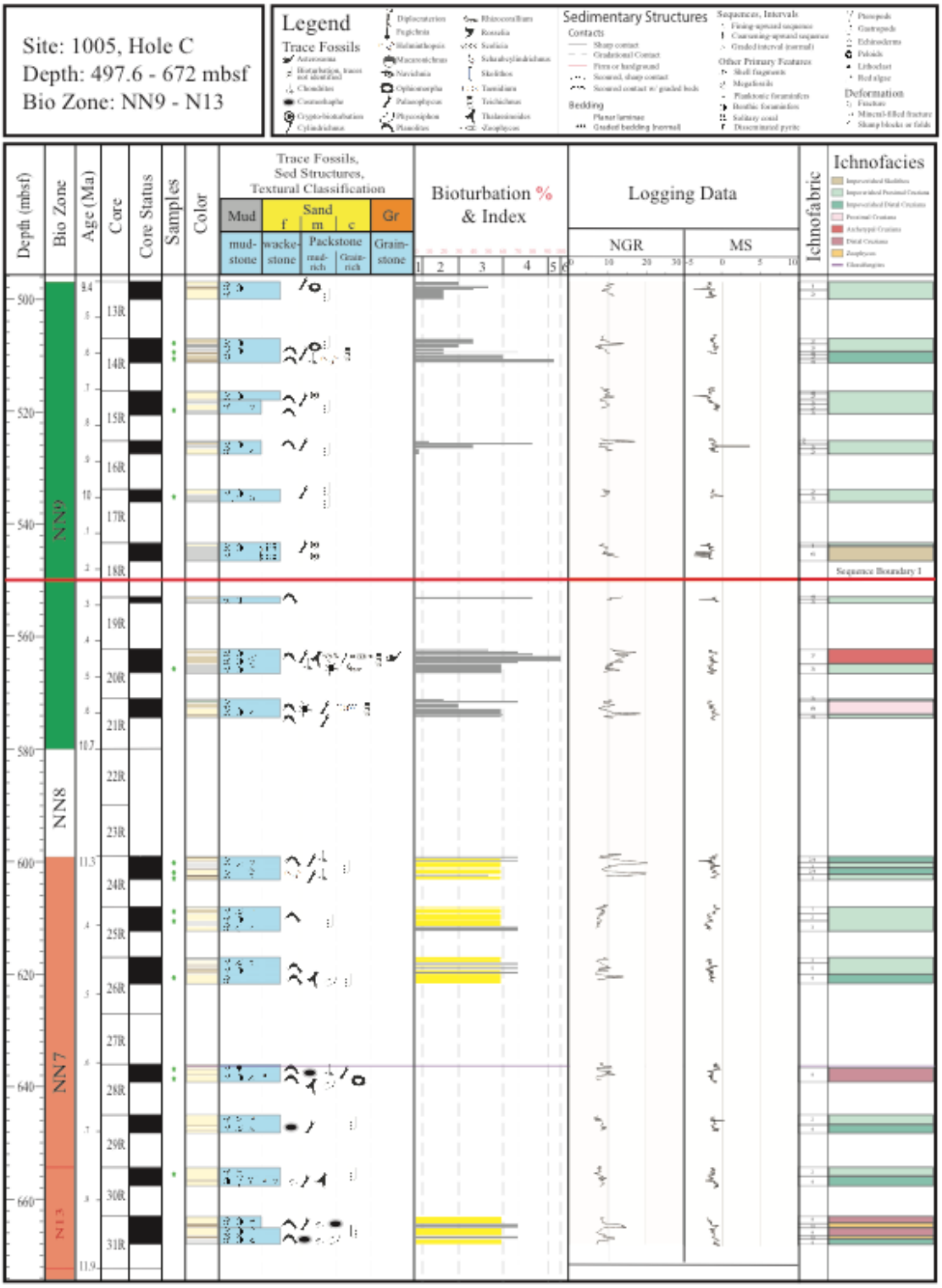
Site: 1005, Hole C
Depth: 497.6 - 672 mbsf
Bio Zone: NN9 - N13
Legend
Trace Fossils
Sedimentary Structures
Contacts
Bedding
Sequences, Intervals
Other Primary Features
Deformation
Depth (mbsf)
Bio Zone
Age (Ma)
Core
Core Status
Samples
Color
Trace Fossils, Sed Structures, Textural Classification
Mud
Sand
Gr
mud-stone
wacke-stone
Packstone
Grain-stone
Bioturbation % & Index
Logging Data
NGR
MS
Ichnofabric
Ichnofacies
NN9
NN8
NN7
N13
Sequence Boundary 1

Figure 13

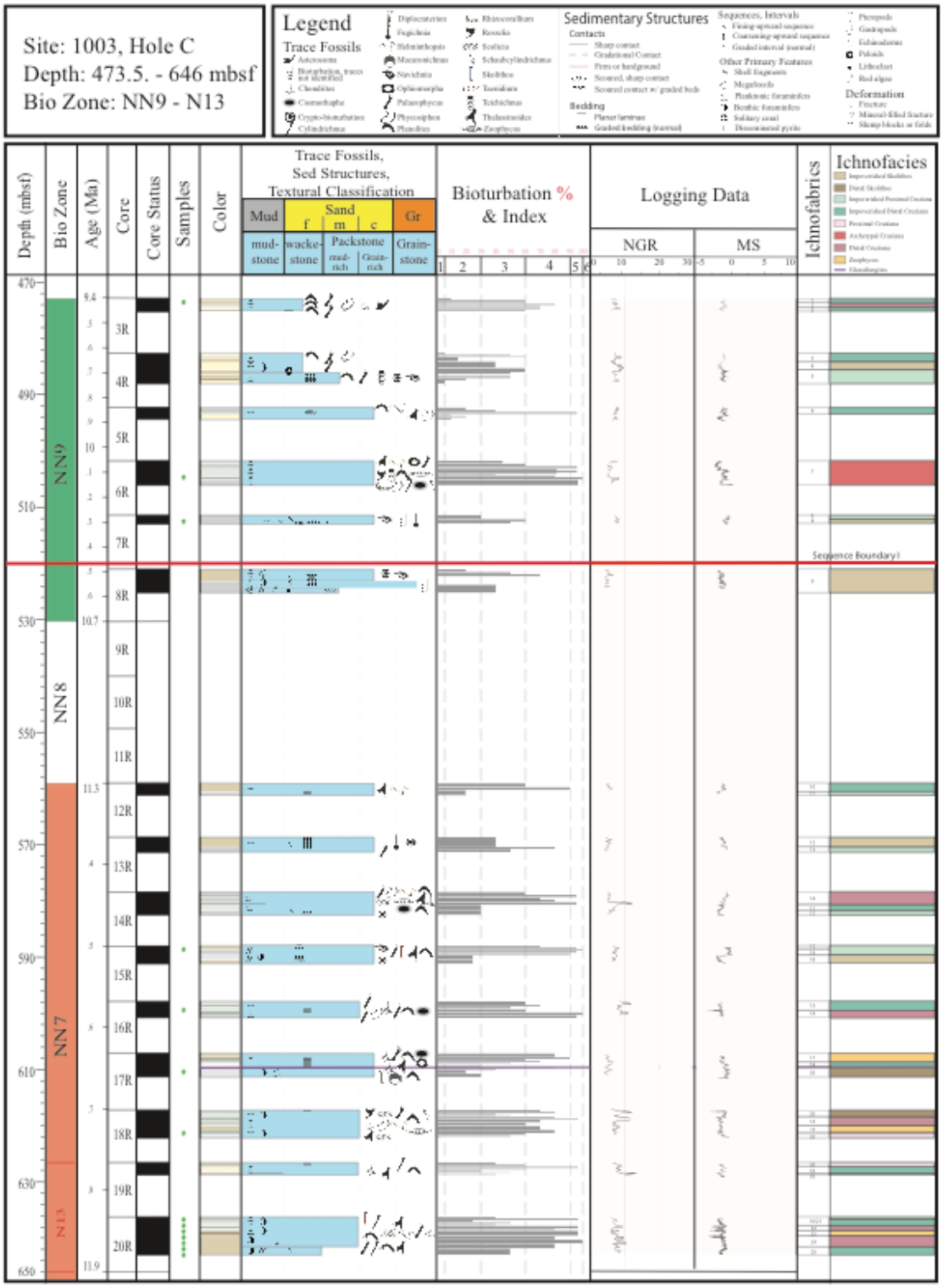
Site: 1003, Hole C
Depth: 473.5. - 646 mbsf
Bio Zone: NN9 - N13
Legend
Trace Fossils
Sedimentary Structures
Depth (mbsf)
Bio Zone
Age (Ma)
Core
Core Status
Samples
Color
Trace Fossils, Sed Structures, Textural Classification
Mud
Sand
Gr
mud-stone
wacke-stone
Packstone
Grain-stone
Bioturbation % & Index
Logging Data
NGR
MS
Ichnofabrics
Ichnofacies
NN9
NN8
NN7
N13
Sequence Boundary I

Figure 14

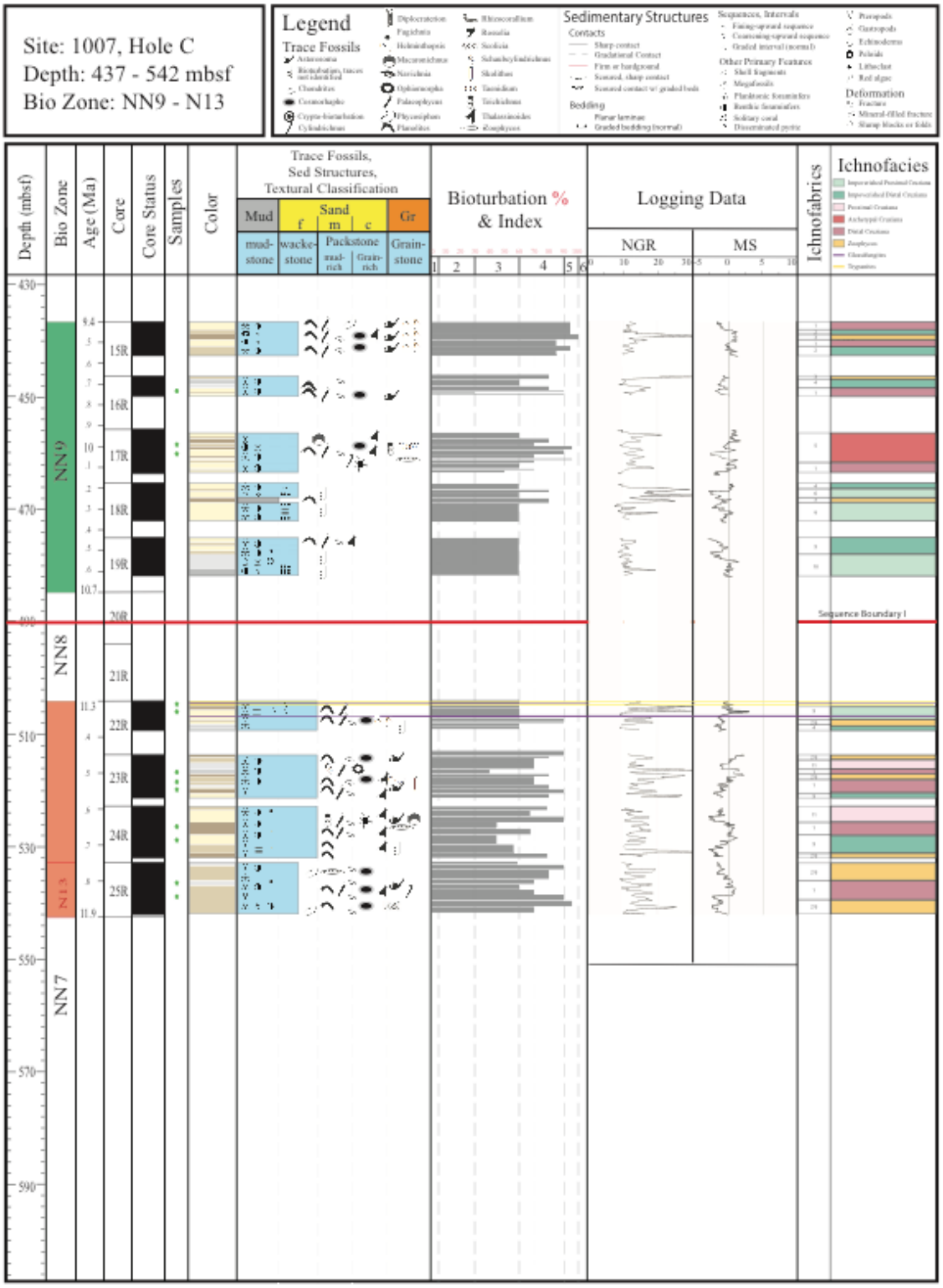
Site: 1007, Hole C
Depth: 437 - 542 mbsf
Bio Zone: NN9 - N13
Legend
Trace Fossils
Sedimentary Structures
Contacts
Bedding
Sequences, Intervals
Other Primary Features
Deformation
Depth (mbsf)
Bio Zone
Age (Ma)
Core
Core Status
Samples
Color
Trace Fossils, Sed Structures, Textural Classification
Mud
Sand
f
m
c
Gr
mud-stone
wacke-stone
Packstone
mud-rich
Grain-rich
Grain-stone
Bioturbation % & Index
Logging Data
NGR
MS
Ichnofabrics
Ichnofacies
NN9
NN8
N13
NN7
15R
16R
17R
18R
19R
20R
21R
22R
23R
24R
25R
Sequence Boundary 1

Figure 15

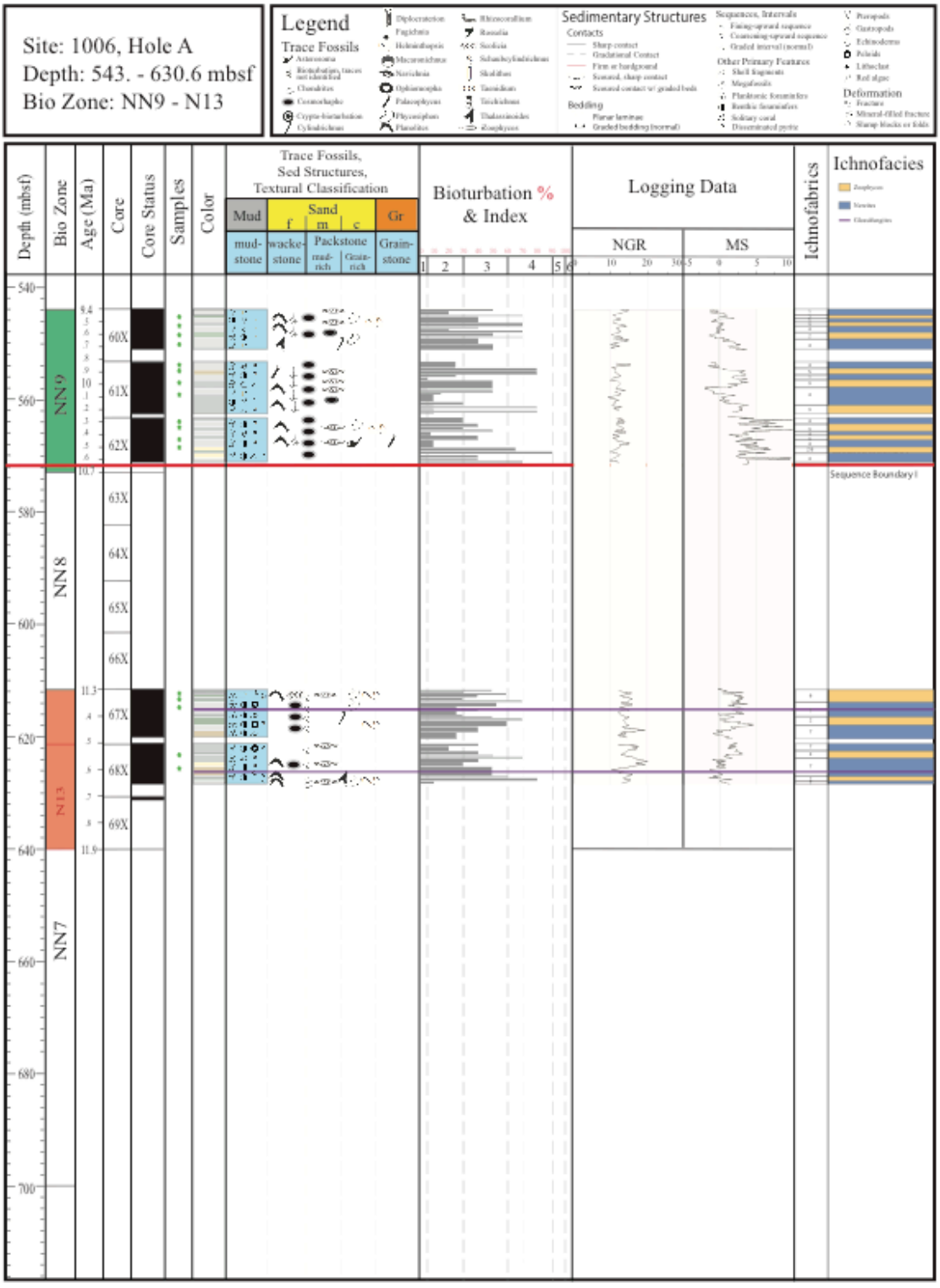
Site: 1006, Hole A
Depth: 543. - 630.6 mbsf
Bio Zone: NN9 - NN13
Legend
Trace Fossils
Sedimentary Structures
Contacts
Bedding
Sequences, Intervals
Other Primary Features
Deformation
Depth (mbsf)
Bio Zone
Age (Ma)
Core
Core Status
Samples
Color
Trace Fossils, Sed Structures, Textural Classification
Mud
Sand
Gr
mud-stone
wacke-stone
Packstone
Grain-stone
Bioturbation % & Index
Logging Data
NGR
MS
Ichnofabrics
Ichnofacies
NN9
NN8
N13
NN7
60X
61X
62X
63X
64X
65X
66X
67X
68X
69X
Sequence Boundary I

Figure 16

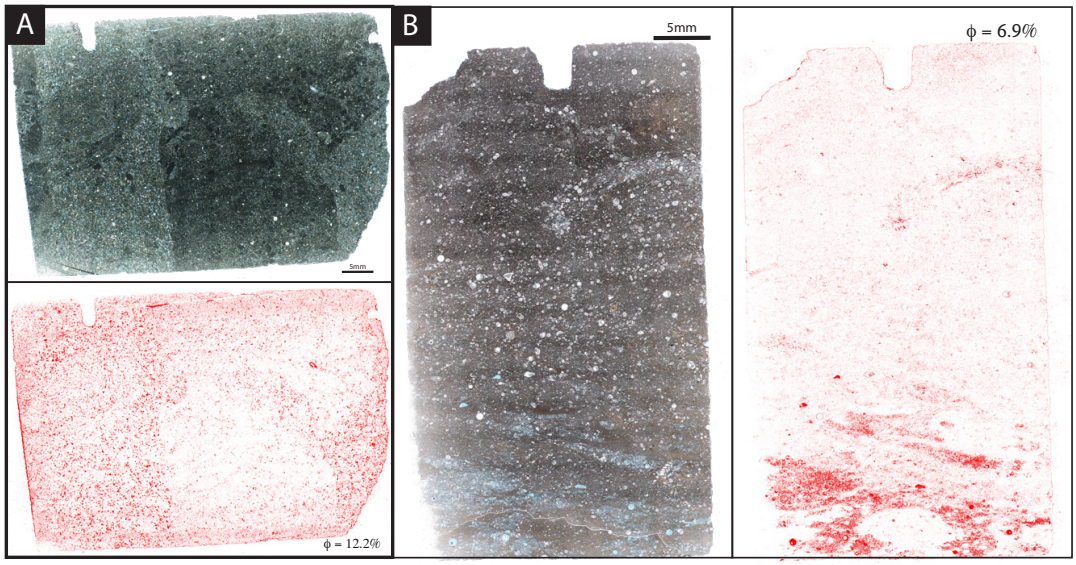

Figure 17

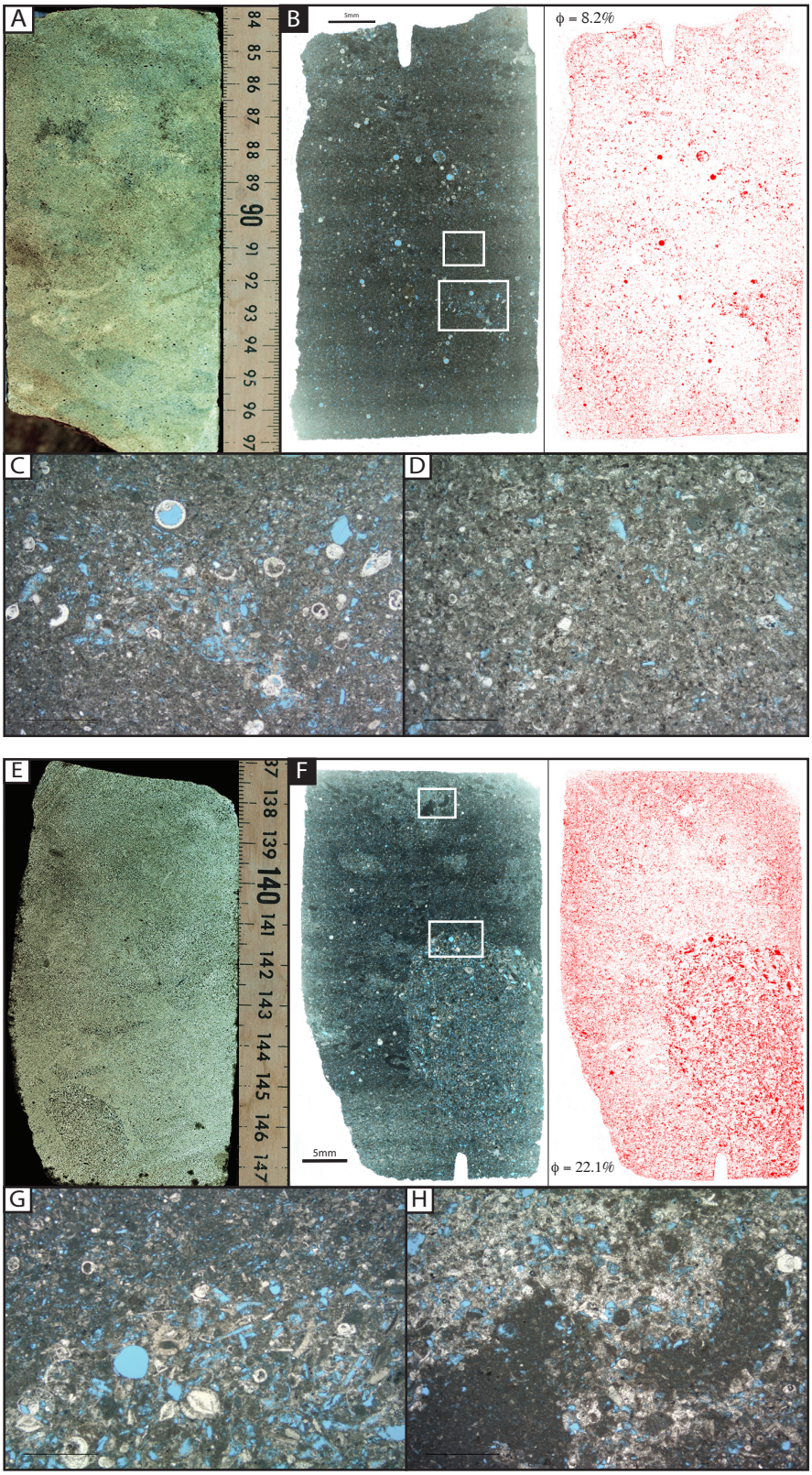

Figure 18

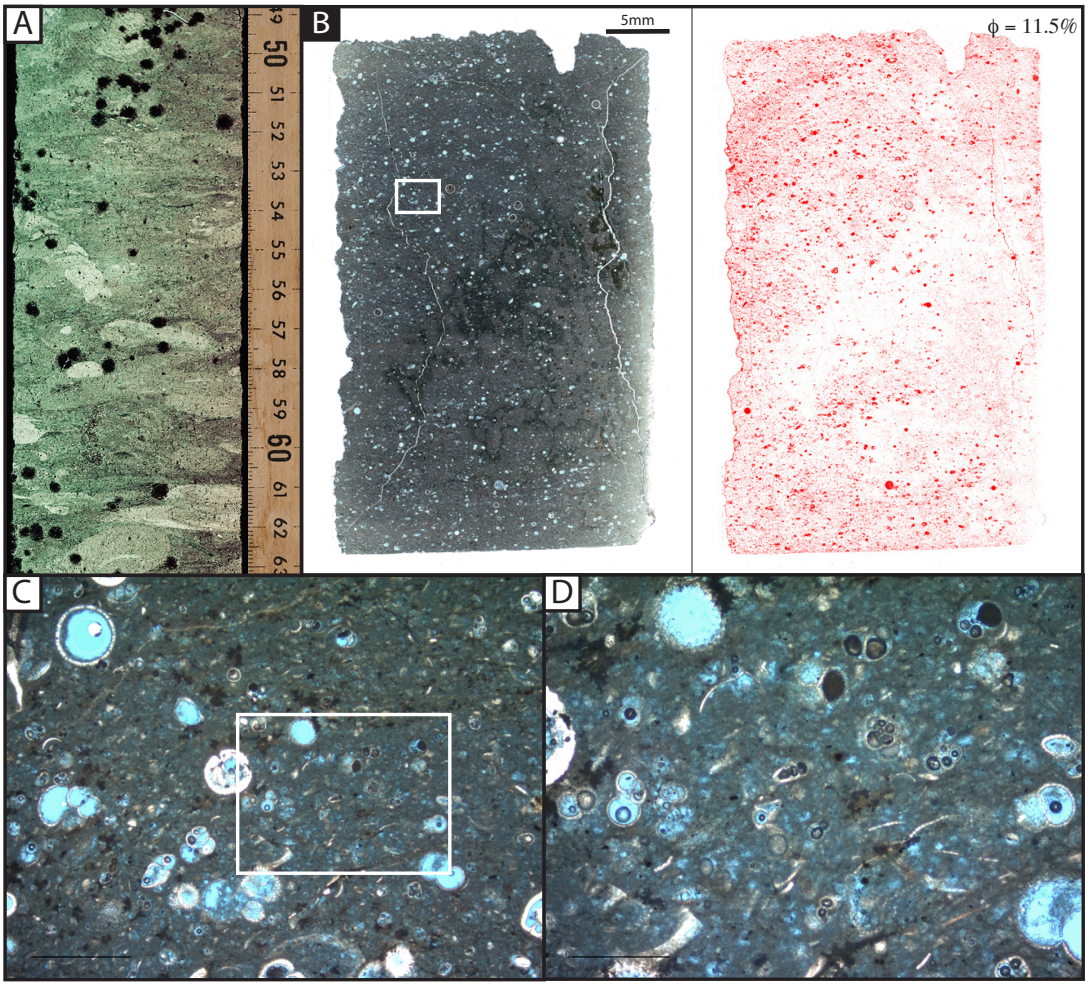

Figure 19

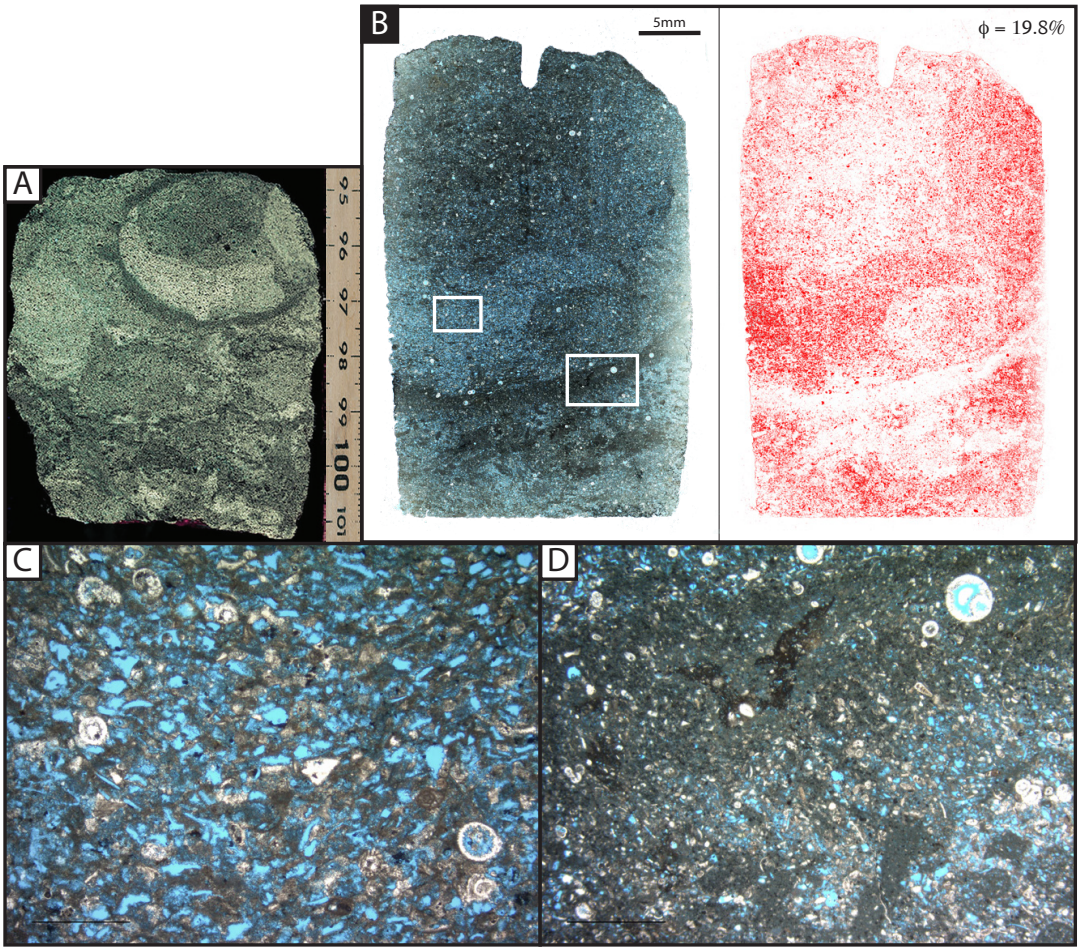

Figure 20

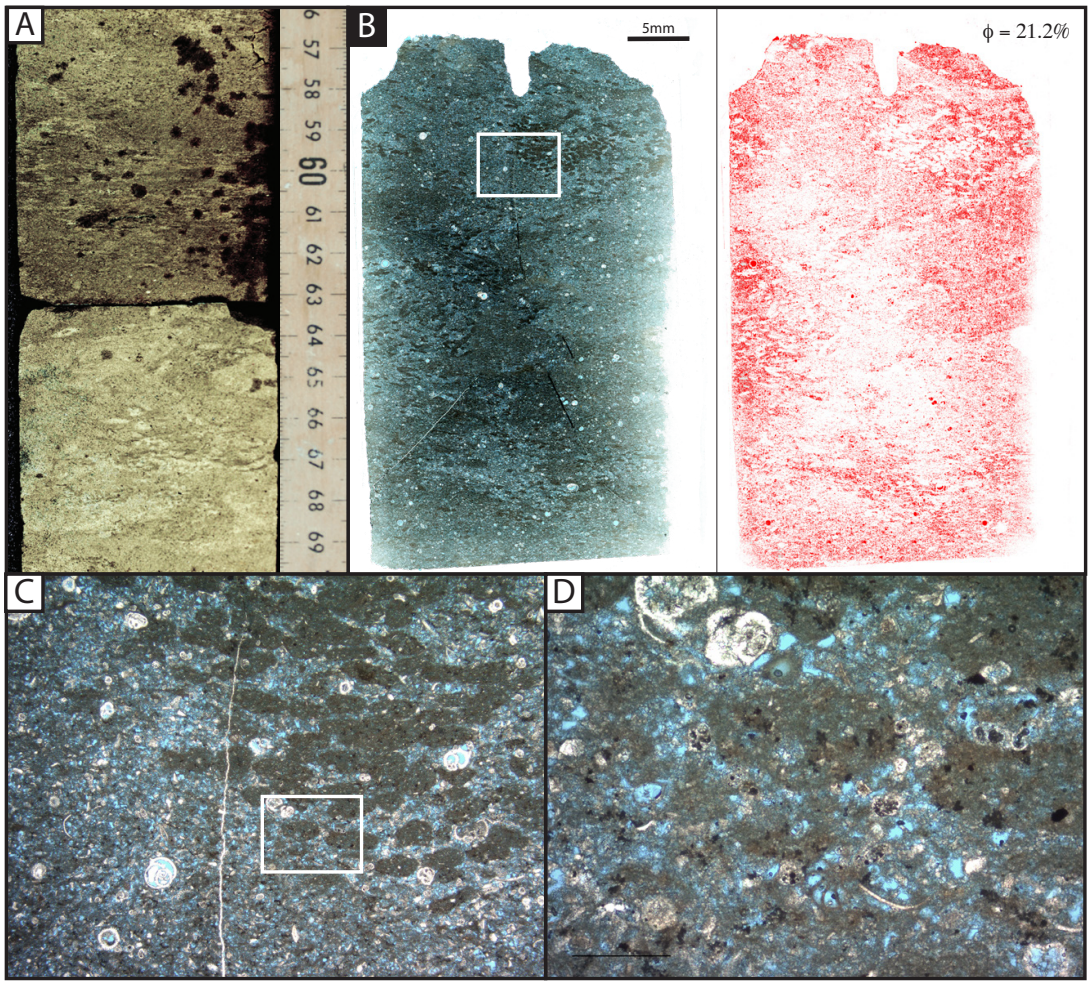

Figure 21

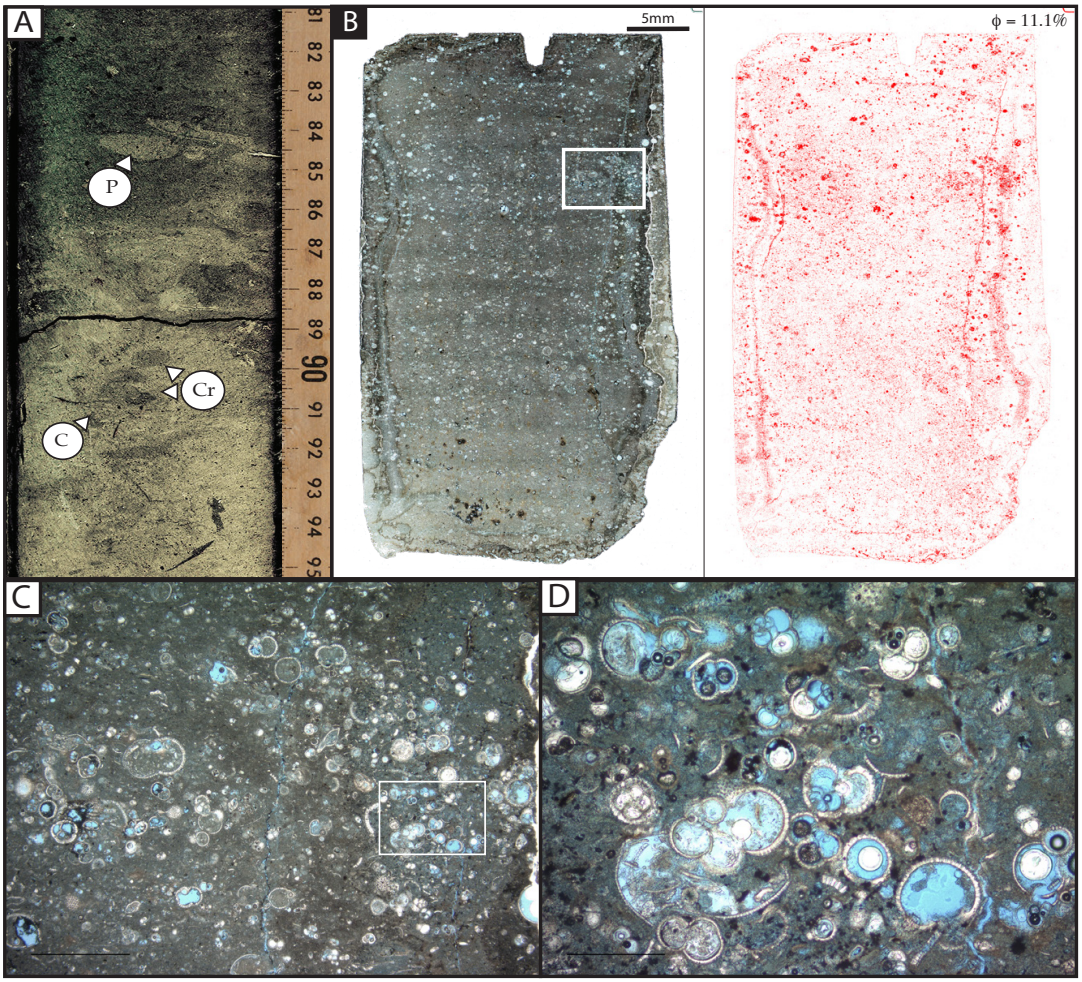

Figure 22

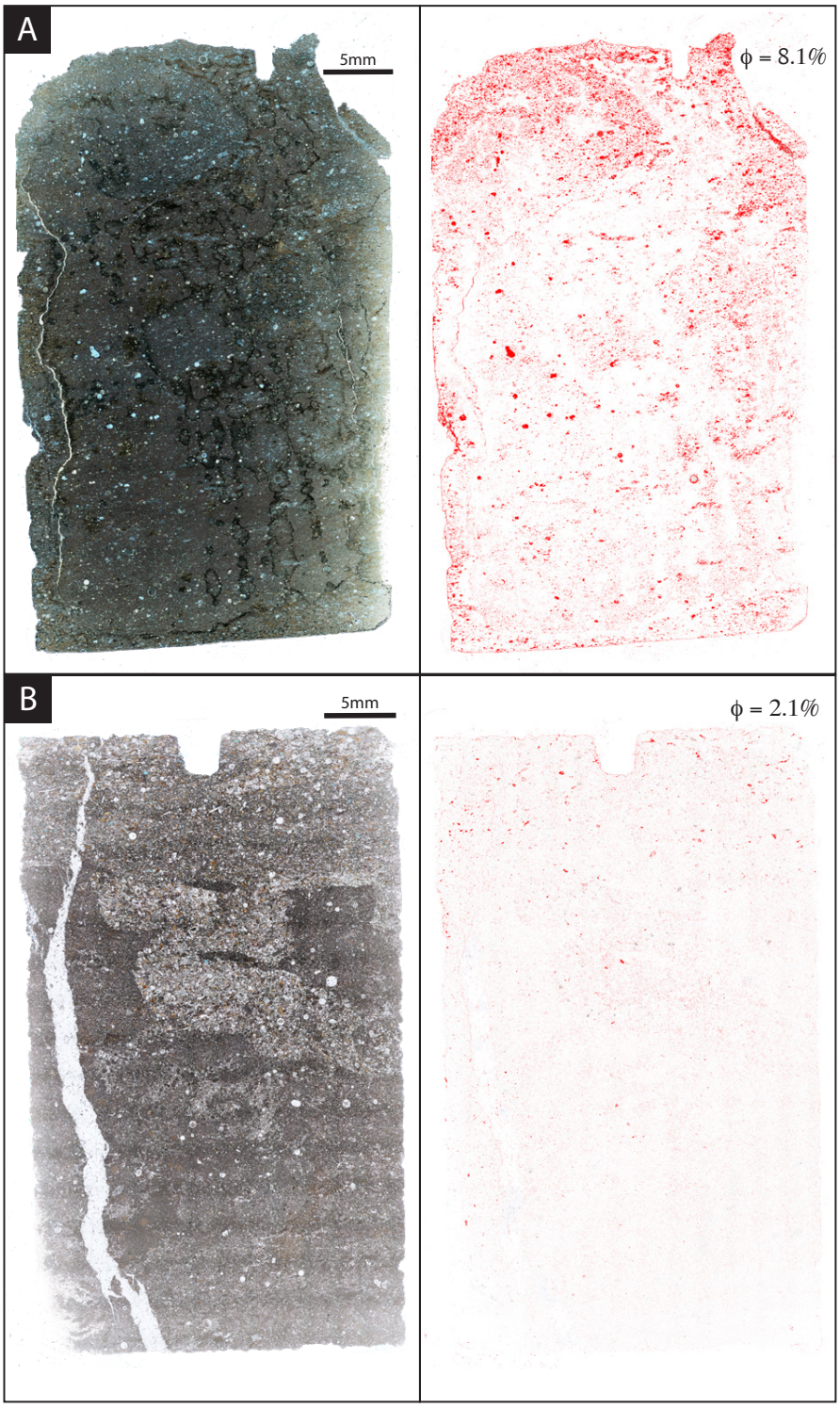

Figure 23

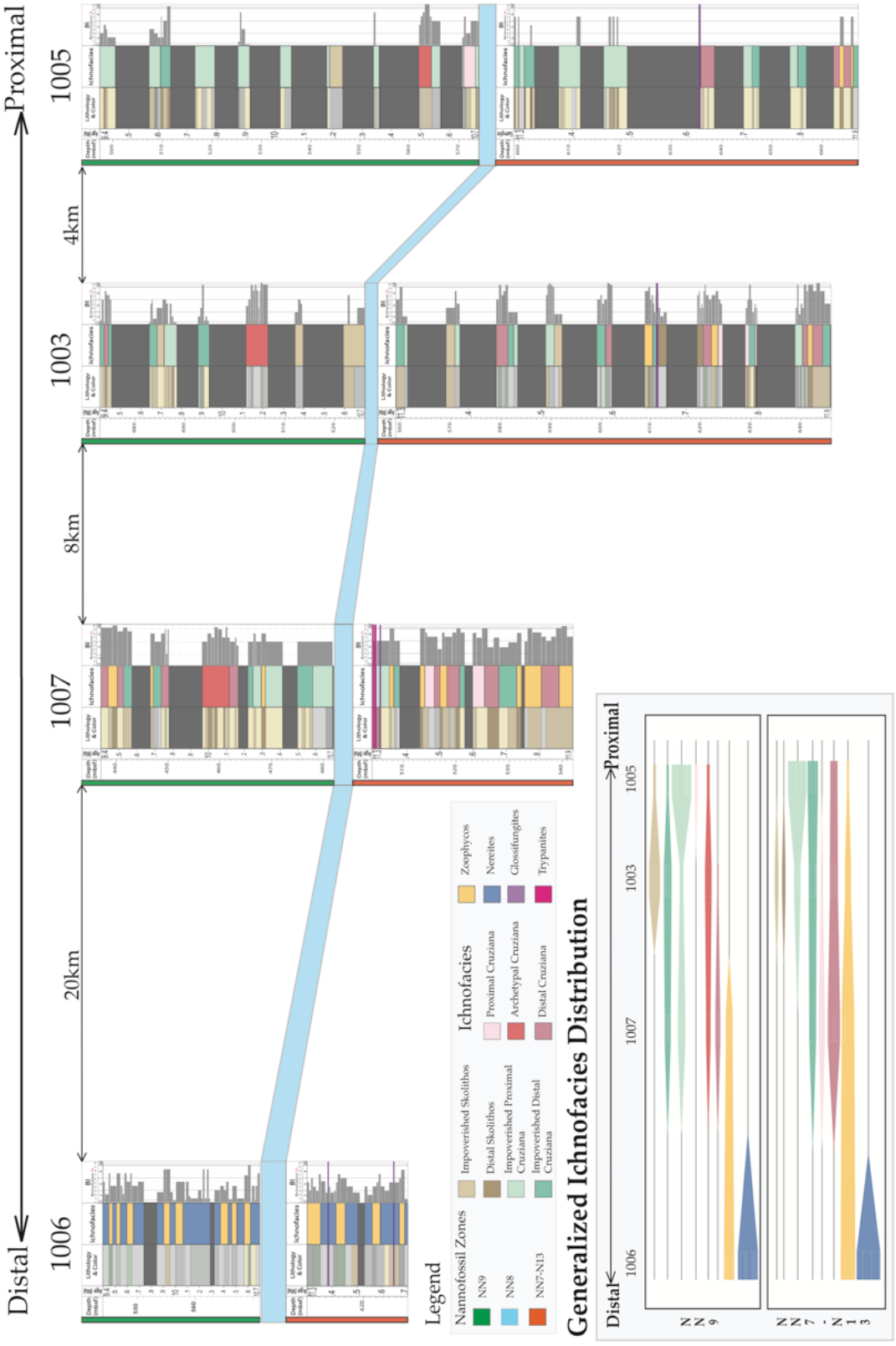
Proximal
Distal
1005
1003
1007
1006
4km
8km
20km
Legend
Nannofossil Zones
NN9
NN8
NN7-N13
Impoverished Skolithos
Distal Skolithos
Impoverished Proximal Cruziana
Impoverished Distal Cruziana
Ichnofacies
Proximal Cruziana
Archetypal Cruziana
Distal Cruziana
Zoophycos
Nereites
Glossifungites
Trypanites
Generalized Ichnofacies Distribution
Distal
Proximal
1006
1007
1003
1005
NN9
NN7-N13

Figure 24

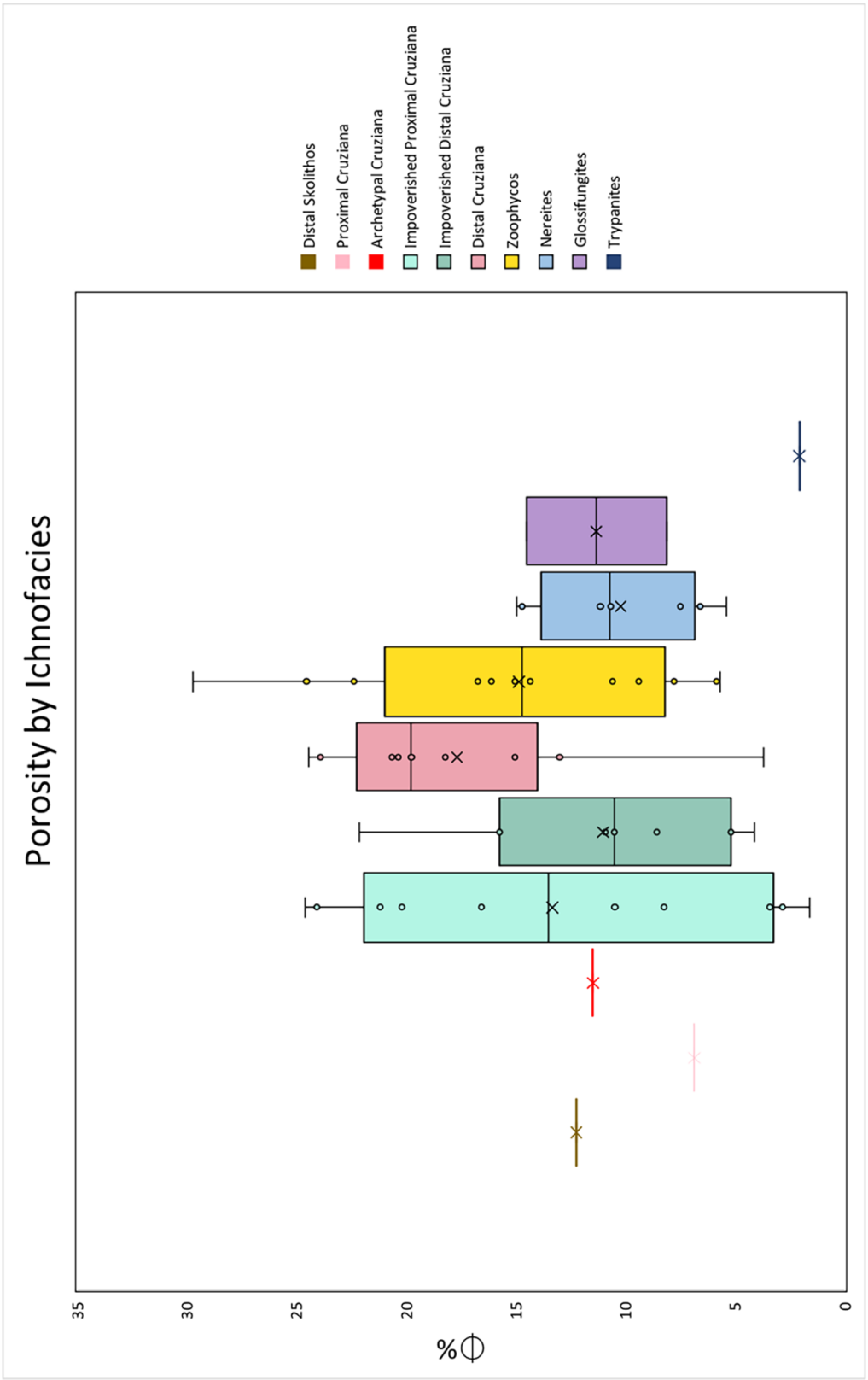
Porosity by Ichnofacies
Distal Skolithos
Proximal Cruziana
Archetypal Cruziana
Impoverished Proximal Cruziana
Impoverished Distal Cruziana
Distal Cruziana
Zoophycos
Nereites
Glossifungites
Trypanites
35
30
25
20
15
10
5
0
%ϕ

Figure 25

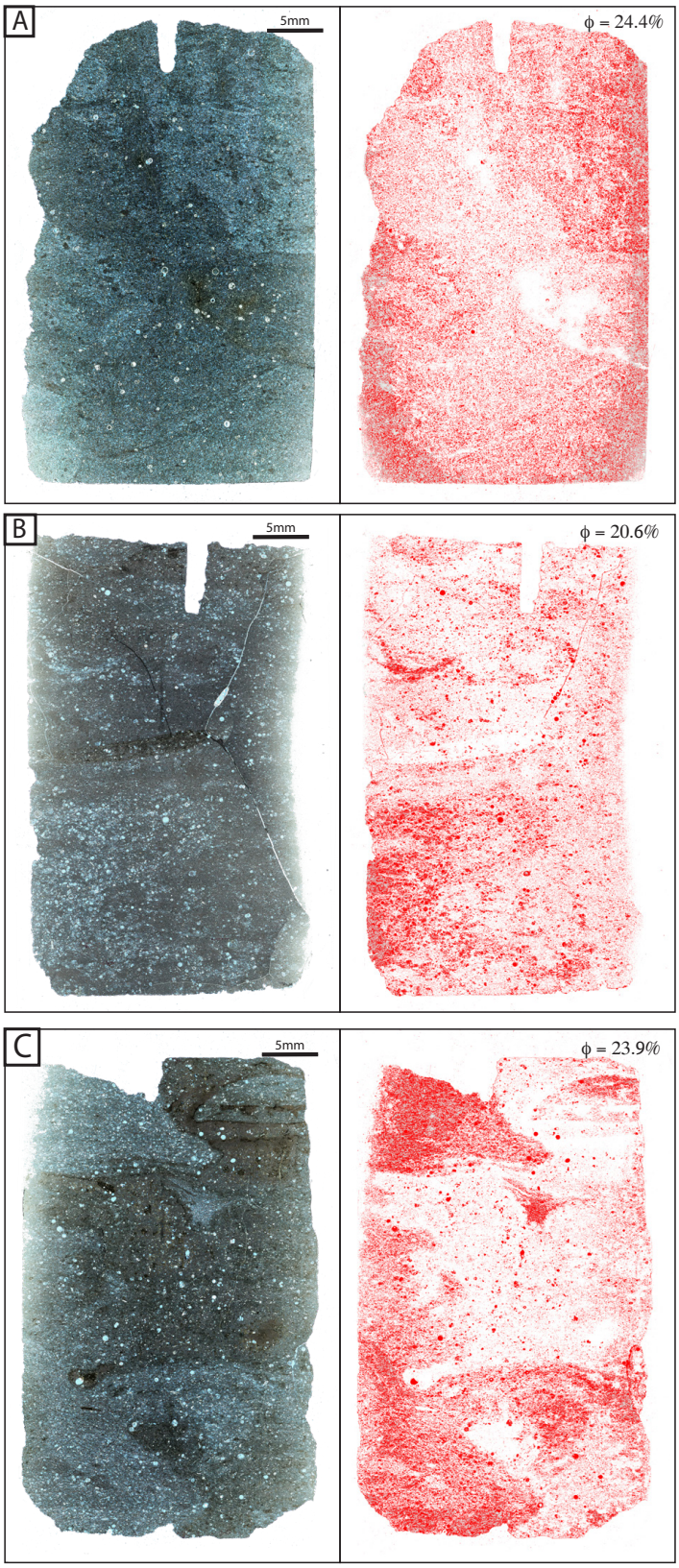

Figure 26

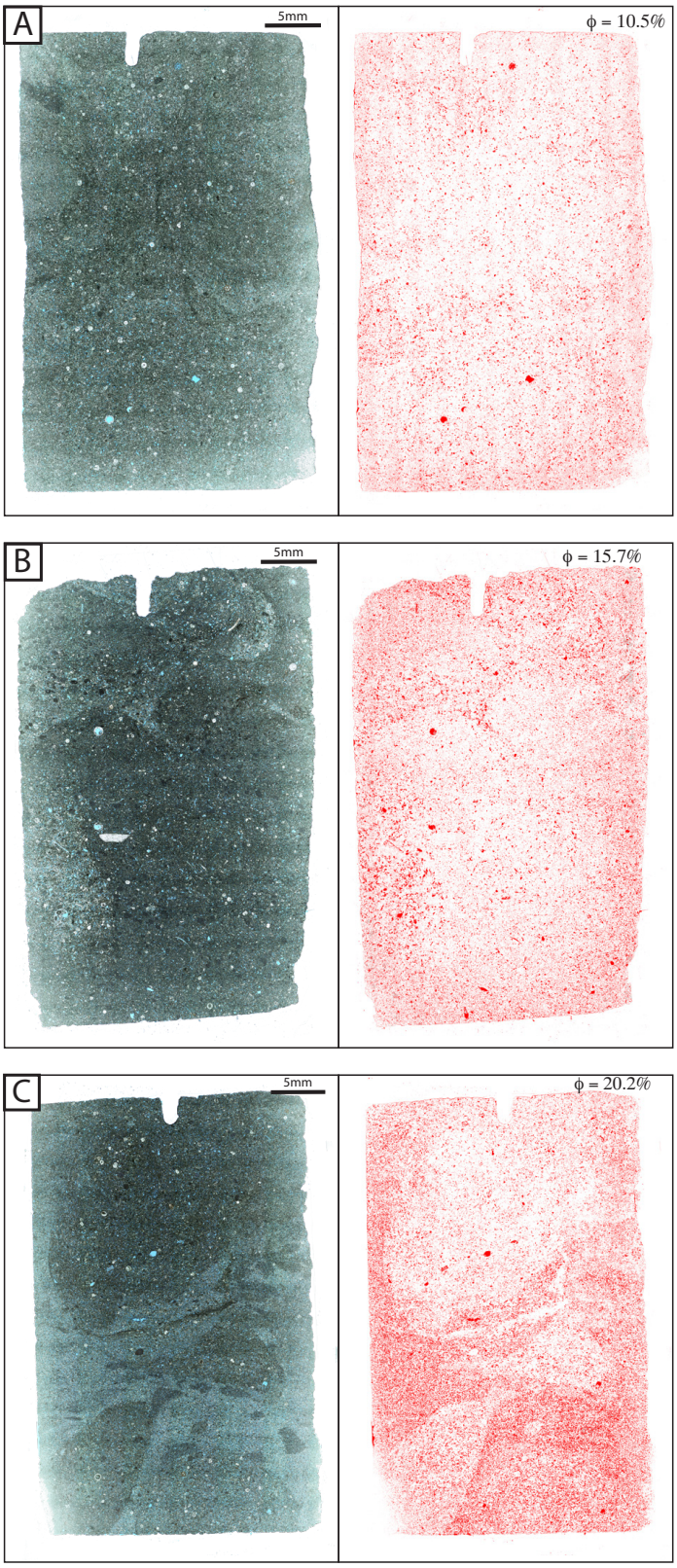

Figure 27

Table 1: Ichnofabric & Ichnofacies

Site	Ichnfabric	Lithology	Color	Sed Structures	Primary Features	Burrow Size	BI & Uniformity of Bioturbation	Ichno genera	Ethologies	Ichnodiversity	Colonization	Colonization Window	Substrate	Tiering	Comments	Sedimentation Rate	Ichnofacies Association	Interpretation
1003	1	Foraminifer Wackestone	Light beige - beige	N/A	Pf	mm-scale common, cm-scale rare	3,4	Planolites, Palaeophycus	Shallow deposit feeding, passive carnivore	Low	Opportunistic-Equilibrium	Moderate-long	Soup-soft	Shallow-middle	Color mottling overprinted by few discrete traces of facies crossers. Impoverished shallow-tier deposit feeding community overprinted by passive carnivore community	Moderate-Low, less stable	Impoverished Proximal Cruziana	Predominantly aggrading background sedimentation from supernormal to semi-dewith potential pulses of redeposited sediment. Also characteristic of salinity stress.
	2	Foraminifer wackestone	Beige to dark beige	N/A	Pf, bf	mm-scale abundant, cm-scale subordinate	4, pervasive	Planolites, Chondrites, Asterosoma, Phycosiphon	Shallow & deep deposit feeding, Systematic feeding	Moderate	Equilibrium	Long	Loose-stiff	Shallow-middle	Impoverished shallow-tier deposit feeding community overprinted by systematic & deep deposit feeding community	Low, stable	Distal Cruziana	Environmental Stability
	3	Foraminifer wackestone	Light beige - beige	Planar laminae	Pf	cm-scale common, mm-scale subordinate	3,4	Planolites, Palaeophycus	Shallow deposit feeding, passive carnivore	Low	Opportunistic-Equilibrium	Moderate	Soup-soft	Shallow-middle	Color mottling overprinted by few discrete traces of facies crossers. Impoverished shallow-tier deposit feeding community overprinted by passive carnivore community	Low-Moderate, stabalizing	Impoverished Proximal Cuatana	Aggrading background sedimentation. Also characteristic of salinity stress.
	4	Mud-rich foraminifer packstone	Brown to gray	Graded bedding (normal), Planar laminae at base	Pf, Bf, Es, P	cm-scale abundant	1-4, sporadic	Planolites, Palaeophycus, Teichichnus, Crypto-bioturbation, Navichnia	Shallow deposit feeding, passive carnivore, up-and-down, locomation under interface	Low-Moderate	Opportunistic	Short	Loose	Shallow	Post event suite	High, variable	Impoverished Skolithos	Episodic deposition
	6	Grain-rich Foraminifer Packstone	Dark gray - brownish gray	Scoured contact a base	Pf	mm-scale abundant, cm-scale common	4-5, pervasive	Planolites, Phycosiphon, Helminthopsis, Thalassinoides	Shallow deposit feeding, systematic Feeding, grazing	Low-Moderate	Equilibrium	Moderate	Loose-stiff	Shallow-middle	Pre-event resident suite	Moderate-Low, less stable	Impoverished Distal Cruziana	Increasing sedimentation rate & hydraulic energy
	7	Grain-rich Bioclastic Grainstone	light grey, dark gray, olive gray	Gradational contacts	Pf	cm-scale abundant, mm-scale abundant	5-6, pervasive	Chondrites, Cosmorhaphe, Cylindrichnus, Helminthopsis, Ophiomorpha Palaeophycus, Phycosiphon, Planolites, Rhizocorallium, Rosselia, Thalassinoides, Zoophycus, Schaubcylindrichnus, Teichichnus	Shallow & deep deposit feeding, living, stabilizing, filter feeding, passive carnivore, interface feeding, systematic feeding, grazing, up-and-down	High	Climax Community	Long	Loose-Cohesive-Stiff	Complex	High infaunal biomass, abundant food resources	Low-Moderate, stable	Archetypal Cruziana	Environmental Stability
	8	Grain-rich Bioclastic Grainstone	Light gray	Scoured contacts with graded beds, fining upward sequences, grade bedding (normal)	Pf	mm-scale common, cm-scale rare	1-5, sporadic	Fugichnia, Navichnia	Fugichnia, Navichnia	Low	Opportunistic	Short	Loose	Shallow	Abundant scoured contacts indicative of erosive turbidite deposition	High, variable	Impoverished skolithos	Pulse of erosive turbidite deposition
	9	Bioclastic Packstone-Grainstone	Light gray - light olive brown	Graded bedding (normal), Planar laminae, Scoured contacts with graded beds, Fining-upward sequences	Pf, Bf, Ga, L, M	mm-scale	1-4, sporadic	Navichnia, Fugichnia, Crypto-bioturbation	Navichnia, locomation under interface	Low	Opportunistic	Short	Loose	Shallow	Only indication of abundant shallow water components within turbidites	High, variable	Impoverished skolithos	Pulse of turbidite deposition
	10	Bioclastic Packstone-Grainstone	Light brown-ish gray	N/A	Pf	mm-scale common, cm-scale subordinate	4-5, pervasive	Helminthopsis, Thalassinoides	Grazing, Living	Low-Moderate	Equilibrium-Opportunistic	Moderate-long	Loose-stiff	Shallow-middle	Impoverished shallow-tier grazers overprinted by middle-tier domichnia	Low, stable	Impoverished Distal Cruziana	Impoverished community in environmentally stable conditions
	11	Bioclastic Packstone-Grainstone	Light gray	Planar laminae	Pf	cm-scale	N/A	N/A	Sediment swimming	Low	Opportunistic	Moderate	Soup-loose	Shallow	Mantle & swirl bioturbational structures / color mottling	Low-moderate, stabilizing	Impoverished	Recovery after pulse of turbidite deposition. Consistently soupy sediment still disturbed by turbid conditions
	12	Bioclastic Packstone-Grainstone	Light brown-ish gray	Graded bedding (normal), Planar laminae, Fining upward sequence	Pf	N/A	1-4, sporadic	Fugichnia, Cryptobioturbation, Navichnia	Escape, locomation under interface	Low	Opportunistic	Short	Loose	Shallow	Post event suite showing strongest evidence of escape	High, variable	Impoverished skolithos	Episodic deposition
	13	Bioclastic Packstone-Grainstone	Light gray	N/A	Pf	mm & cm scale common	3-4, even	Paleophycus	Passive carnivore	Low	Equilibrium-Opportunistic	Moderate-short	Loose	Shallow-middle	Color mottling overprinted with few discrete trace of facies crossers. Opportunistic shallow-tier deposit feeding community overprinted by passive carnivore community	Moderate-Low, less stable	Impoverished Proximal Cruziana	Increasing sedimentation rate & hydraulic energy. Also characteristic of salinity stress.
	14	Bioclastic Packstone-Grainstone	light gray, dark gray, olive gray	Gradational contacts	Pf	mm-scale abundant, cm-scale common	4-5, pervasive	Chondrites, Cosmorhaphe, Helminthopsis, Palaeophycus, Phycosiphon, Planolites, Thalassinoides, Zoophycus	Shallow & deep deposit feeding, systematic feeding, passive carnivore, grazing	Moderate-High	Equilibrium-Climax	Long	Loose-Cohesive-Stiff	Shallow-middle-deep	Very high infaunal biomass, dissolved oxygen high enough to support large animals at the seafloor, abundant food resources	Low, stable	Distal Cruziana	Environmental Stability
	15	Bioclastic Packstone-Grainstone	Brown-ish gray - light gray	Planar laminae	Pf, Bf	cm-scale common, mm-scale subordinate	5, pervasive	Navichnia, Skolithos, Planolites, Palaeophycus, Thalassinoides	Filter-feeding, passive carnivore	Low-Moderate	Opportunistic	Moderate	Soup-loose	Shallow-middle	Color mottling overprinted with few discrete traces. Opportunistic colonizers in between sedimentation events.	Moderate-Low, stabilizing	Proximal Cruziana	Recovery after turbidite deposition
	16	Bioclastic Packstone-Grainstone	Light gray	Graded bedding (normal), Planar laminae, Scoured contact with grade d beds	Pf, Bf	mm-scale	1-5 sporadic	Navichnia, Cryptobioturbation	Sediment swimming	Low	Opportunistic	Short	Soup-loose	Shallow	Post event suite after turbidite deposition	High, variable	Impoverished Skolithos	Episodic deposition, erosive at base
	17	Bioclastic Packstone-Grainstone	Gray - olive gray	N/A	Pf	mm & cm scale common	5-6, pervasive	Planolites, Paleophycus, Chondrites, Cosmorhaphe, Phycosiphon	Shallow & deep deposit feeding, passive carnivore, systematic feeding	Moderate	Equilibrium-Climax	Long	Loose-Cohesive-Stiff	Shallow-middle-deep	Shallow-tier grazers overprinted by middle-tier domiciles, overprinted by complex deposit feeders	Low, stable	Zoophycos	Environmental Stability
	18	Bioclastic Packstone-Grainstone	Light gray - gray	Planar laminae	Pf	cm-scale	3,4 sporadic	Planolites, Paleophycus, Ophiomorpha	Shallow deposit feeding, passive carnivore, living, stabilizing	Low-Moderate	Opportunistic	Moderate	Soup-loose	Shallow-middle	Color mottling overprinted by few discrete traces of facies crossers. Impoverished shallow-tier deposit feeding community overprinted by passive carnivore community	Low-Moderate, stabalizing	Impoverished Proximal Cruziana	Predominantly aggrading background sedimentation from supernormal to semi-dewith potential pulses of redeposited sediment. Also characteristic of salinity stress.
	19	Bioclastic Packstone-Grainstone	Dark gray	Sharp contact	Pf	cm-scale common, mm-scale subordinate	4, pervasive	Planolites, Chondrites, Thalassinoides	Shallow & deep deposit feeding, systematic feeding	Low	Opportunistic-Equilibrium	Moderate-long	Stiff-Firm	Shallow-middle-deep	Exhumation of stiff to firm substrate. Thalassinoides shows slight evidence of compaction	N/A	Glossifungites	Auto vs. allocyclic?
	20	Bioclastic Packstone-Grainstone	Light gray-gray	Planar Laminae	Bf, Ga	cm-scale	3-4, even	Macaronichnus, Diplocraterion, Rosselia, Cylindrichnus	Filter-feeding, interface feeding, shallow deposit feeding, up-and-down	Low	Equilibrium-Opportunistic	Short-Moderate	Soup-loose	Shallow-middle	This suite is unique	Moderate-High	Distal Skolithos/Proximal Cruziana	Increased sedimentation rate without evidence of mass wasting
	21	Bioclastic Packstone-Grainstone	Light-gray	Planar laminae, Sharp contact at base	Pf	mm-cm scale	2, sporadic	Skolithos, potential Ammicnites	Filter-feeding	Low	Opportunistic	Short	Soup-loose	Single Tier	Post event suite	High, Variable	Impoverished Skolithos	Episodic deposition
	22	Bioclastic Packstone-Grainstone	Light gray dark gray	Abundant gradational and sharp contacts	Pf, Bf	mm-scale & cm-scale common	3-5, pervasive	Thalassinoides, Cylindrichnus, Planolites, Chondrites, Helminthopsis	Filter-feeding, interface feeding, deep deposit feeding, systematic feeding, grazing	Moderate	Equilibrium	Moderate	Loose-stiff	Shallow-middle	Higher abundance of filter-feeding and equilibrium	Moderate, less stable	Proximal Cruziana	Increased sedimentation rate without evidence of mass wasting
	23	Bioclastic Packstone-Grainstone	Brown	Gradational contacts	Pf, Bf	mm-scale abundant, cm, scale common	5-6, pervasive	Scolicia, Chondrites, Planolites, Paleophycus, Helminthopsis	Shallow & deep deposit feeding, systematic feeding, passive carnivore, grazing	Moderate	Equilibrium-Climax	Long	Loose-Cohesive-Stiff	Shallow-middle-deep	High infaunal biomass, abundant food resources	Low, stable	Zoophycos	Environmental Stability
	24	Bioclastic Packstone-Grainstone	Light brown	Gradational contacts	Bf, Ga	cm-scale abundant	5-6, pervasive	Thalassinoides, Cylindrichnus, Planolites, Chondrites, Paleophycus	Filter-feeding, interface feeding, shallow & deep deposit feeding, systematic feeding	Moderate	Equilibrium-Climax	Long	Loose-Cohesive-Stiff	Shallow-middle-deep	High infaunal biomass, abundant food resources	Low, stable	Distal Cruziana	Environmental Stability
	25	Bioclastic Wackestone-Packstone	Light brown	Planar Laminae, Fining Upward Sequences	Pf, Bf	N/A	2, even or sporadic	N/A	N/A	Low	Opportunistic	Moderate	Loose	Shallow		Low-Moderate, stabalizing	Impoverished Distal Cruziana	Potential turbidite suite
1005	1	Foraminifer Wackestone	Beige-Dark beige	N/A	Pf, Bf	cm-scale & mm-scale	3, pervasive	Palaeophycus, Ophiomorpha, Thalassinoides	Passive carnivore, living, stabilizing	Low	Equilibrium-Opportunistic	Moderate	Soup-soft	Shallow-middle	Biodeformational structures / color mottling overprinted by few discrete traces. Opportunistic shallow-tier deposit feeding community overprinted by Palaeophycus & Ophiomorpha	Moderate-low, variable	Impoverished Proximal Cruziana	Ambient Conditions but still stressed. Characteristic of salinity stress
	2	Foraminifer Wackestone	Light beige-Beige	N/A	Pf	mm-scale	2-3, even	N/A	Deposit feeding or navichnia	Low	Opportunistic	Moderate-short	Soup	Shallow-middle	Mottled fabric, very few to no discrete traces. Shallow-tier opportunistic deposit feeding community	Moderate, variable	Impoverished Proximal Cruziana	Turbid conditions constantly disrupting soupy sediment or reworking of slowly aggrading seafloor
	3	Foraminifer Wackestone	Gray - light gray - light brown-ish gray	N/A	Pf, Sf, Ga	cm-scale	2, 3, even	Rare Ophiomorpha, Planolites	Living, Stabalizing, Shallow deposit feeding	Low	Opportunistic	Moderate-short	Soup	Shallow-middle	The lack of sedimentary structures indicates disipation time is great enough to disrupt all intrial sedimentary fabric	Moderate, variable	Impoverished Proximal Cruziana	Potential post event suite. Also characteristic of salinity stress
	4	Foraminifer Wackestone	Dark Beige	Sharp Contacts	Pf, Bf	mm-scale abundant, cm-scale common	4-5, pervasive	Planolites, Palaeophycus, Helminthopsis, Cosmorhaphe Chondrites	Shallow deposit & deep deposit feeding, systematic feeding	Low	Equilibrium-Opportunistic	Moderate	Soup-Soft	Shallow-middle	Flattened planolites over-printing mined background fabric	Moderate, steady	Impoverished Distal Cruziana	Ambient conditions (mostly pelagic sedimentation)
	5	Foraminifer Wackestone	Beige	Sharp Contacts	Pf, Bf	cm-scale, mm-scale common	3-4, even	Planolites, Palaeophycus	Shallow deposit feeding, Passive carnivore	Low	Equilibrium-Opportunistic	Moderate	Soup-Soft	Shallow-middle	Abundant facies crossers	Moderate-Low, variable	Impoverished Proximal Cruziana	Sharp boundaries point to more episodic or sporadic depositional energies
	6	Foraminifer Wackestone	Grey - light gray - light brown-ish gray	Fining Upward Sequences, Normally graded beds	Pf, Bf	mm-scale	1-5, Sporadic	N/A	N/A	Low	Opportunistic	Moderate-short	Soup	Shallow	Color mottling with few-no discrete traces	High, variable	Impoverished Skolithos	Episodic turbidite deposition
	7	Foraminifer Wackestone	Beige	Gradational Contacts	Pf, Bf	cm-scale abundant	5-6, pervasive	Planolites, Paleophycus, Thalassinoides, Cylindrichnus, Scolicia, Asterosoma, Rhizocorallium, Rhodolinus, Zoophycos, Teichichnus, Chondrites	Shallow & deep deposit feeding, systematic feeding, interface feeding, living, passive carnivore, rare filter feeding, up-and-down	High	Climax	Moderate-long	Soft-stiff	Complex	Very high infaunal biomass, dissolved oxygen high enough to support large animals at the seafloor, abundant food resources	Low, steady	Archetypal Cruziana	Environmental Stability
	8	Foraminifer Wackestone	Light beige-Beige	Gradational Contacts	Pf, Bf	cm-scale & mm-scale	4-5, pervasive	Paleophycus, Poeteichnus, Teichichnus, Taenidium	Passive carnivore, equilibrium, shallow deposit feeding	Moderate-low	Equilibrium-Opportunistic	Moderate	Soup-soft	Shallow-middle	Higher abundance of equilibrium structures	Moderate, steady	Proximal Cruziana	Increased sedimentation rate without evidence of mass wasting
	9	Foraminifer Wackestone	Beige-Dark Beige	Gradational Contacts	Pf, Bf, Sf, Pt	cm-mm scale common	4,5 pervasive	Chondrites, Cosmorhaphe, Planolites, Paleophycus, Phycosiphon, Thalassinoides, Ophiomorpha	Shallow & deep deposit feeding, systematic feeding, grazing, dwelling	Moderate	Equilibrium-climax	Moderate-long	Soft-stiff	Shallow-middle-deep	High infaunal biomass, abundant food resources	Low, steady	Distal Cruziana	Environmental Stability
	10	Foraminifer Wackestone	Dark Beige	gradational Contacts	Pf, Bf, Sf	mm-scale abundant, cm-scale common	5,6 pervasive	Chondrites, Cosmorhaphe, Planolites, Paleophycus, Phycosiphon	Shallow & deep deposit feeding, systematic feeding, grazing	Moderate	Equilibrium-climax	Moderate-long	Soft-stiff	Shallow-middle-deep	Dominated by chondrites and cosmorhaphe	Low, steady	Zoophycos	Ambient Conditions
1007	1	Foraminifer Wackestone	Light beige-beige	N/A	Pf, Bf	cm-scale overprint mm scale	5-6, pervasive	Asterosoma, Planolites, Paleophycus, Helminthopsis, Phycosiphon	Deep deposit feeding, Passive carnivore, grazing	Moderate-low	Equilibrium	Long	Soup-soft	Shallow-middle	Moderate-high infaunal biomass	Low-moderate, stable	Distal Cruziana	Environmental Stability, background sedimentation
	2	Foraminifer Wackestone	Beige	N/A	Pf, P	cm-scale abundant, mm-scale subordinate	5, pervasive	Planolites, Paleophycus, Phycosiphon	Shallow deposit feeding, passive carnivore, systematic feeding	Low-moderate	Opportunistic-Equilibrium	Moderate	Soup-soft	Shallow abundant		Low-moderate, less stable	Impoverished Distal Cruziana	Predominantly aggrading background sedimentation from supernormal to semi-dewith potential pulses of redeposited sediment. Also characteristic of salinity stress.
	3	Foraminifer Wackestone	Dark-beige	N/A	Pf	cm-scale abundant	5-6, pervasive	Asterosoma, Planolites, Paleophycus, Helminthopsis, Chondrites, Cosmorhaphe, Thalassinoides	Passive carnivore, shallow & deep deposit feeding, systematic feeding, grazing	Moderate	Equilibrium-Climax	Long	Soup-soft-firm	Complex	High infaunal biomass	Low	Zoophycos	Environmental Stability, slow background sedimentation
	4	Foraminifer Wackestone	Light gray	N/A	Pf, Bf	cm-scale	3-5 pervasive	Planolites, Paleophycus, Chondrites	Shallow deposit feeding, rare deep deposit feeding	Low	Opportunistic-Equilibrium	Moderate	Soup	Shallow-middle	Mottled fabric, very few to no discrete traces	Moderate, less stable	Impoverished Distal Cruziana	Poor substrate consistency
	5	Foraminifer Wackestone	Dark beige - beige	Sharp contacts at base, abundant gradational contacts	Pf, Bf	cm-scale abundant	5-6, pervasive	Planolites, Paleophycus, Thalassinoides, Cylindrichnus, Teichichnus, Cosmorhaphe, Chondrites, Macaronichnus, Zoophycos, Phoebichnus, Taenidium	Shallow & deep deposit feeding, passive carnivore	High	Climax	Long	Soup-soft-firm	Complex	Very high infaunal biomass, dissolved oxygen high enough to support large animals at the seafloor, abundant food resources	Low	Archetypal Cruziana	Transition from shedding into more background sedimentation
	6	Foraminifer Wackestone	Light beige-beige	Slumped intervals with erosional bases, normally graded bedding	Bf, Sf, Fr	cm-scale	3-4, sporadic	N/A	N/A	Low	Opportunistic	Short	Soup	Shallow	Color mottling overprinted with few discrete traces of facies crossers. Opportunistic shallow-tier deposit feeding community overprinted by Thalassinoides ?	Moderate-High, variable	Impoverished Proximal Cruziana	Episodic deposition
	7	Claystone	Dark Gray	N/A	Pf, Bf, Sf	cm-scale abundant, mm-scale subordinate	4-5, pervasive	Planolites, Chondrites, Phycosiphon	Shallow & deep deposit feeding, systematic feeding	Moderat e-low	Equilibrium-opportunistic	Long	Soup-soft	Shallow-middle		Low, stable	Zoophycos	Environmental Stability, slow background sedimentation
	8	Foraminifer Wackestone	Light beige-gray	Planar Laminae, Normally graded beddin	Pf, Bf	cm-scale	3,4 sporadic	N/A	N/A	Low	Opportunistic	Short	Soup	Shallow	Color mottling overprinted with few discrete traces of facies crossers. Opportunistic shallow-tier deposit feeding community	Moderate-High, variable	Impoverished Proximal Cruziana	Episodic deposition

Table 1(continued): Ichnofabric & Ichnofacies

	9	Foraminifer Wackestone	Light beige-beige	Gradational contacts, some planar laminae, some fining upward sequences	Pf, Bf, P	cm-scale	3-5, pervasive	Planolites, Palaeophycus, Thalassinoides, Chondrites	Shallow & deep deposit feeding, passive carnivore	Low-moderate	Opportunistic-Equilibrium	Moderate	Soup-soft	Shallow-middle		Low-moderate	Impoverished Distal Cruziana	Recovery during intermittent times of quiesence
	10	Foraminifer Wackestone	Light gray - gray	Normally graded bedding	Pf, Bf, Sc, Es	N/A	3,4 sporadic	N/A	N/A	Low	Opportunistic	Short	Soup	Shallow			Impoverished Proximal Cruziana	Episodic deposition
	11	Foraminifer Wackestone	Light gray - gray	N/A	Pf, Bf	cm-scale common	3-5, even	Ophiomorpha, Chondrites, Schaubcylindrichnus, Teichichnus, Palaeophycus, Phoebichnus, Asterosoma, Macaronichnus	Livign, stabilizing, passive carnivore, equilibrium shallow & deep deposit feeding	Moderate-low	Equilibrium-opportunistic	Moderate	Soup-soft	Shallow-middle	This suite is unique	Moderate	Proximal Cruziana	increased sedimentation without evidence for mass-wasting
1006	1	Nannofossil Chalk	Light gray or light tan	N/A	Pf, P	mm-scale common, cm-scale rare	2-3, pervasive	Cosmorhaphe, Zoophycos	Systematic feeding, deep deposit feeding	Low	Equilibrium	Long	Soup	Shallow-deep	Common color mottling and biodeformational structures overprinted by few discrete traces. Most impoverished fabric at site 1006	Low, steady	Nereites	Steady bottom current energy
	2	Nannofossil Chalk	Greenish-gray	Sharp contacts	Bf, Pf, P	mm-scale abundant	5-6, pervasive	Chondrites, Cosmorhaphe, Helminthopsis, Phycosiphon, Planolites, Zoophycos	Shallow and deep deposit feeding, mining, grazing	Low-moderate	Equilibrium	Long	Soft-stiff	Shallow-middle-deep	Lower oxygenation within sediments, slightly reducing conditions	Low, steady	Zoophycos	Weak bottom currents
	3	Nannofossil Chalk	Gray	Gradational contact at base	Pf, P, Sf	mm-scale common	4-5, pervasive	Chondrites, Cosmorhaphe, Helminthopsis, Phycosiphon, Planolites, Zoophycos	Shallow and deep deposit feeding, mining, grazing, systematic feeding	Low-moderate	Equilibrium	Long	Soup-soft	Shallow-middle-deep	Comon color mottling and biodeformational structures overprinted by systematic feeding traces.	Low, steady	Zoophycos	Weakening bottom current energy
	4	Nannofossil Chalk	Light gray	Gradational contacts	Pf, Bf, P, Sf, Es	cm-scale common	3-4, pervasive, increasing towards top	Chondrites, Cosmorhaphe, Cylindrichnus, Nereites or Neonerites, Planolites, Thalassinoides	Shallow deposit feeding, systematic feeding, interface feeding, dwelling	Low-moderate	Equilibrium	Long	Soup-soft	Shallow	Comon color mottling and biodeformational structures overprinted by mud-filled meanders	Low, steady	Nerites	Steady bottom current energy
	5	Nannofossil Chalk	Brownish-Gray	N/A	Pf, Bf, P	cm & mm scale common	4-5, pervasive	Asterosoma, Chondrites, Helminthopsis, Phycosiphon, Planolites, Palaeophycus, Zoophycos	Shallow & deep deposit feeding, systematic feeding, grazing, passive carnivore	Low-moderate	Equilibrium	Long	Soup-soft	Shallow-middle-deep	Bordering on distal cruziana expression	Low, steady	Zoophycos	Variable bottom current energy
	6	Nannofossil Chalk	Dark gray	Gradational contacts, fining upward and coarsening upward sequences	Pf, P	cm & mm scale common	4,5, pervasive	Chondrites, Helminthopsis, Phycosiphon, Planolites, Scolicia, Zoophycos	Shallow & deep deposit feeding, systematic feeding, grazing, passive carnivore	Low-moderate	Equilibrium	Long	Soup-soft	Shallow-middle-deep		Low but more variable	Zoophycos	Variable bottom current energy
	7	Nannofossil Chalk	Light gray or light tan	Rare gradational contacts	Pf, Bf, P, Sf, Pi	cm & mm scale common	3-4, pervasive, increasing towards top	Chondrites, Cosmorhaphe, Cylindrichnus, Nereites or Neonerites, Planolites, Thalassinoides	Shallow deposit feeding, systematic feeding, interface feeding, dwelling, filter-feeding	Low-moderate	Equilibrium	Long	soup-soft	Shallow-middle		Low, steady	Nereites	Steady bottom current energy
	8	Nannofossil Chalk	Dark gray	N/A	N/A	cm & mm scale common	3-4, even	Chondrites, Planolites, Thalassinoides	Shallow & deep deposit feeding, dwelling	Low-moderate	N/A	Long	stiff-firm	Shallow-middle-deep	Semi-consolidated firmground	N/A	Glossifungites	Depositional hiatus/exumation by increased power of contour currents

Bf = Benthic Foraminifers
Es = Echinoderm Spines
Fr = Fracture
Ga = Gastropods
L = Lithoclasts
M = Megafossils
P = Pyrite
Pf = Planktonic Foraminifers
Pi = Peloids
Pt = Pteropods
Sc = Solitary coral
Sf = Shell Fragments